UNIVERSIDAD
REY JUAN CARLOS

INGENIERÍA DE TELECOMUNICACIÓN

INGENIERÍA TECNICA EN INFORMÁTICA DE SISTEMAS

Curso Académico 2014/2015

Proyecto Fin de Carrera

ENERGY HARVESTING FROM MOVEMENT

Author : Álvaro Collado Alsina

Tutor : Dr. Gregorio Robles (Spain)

Cotutor : Dr. Piotr Dziurdzia (Poland)

Proyecto Fin de Carrera

ENERGY HARVESTING FROM MOVEMENT

Autor : Álvaro Collado Alsina

Tutor : Dr. Gregorio Robles Martínez

Co-tutor : Dr. Piotr Dziurdzia

La defensa del presente Proyecto Fin de Carrera se realizó el día de de 2015, siendo calificada por el siguiente tribunal:

Presidente:

Secretario:

Vocal:

y habiendo obtenido la siguiente calificación:

Calificación:

Fuenlabrada, a de de 2015

Dedicate to

all people who supported me and believed in me

Acknowledgments

Los agradecimientos será la única parte en español del proyecto porque es muy difícil expresar todo lo que siento en otro idioma.

Quiero darle las gracias a mis padres, Pedro y Amparo, a mi hermana, Andrea y a mi abuela Esperanza, porque sin su apoyo, su fuerza no habría sido capaz de llegar hasta aquí. También tengo muchísimo que agradecer a Ana, mi novia, por soportar todo este curso a mi lado incluyendo estrés, nervios y enfados que ha generado este ultimo curso de carrera tan estresante. A Joshua y Pablo porque siempre están ahi cuando necesito echar unas risas, unas cervezas o lo que haga falta.

Me gustaría también agradecer a todos los compañeros que me han acompañado y ayudado en la carrera. Quiero hacer especial mención a Carlos porque que seria de Polonia sin ese gran año juntos y todo lo que paso es un trocito muy importante en mi vida ya lo sabes. A Joel por tantas cosas que me aportas en el día a día siempre apoyando en todo y haciendo reír a todo el mundo eres genial. A Franco porque es el mejor ”basketcista” de toda europa y mejor persona, y aporta el punto de seriedad que muchas veces me ha hecho falta. Raquel, gracias por todas las charlas que he tenido de tantas cosas contigo. Peligros por estar siempre ahi aunque estemos lejos y quiero agradecer también a Macarena por toda la fuerza que durante este curso me ha dado para seguir luchando.

Quiero hacer un aparte a la gente que he conocido en Polonia desde Cesar,Anabel, Moni, Justyna, Marcin, Aldona, Pablo, Guillaume... Porque me han aportado muchísimas cosas y me han ayudado a que la adaptación al nuevo país sea inmejorable y me sienta genial cada día en Cracovia.

En definitiva quiero agradecer a todos por estar a mi lado por darme lo mejor y por estar de una forma u otra en mi vida. Os quiero.

Por ultimo, gracias a Gregorio Robles por facilitarme la realización del proyecto a distancia y por ayudarme a realizarlo de la mejor manera no se me ocurre otro profesor que me hubiera ayudado mejor.

Y para acabar serdecznie dziekuje Doktorowi Piotrowi Dziurdzia za pomoc udzielona nie tylko przy tym projekcie, ale w ciagu calego roku.

Muchas gracias a todos

Summary

Energy is wasted everyday in every place and nowadays is really important the use of green energy or renewable energy. Parallel to this type of energy, appeared few years ago the concept of energy harvesting, which has a lot of different types and applications.

This thesis is based on the study of energy harvesting on the move. Energy harvesting is the use of energy that is wasted each day. In recent years there have been many experiments related to this topic and this is one more. Among the different types of possible ways to take this energy I have selected one of them which is electromagnetism.

The main objective of my thesis is the search for a prototype to charge the battery of your own device whether smartphone, bike-pc or anything else. Currently the batteries are less durable and in a few hours you have to charge them to carry on working with them, thanks to the movement that I made in our bike these batteries could be charged during our journey on the bicycle.

During the process of my thesis I have researched on energy requirements and systems that could the prototype need for the las target. I used circuit simulation tools such as LTSpice and I also installed a prototype of bicycle in the laboratory to manage with all the testing needed.

Contents

List of Figures

List of Tables

Chapter 1

Introduction

“To convince people to back your idea, you’ve got to sell it to yourself and know
when it’s the moment. Sometimes that means waiting. It’s like surfing.
You don’t create energy, you just harvest energy already out there.”

In this chapter I will make a brief introduction of this final project. Explain the motivation that led us to realize as well as the goals I want to achieve. Also expose the memory structure of a short form to put in situation the reader of what will be found throughout the following chapters.

The purpose of this Final Project to be understood and improve the way in which I waste energy, such as the energy that is lost in the movements, body temperature. . .

For this reason I decided to get involved with energy harvesting looking for a project that could exploit the energy to so I can improve the utilization of this lost energy. At first I choose to orient toward the human body or something more electronic finally decided to get involved in the simulation, creation and optimization this prototype autonomous charger on a bicycle.

1.1 Context

The increase of energy consumption, has created the need to implement new methods of harvesting, conserving and optimally using energy. Movement in devices wheels, motor. . . is just one example of the multitude of untapped energy source on everyday life, that can be used to get amount of energy. Developing methods to harvest energy from these movements is a particular challenge, because there is a lot of applications for these methods.

Movement of wheels provides excellent case-study to explore the energy harvesting related with magnetic fields. In present day there is no way to get energy on bike for bike-computer, GPS... A solution to these inconveniences would be a circuit that can get energy from the movement of the bike for the devices.

1.2 Motivation

it all started when speaking with my tutor in Poland, he commented to me about the research he has being conducted. Dr. Dziurdzia sent me several articles based on energy harvesting and I was very interesting on the topic from the first sentences I read about it. I started researching about this fear and finally chose energy harvesting with electromagnetic fields.

1.3 Objectives

The goal of this thesis is to create models to serve as a designs aid and optimization tool for system that harvest energy from movement.

The focus of this thesis is to prove the feasibility of such a system and document the creation of a proof-of-concept prototype.

1.4 Structure

In Chapter 2 of this thesis I will describe what is Energy Harvesting, which are the most commonly used methods and the different magnetic harvesting that exists.

During Chapter 3 I will make a brief explanation about which are the different technologies I use during the thesis.

On Chapter 4 I will explain all the main process I have done for this thesis. Firstly I will describe the simulation I did using LTSpice software and why I change the simulations few times. Also, I will explain the different Integrated circuit I can use for my thesis and which it is the most suitable for my target.

Finally in chapter 5 and 6 it will be shown the results and conclusion about the thesis.

Chapter 2

Energy harvesting

Energy harvesting is possible to implemented in different ways. Calculate the energy requirements of an applications is really important to select the appropriate energy harvesting strategy. This chapter discusses the energy requirements of the bicycle and the selection of an energy harvesting strategy to meet these specifications. The whole theoretical calculations and formulas will be on Appendix A.

2.1 Energy Requirements

Firstly is necessary to identify the energy requirements of the system and determining if the energy harvesting is a viable approach to satisfy them. The energy requirements for our objective are specified in terms of power budget. The current system of energy harvesting in bicycle is the dynamo. The new efficient system will provide the rider the chance to have a charger on his bike. The power requirement for a charger is around 3.3V.

2.2 Energy Requirements Systems

There are many ways of harvesting energy from vibrations. Three of the most common methods are: Variable Capacitance Systems, Piezoelectric Material Systems, and Magnetic Induction Systems. Each of these will be studied and their typical power outputs evaluated. Table 2.1 shows a comparison table of the three options.

2.2.1 Variable Capacitance Systems

Variable capacitance systems employ parallel-plate capacitors with movable plates. The plates are charged to a specified voltage. The plates are then mechanically moved apart by the input vibrations. Increasing the distance between the plates causes energy to be stored in the capacitor.

This energy can be harvested when the plates are brought closer to each other again. The magnitude of energy that can be harvested from such systems is generally on the order of micro watts.

2.2.2 Piezoelectric Material Systems

Piezoelectric materials build up a voltage differential across their ends when they are subjected to mechanical deformation. When energy from vibrations is harnessed to cause deformation in such materials, the voltage difference generated can be used to charge a capacitor or other energy-storage device. The magnitude of energy harvested from piezoelectric systems can vary from micro watts to watts.

2.2.3 Magnetic Induction Systems

Magnetic induction systems generate power through relative motion between a coil of wire and a magnet. This causes the magnetic flux through the coil to change, which leads the generation of a voltage differential across the ends of the wire coil. This voltage difference can be used to charge a capacitor or other energy-storage device. The magnitude of energy harvested from magnetic induction systems can range up to kilowatts depending on the size of the system.

	Variable Capacitance	Piezo Material	Magnetic Induction
Power generation	μW	μW-W	mW-kW
Vibration amplitude	μm	μ-m	mm-cm
Driving frequency	Any range	Tens of Hz	Any range
Ease of system design	Difficult	Easy	Easy
Cost	High	High	Modest
Lifetime	Low	High	High

Table 2.1: Comparison of energy harvesting strategies.

2.3 Magnetic Induction System Design

Magnetic induction systems generate power through relative motion between a coil of wire and a magnet. The result of this is the magnetic flux through the coil to change, which leads the generation of a voltage differential across the ends of the wire coil. This voltage difference can be used to charge a energy-storage device. The magnitude of energy harvested from magnetic induction systems can range up to kilowatts depending on the size of the system. The comparison table (Table 2.1) shows this to be the most cost-effective and promising option for our experiment.

The power that can be harvested by a magnetic induction system depends on many things, including the size and geometric configuration, the magnetic flux density of the magnets, the number of turns of wire in the coil, and the excitation frequency. There are two magnetic induction systems – magnet-through-coil and magnet-across-coils – in order to enable an understanding of how these systems can be designed and optimized for specific applications, this methods will be evaluate.

The objective of analyzing these magnetic induction systems is to calculate their output voltage and power, this parameters are the most interesting one in the project.

Firstly is necessary to calculate the magnetic field, H, in the system. The magnetic field gives the magnitude of magnetic flux density, B, and hence the magnetic flux, A, through the coils. Once the flux through the coils is known, the open-circuit voltage across them, V, can be calculated using Faraday's Law. Ohm's Law and Kirchhoff's Laws are then used to determine the average power, P, dissipated through a load resistor attached to the system. Figure 2.1 shows a flowchart of the steps involved in the analysis of magnetic induction systems.

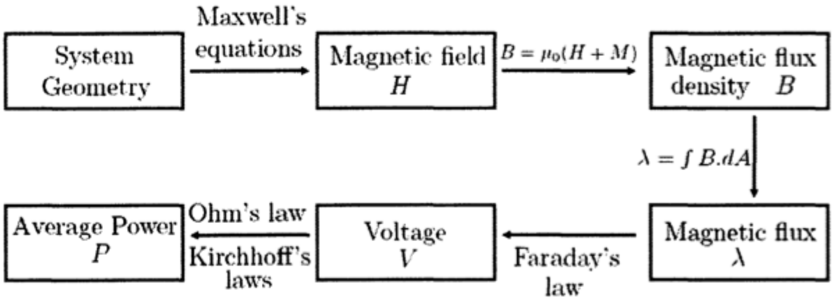

Figure 2.1: Flowchart of steps

2.3.1 Magnet-through-coil Induction

Description of the governing equations for voltage generate by a magnet through a coil. The advantage of this system is the easy way to build it; the disadvantage that the flux reversal of the coil never is complete, and the voltage and power is low. The most common example is a shaker flashlight. The device is powered by the movement of a magnetic relative to a coil when is shaken.

The magnet-through-coil induction system consists of a cylindrical coil that translates relative to a bar magnet of height l_m and radius r_m. The longitudinal axis of the magnet is set along the y-axis, with its midpoint at the origin. The coil, made of N turns of wire, has height I_c, inner diameter d_min and outer diameter d_max. The average radius of the coil, r_c, is calculated as:

$$r_c = \frac{d_{min} + d_{max}}{4} \tag{2.1}$$

The average diameter of the coil, d_c, is $2r_c$. The cross sectional area of the coil, A_c, is calculated as

$$A_c = \pi r_c^2 \tag{2.2}$$

The magnet is fixed in place while the coil moves along the y-axis. The y-coordinate of the lower end of the coil is defined as h. The coil is assumed to vibrate with a fixed amplitude, a, at a single frequency, f, with the motion centered at the y-coordinate dc. Figure 2.2 shows the labeled geometry of this system.

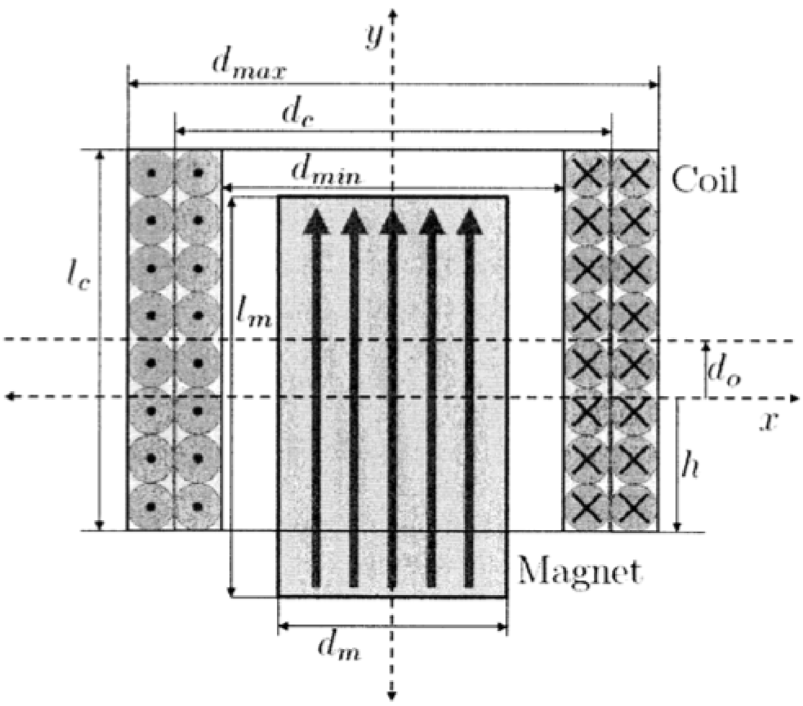

Figure 2.2: A cross-sectional view of the magnet-through-coil induction system.

2.3.2 Magnet-across-coils Induction

The magnets-across-coils induction system consists of a layer of magnets separated by an air gap from a layer of coils. The magnets move across the coils, causing a change in magnetic flux and generating a voltage across the coil ends. The system has three phases: A, B and C. Figure 2.3 shows a schematic of the system to be analyzed.

Since the permeability of a magnetic material like steel is typically orders of magnitude higher than that of air, the magnetic backing for the coils and magnets is assumed to have infinite permeability. The now simplified problem is to solve for the magnetic fields in the gap between the two layers of magnetically permeable material, where magnetic fields are generated by the magnets and by coil current.

As all the elements of the system are linear, the fields due to the magnets and coils can each be calculated separately and then added by superposition. This breaks the problem into three smaller tasks: (1) calculation of the magnetic field due to the magnets; (2) calculation of the fields due to the flow of current in the coils; and (3) adding them by superposition and finding the total voltage and power generated.

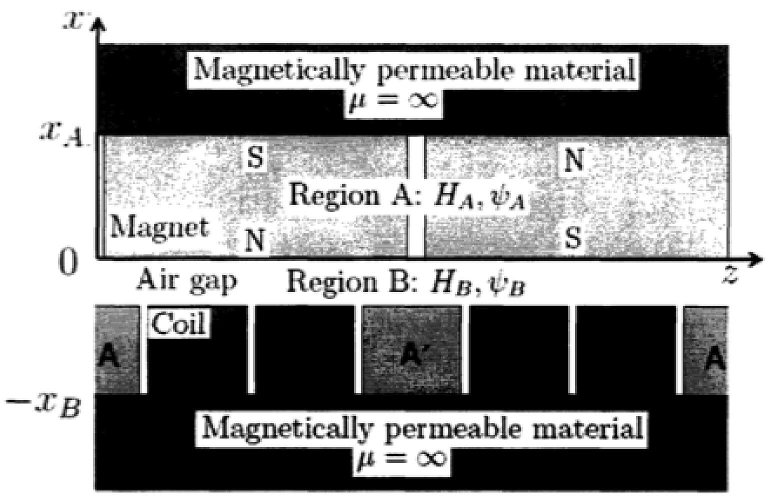

Figure 2.3: Magnet-across-coils induction system

Chapter 3

State of the art

This chapter aims to give an overview of the technical and technological tools that have been taken into account during this project. In this chapter the technologies are presented, in the next chapter is shown how have been used in this project.

For the preparation of this chapter has been used by multiple sources, mainly web pages, books and articles. All are properly referenced.

3.1 LTspice

LTspice[1] is a high performance SPICE simulator, schematic capture and waveform viewer with enhancements and models for easing the simulation of switching regulators. Our enhancements to SPICE have made simulating switching regulators extremely fast compared to normal SPICE simulators, allowing the user to view waveforms for most switching regulators in just a few minutes. Included in this download are LTspice IV, Macro Models for 80% of Linear Technology's switching regulators, over 200 op amp models, as well as resistors, transistors and MOSFET models.

[1] http://www.linear.com

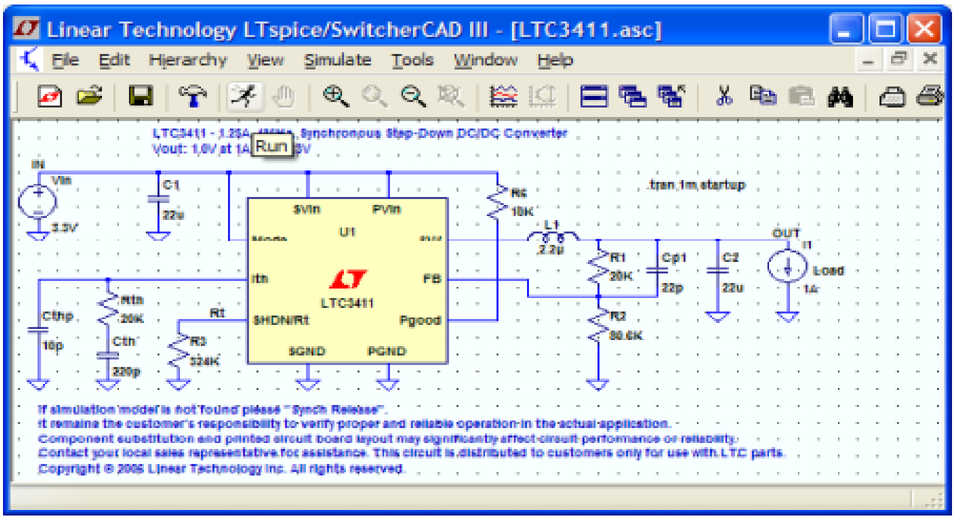

Figure 3.1: LTspice circuit Example

3.2 Altium Designer

Altium Designer[2] is an electronic design automation software package for printed circuit board, FPGA and embedded software design, and associated library and release management automation. it is developed and marketed by Altium Limited of Australia.

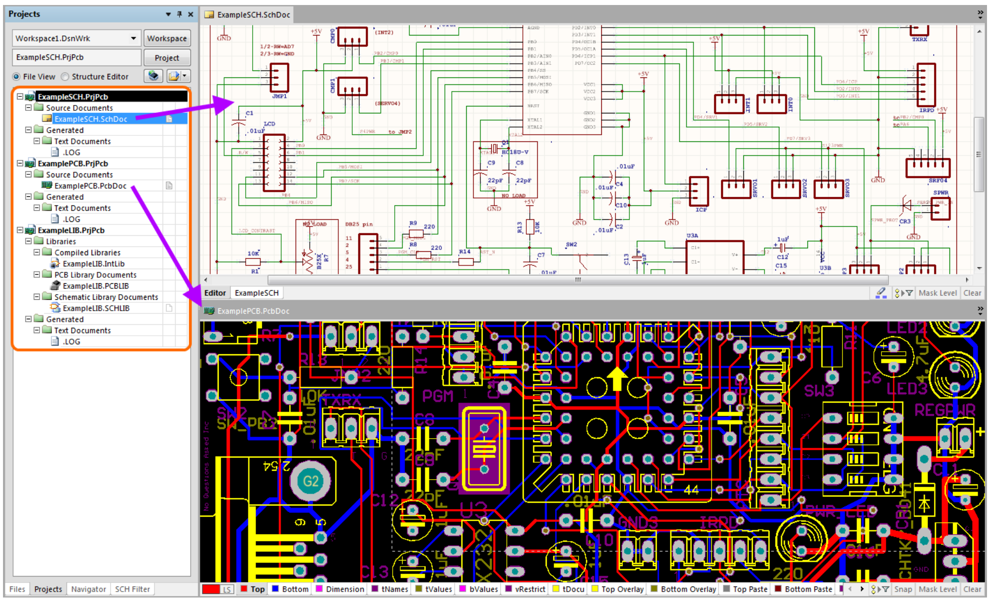

Figure 3.2: Eagle Board Example

2http://www.altium.com/altium-designer/overview

Chapter 4

Design and Implementation

This chapter explains the design of the prototype of my thesis, and also the changes that I have made in this prototype during the time. At the same time of the design, are shown corresponding simulations with the design state at that time.

4.1 Prototype components

This section describes the different kinds of components which are necessary to implement the final set-up of the laboratory.

4.1.1 Motor

A motor is an electrical machine that converts the electrical energy into mechanical energy. There are tow different kinds of motors, DC and AC. In our case DC motor is the one used on the prototype. The DC motor gets the electrical energy from a Power Supply.

Figure 4.1: Different motors

4.1.2 Roller

it is a component designed to roll, in the project it is related to the movement of the DC motor shaft.

4.1.3 Wheel

it is a circular component that has rotates on an axial bearing. A bicycle wheel, most commonly a wire wheel,is one wheel designed for a bicycle. A pair is often called a wheelset. A typical modern wheel has a metal hub, wire tension spokes and a metal or carbon fiber rim which holds a pneumatic rubber tire.

Figure 4.2: Bicycle wheel

4.1.4 Holder

The holder is the part where all the rest of the prototype is attached to with screws, glue or different fastening methods.

4.1.5 Tachometer

A tachometer is an instrument to measure the rotation speed of shaft, disk or more. Normally these devices shows Revolutions per minute (RPM) on an analog dial, but nowadays also are common the digital ones.

Figure 4.3: Tachometer

4.1.6 Magnets

Magnet is a material or object than can generate magnetic fields. This field generates a force that pulls from some material and attracts others.

Figure 4.4: Magnets

4.1.7 Coil

A coil is an electrical conductor like a wire in spiral or helix. Electromagnetic coils are used, in applications where electric currents produce magnetic fields, in devices like inducts, electromagnets, transformers...

Figure 4.5: Coils

4.1.8 Transformers

A transformer is an electrical device that transfers energy between two or more circuits through electromagnetic induction. Commonly, transformers are used to increase or decrease the voltages of alternating current in electric power applications.

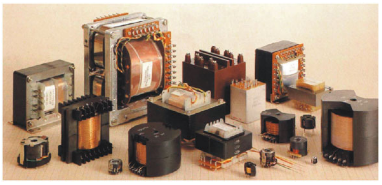

Figure 4.6: transformers

4.1.9 Integrated Circuits

An integrated circuit is a joint of circuits on a chip of semiconductor material. This is smaller than a typical circuit, it has a lot of transistors and other components and is not much bigger than a fingerprint.

Figure 4.7: integrated circuits

4.1.10 Components for IC

Capacitors and resistor are electrical components needed on the IC circuit.

4.2 Uses of components of the prototype

4.2.1 Motor

In the prototype, a motor is arranged to generate the movement that would be generated by a person pedlling the bicycle. This movement is the mechanical energy that the DC motor generates on the shaft by the rotation of this part.

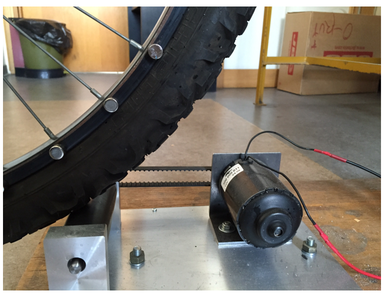

Figure 4.8: DC motor

4.2.2 Roller

In Figure 4.8 it is possible to see that there is a roller to move the wheel in a better way, because the DC motor generates a movement that can?t move the wheel with the shaft. In order to have a good movement of the wheel, it was prepared like this the DC motor with this roller.

Figure 4.9: Roller

4.2.3 Wheel

it is the main part of the prototype which will move and generate the magnetic field. This movement is produced by the whole set of the DC Motor and Roller.

Figure 4.10: Wheel of the prototype

4.2.4 Tachometer

The tachometer will get the value of the RPM of the wheel. To use the tachometer it is necessary to have a small reflective material on the wheel.

Figure 4.11: Tachometer

4.2.5 Magnets

The magnets will be distributed around the rim to produce a constant magnetic field. They are one of the important parts of the prototype to generate our final voltage.

Figure 4.12: Magnets on the wheel

4.2.6 Coil

The coil will be established closed to the rim of the bicycle. The coil will generate electrical energy because of the movement of the magnets. First I used coils that I can have on the market like the one on Figure 4.13 and also figure 4.14.

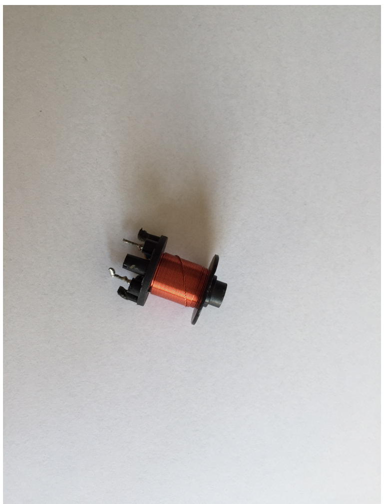

Figure 4.13: First coil

Figure 4.14: Second coil

Finally I decided to create our own coil. I create this coil with a wire of 0.5 millimeter of thickness, and with 100 round.

Figure 4.15: Costume coil

Inside the coil from Figure 4.15 I put inside some ferromagnetic as is shown in the Figure 4.16.

Figure 4.16: Ferromagnetic Material

4.2.7 Transformers

The use of the transformers in the prototype its really important because they will increase the value of the voltage obtained on the coil to a necessary voltage for properly operation of the IC.

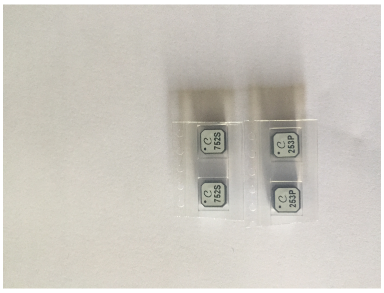

Figure 4.17: Different Transformers

4.2.8 Integrated Circuits

The integrated circuits are circuits focused on energy harvesting that can convert a really slow voltage into one enough to charge a battery.

4.3 Design and simulation history

The first step in the project, was to mount the prototype for the laboratory and set up everything (dc motor, wheel, holder, roller) to start getting some values. This first part it is really important because it is useful to know the range of voltage I will have on the prototype.

Figure 4.18: First prototype

With the first range of voltage's value I was able to perform a simulation on LTSpice based on LTC3108 converter. Firstly the simulation with the converter was focused on obtaining in which range I can start simulating, so I decided to have the same configuration of the circuit changing the values of the voltage 3V or 5V and changing the frequency of the V_{in}.[1] At this moment I was just checking which IC would be more suitable for my prototype, so looking at data sheet of LTC3108[2], it is possible to verify the different kinds of applications.

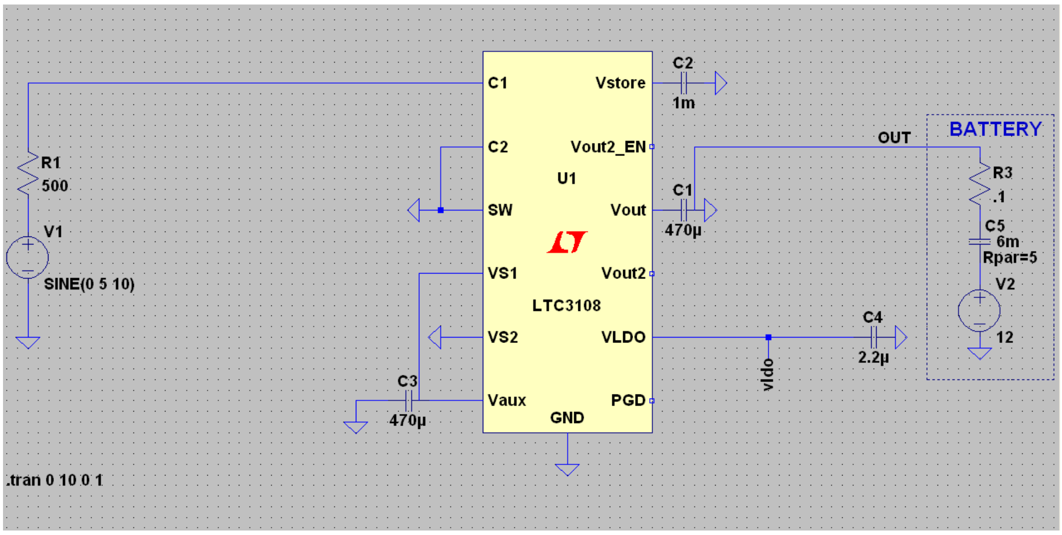

Figure 4.19: Simulation circuit 1

As it can be verified on the data sheet the first configuration was wrong. It is not necessary to connect C_2 to SW and also the values of the capacitor are not correct. So as I can see in Figure 4.19 I took out the battery because I didn't need it for the simulation. Just getting the right value at the V_{out} would be perfect to achieve my target.

[1]All results about simulation will be describe in next chapter.

[2]Data sheet LTC3108 is in the Appendix B.

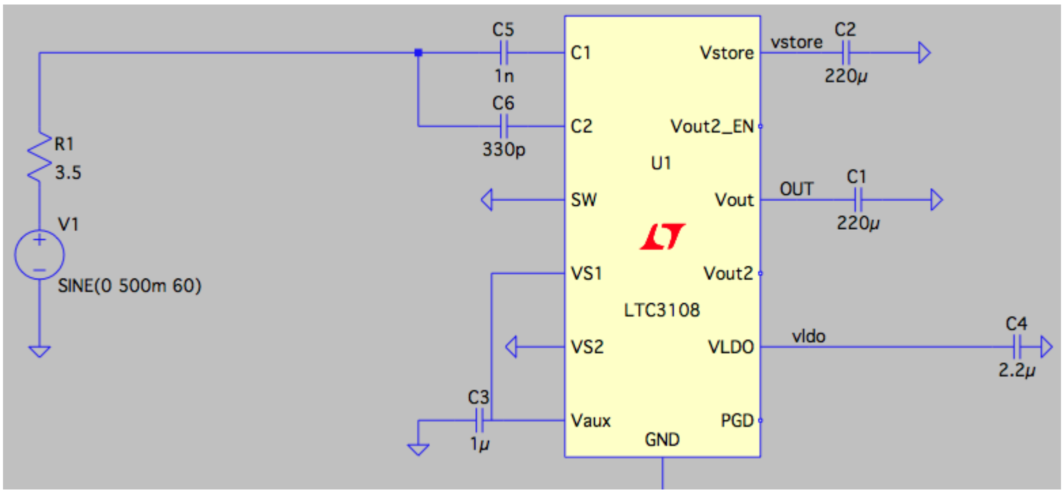

Figure 4.20: Simulation circuit 2

At the same time I was working on the simulation with LTSpice, I was working to improve the prototype with different coils to generate more voltage and also to get a more stable voltage. Finally I decided to create my own coil[3] and I attached the coil to the holder of my prototype to keep it stable and close to the rim of the wheel.

Figure 4.21: Homemade coil attached to the prototype

[3]Values of the homemade coil will be describe in next chapter

The next modification in the simulation circuit was to attach a transformer just to get a greater value of the V_{in} in the converter, because I realized that the voltage with the higher speed it was around 1.1V. So the next changes in the circuit were related to the different ratio of the transformer 1:20, 1:50 or 1:100.

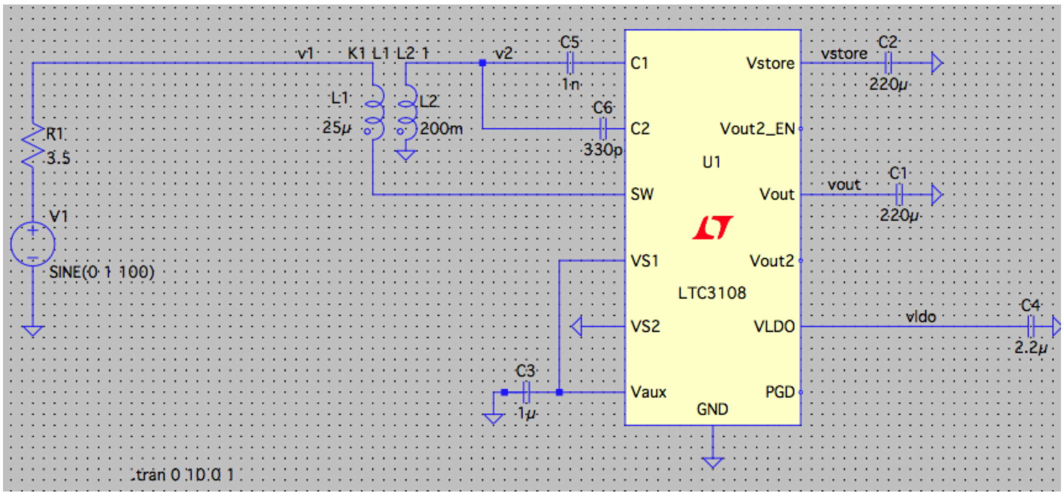

Figure 4.22: Simulation circuit ratio 1:20

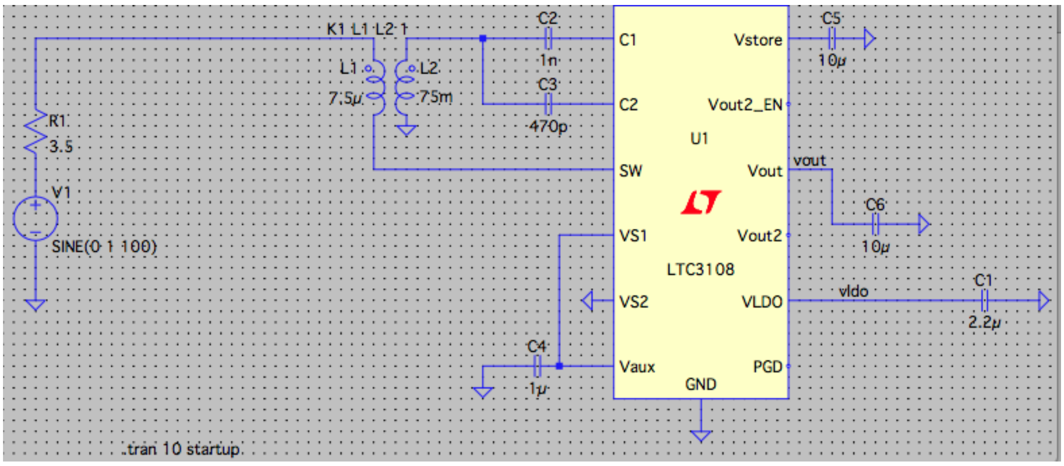

Figure 4.23: Simulation circuit ratio 1:100

At this part of the project my tutor told me to take a look also at LTC3109 as it could be suitable for my objective. So taking a look at the data-sheet[4] I prepared a simulation for this new IC than could be used in with the prototype.

[4]Data sheet LTC3109 is in the Appendix C

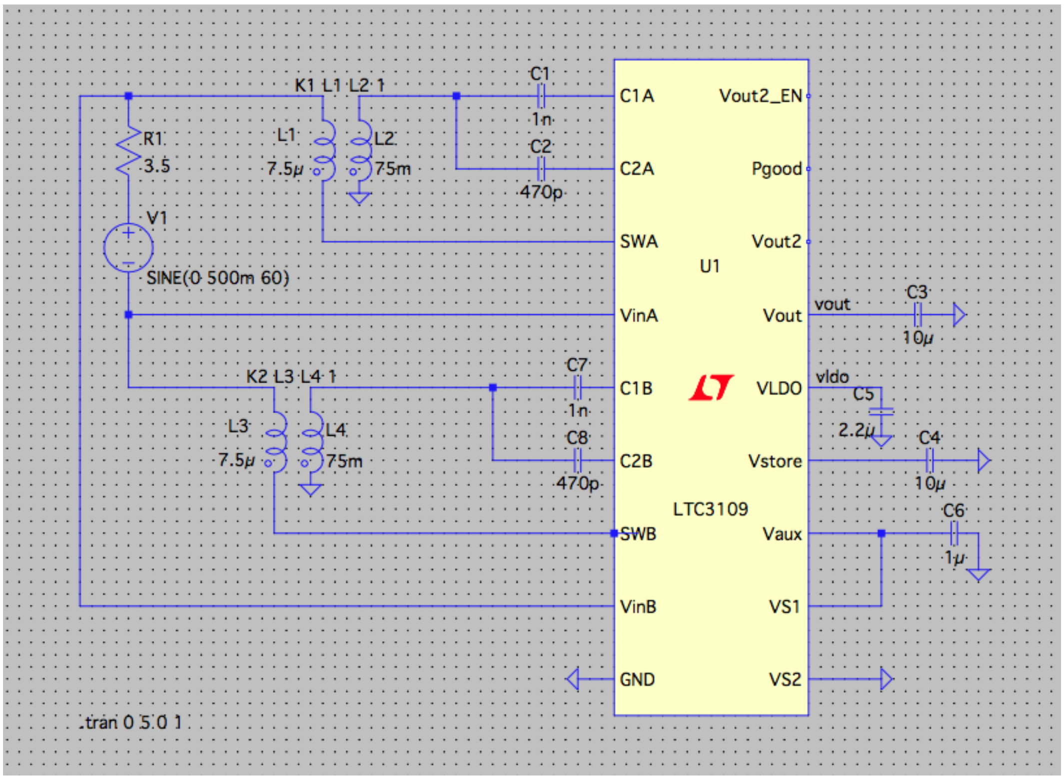

Figure 4.24: Simulation with LTC3109

With this simulation there were some troubles on the V_{out} values and it was necessary to attach a resistor on the negative part of V_{in} as is shown in Figure 4.24.

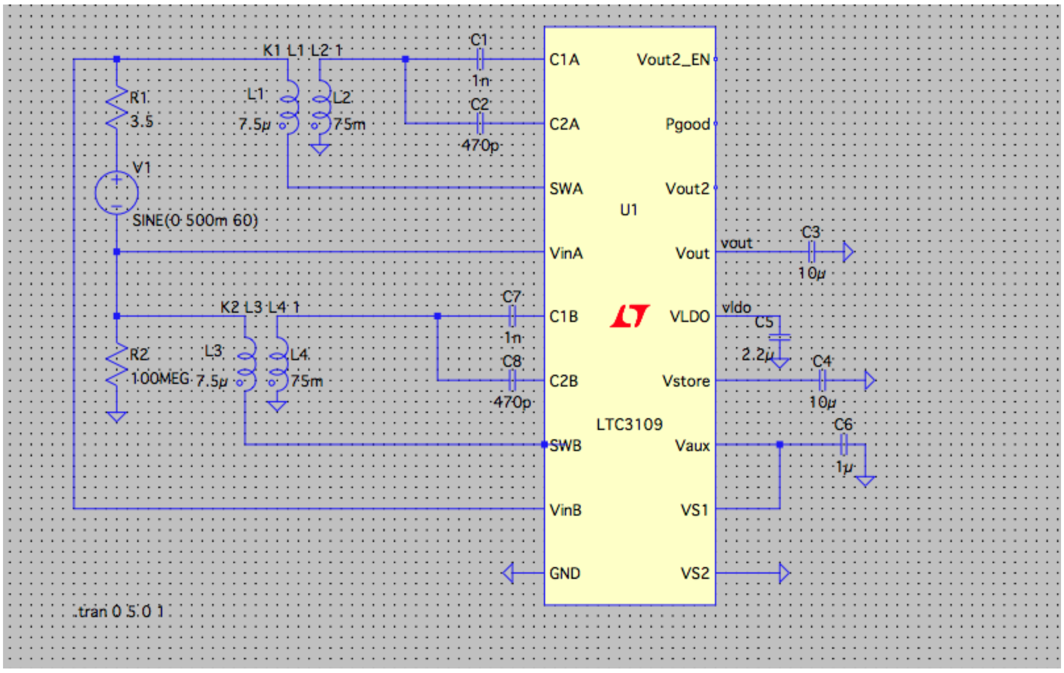

Figure 4.25: Simulation with LTC3109 and resistor

After this point the simulation of my circuits in LTSpice are finished and I was able to start with the simulation of the PCB board that I would use on my prototype. So, first of all I needed to create a necessary scheme of the whole circuit with all the connections from the IC to the output and also create a model of how I weld all components in the PCB board. On the figures below is shown both the scheme and the model for each IC LTC3108 and LTC3109, for this issue I used the Altium Designer.

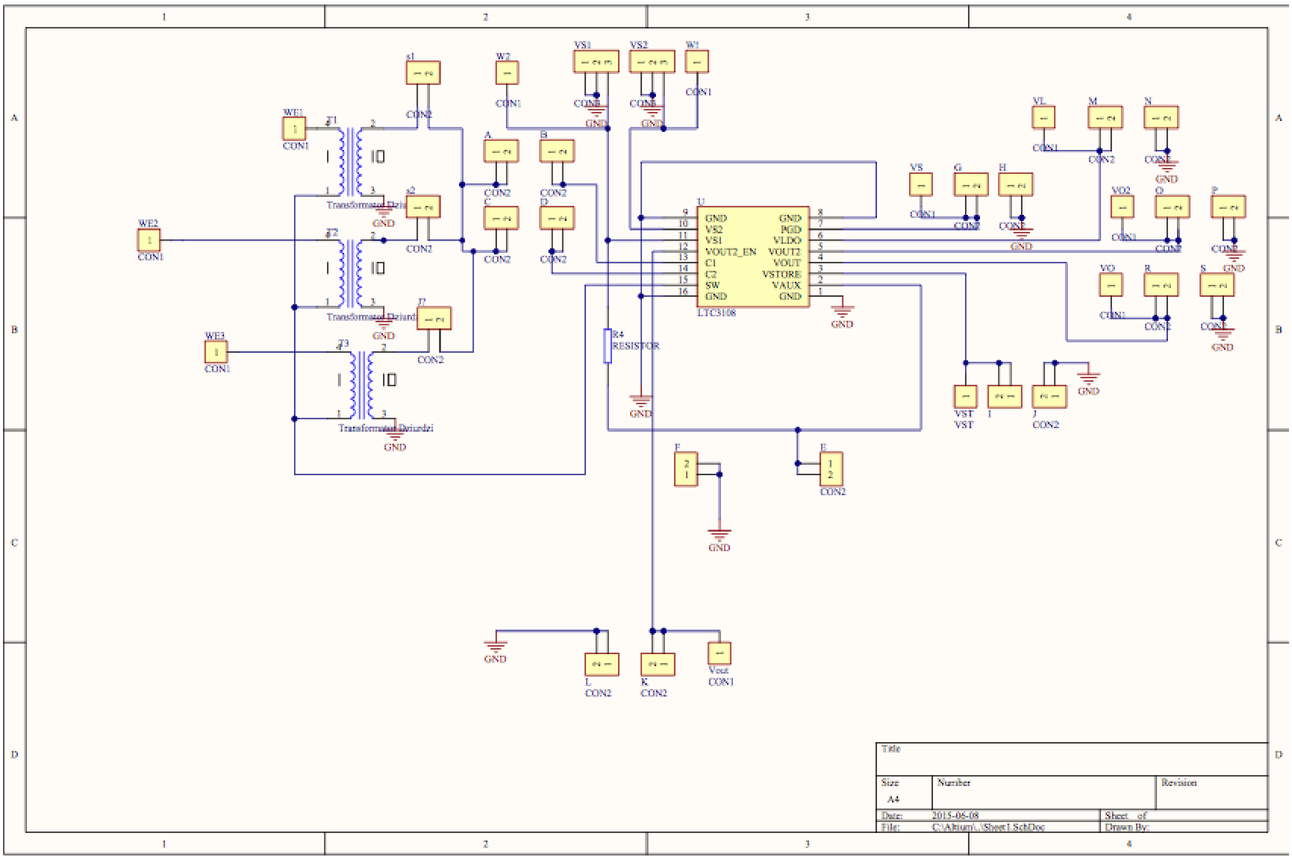

Figure 4.26: Scheme of LTC3108 circuit

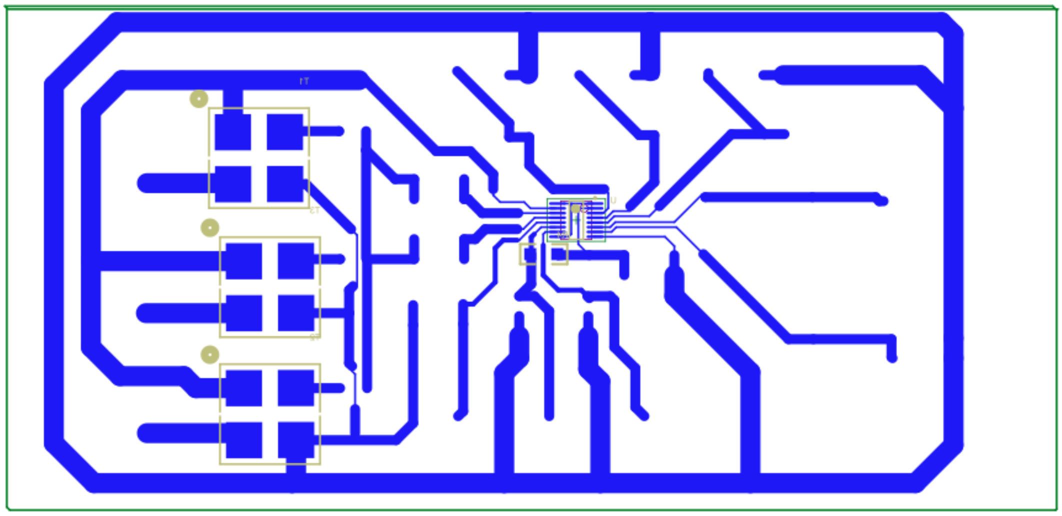

Figure 4.27: Welding simulation LTC3108 circuit

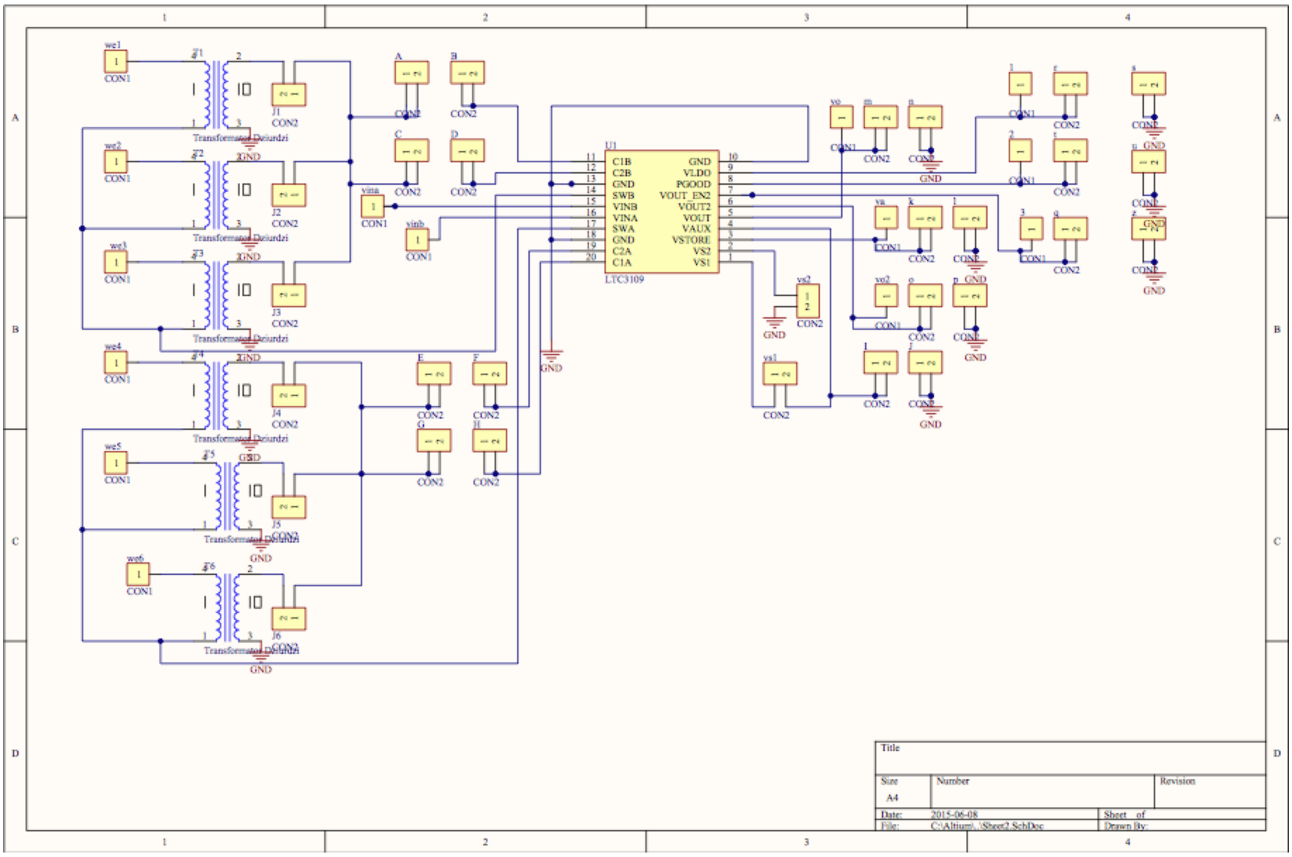

Figure 4.28: Scheme of LTC3109 circuit

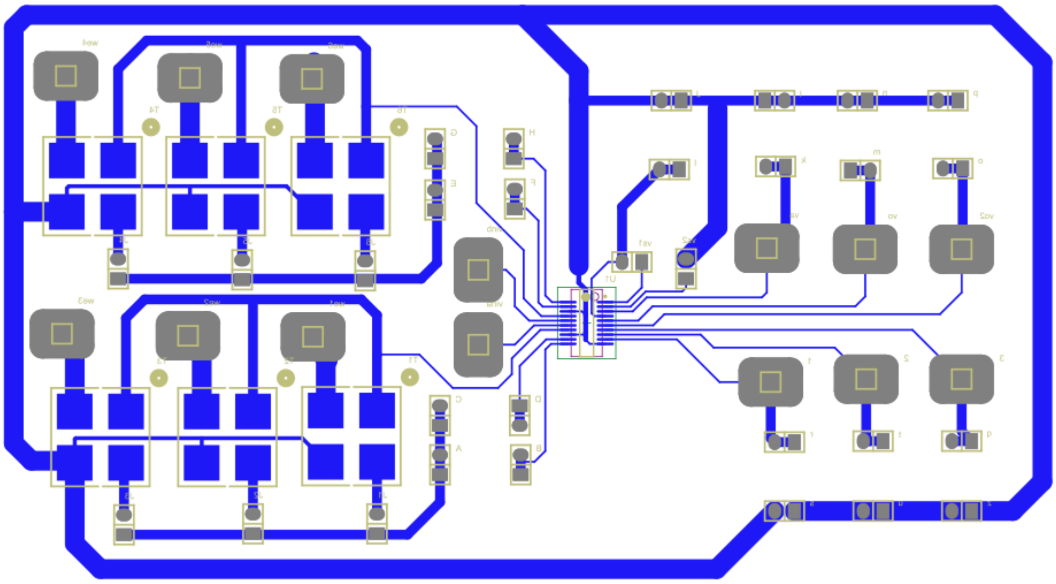

Figure 4.29: Welding simulation LTC3109 circuit

Chapter 5

Results

In this chapter I will describe and discuss all the results form the simulation and after this the results from the prototype. I will reference all the time to the Section 4.3 Design and simulation history.

At the first part of the results, I started with the simulation circuit from Figure 4.18. I got two values of input voltage (3V and 5V) and I also changed the frequency of V_{in} to get how this change of the frequency affects to my circuit.

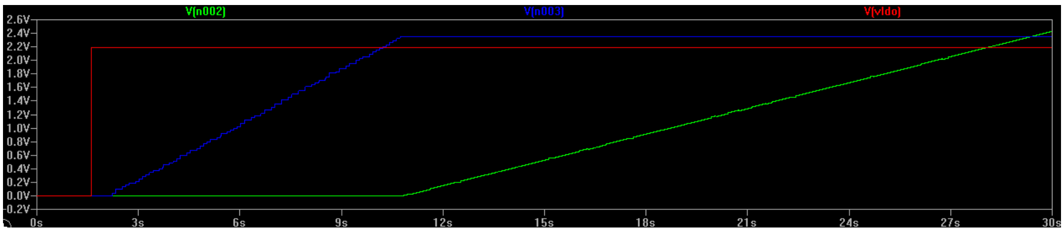

Figure 5.1: Simulation LTC3108 values:3V 10Hz

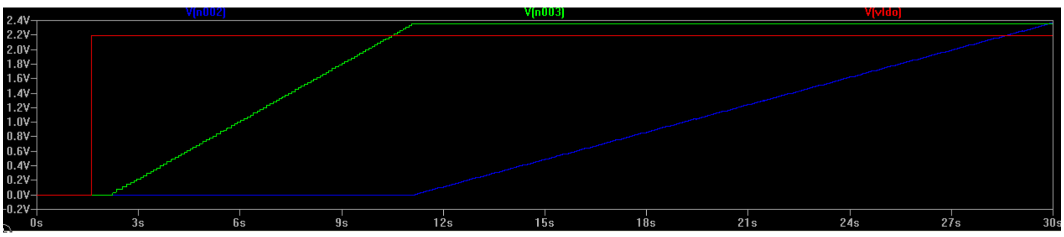

Figure 5.2: Simulation LTC3108 values: 3V 60Hz

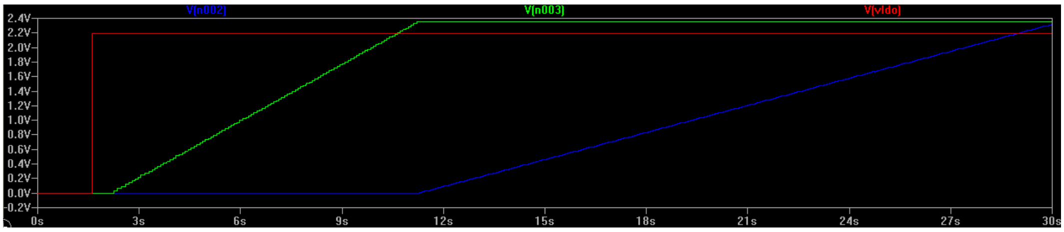

Figure 5.3: Simulation LTC3108 values: 3V 100Hz

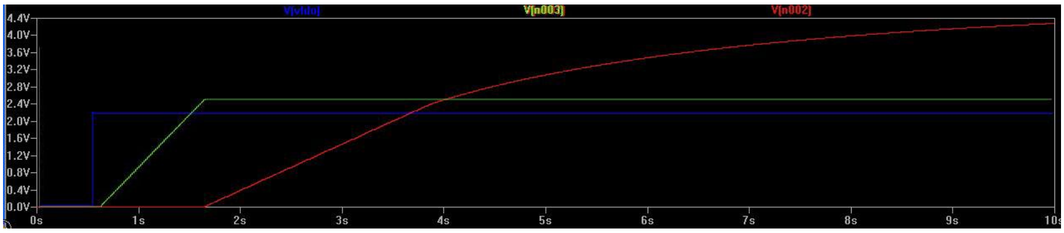

Figure 5.4: Simulation LTC3108 values: 5V 10Hz

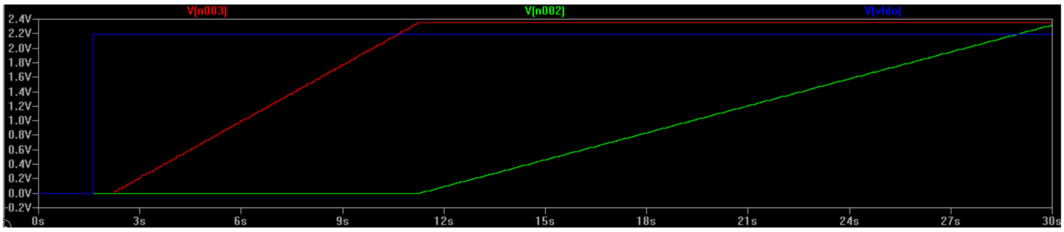

Figure 5.5: Simulation LTC3108 values: 5V 100Hz

It was possible to observe some errors in this simulation. First when I looked again in the data sheet of 3108 I knew that it was not necessary to connect C_2 to SW. So I changed it as we can see on Figure 4.19.

Second, as it was possible to see V_{out} couldn't reach the expected value to charge a battery. This value has to be 3.3V and in the first simulation the graph for V_{out} reached 2.2V. To fix this problem I noticed that the connection of C_3 didn't exist as I can see there is no a dot in the wire that means there is no connection. Thats why I got in V_{out} 2.35 V instead of 3.3 V.

Third, there was no change if I increased or decreased the frequency of the V_{in}. I obtained the same values for each frequency 10Hz, 60Hz or 100Hz. So for the next simulation it was not important which frequency I would use to simulate the circuit.

On the other hand, I prepared my homemade coil. I decided to do it like this because with this method I was able to decide all the specifications of my coil.

	Homemade Coil
Wire Thickness	0,5 mm W
Bounds	100
Length	7cm
Internal Resistance	$3,5\Omega$
Inductance without Ferromagnetic's	0,54mH
Inductance with Ferromagnetic's	9,2 mH

Table 5.1: Homemade Coil Values

As it is possible to see on Figure 4.20, I attached the coil to my prototype and I did some tests on the prototype because it was the last change on the laboratory prototype. This part of the project was really important, I got a range of Voltage in the output of the homemade coil from 0.3V to 1.1V.

This testing changed the whole simulation because I was simulating with a wrong range. Also, I needed to change the value of R_1.

Because of this change in the range of voltage it was necessary to attach a transformer between the coil and the input of LTC3108. It was necessary to increase the value that goes to the IC because now the maximum value V_{in} it wasn't enough for the IC input.

As it is possible to see on the Figure 5.6 after attaching the transformer, I was able to improve the voltage value (V_1 = voltage before transformer V_2 = voltage after transformer) that would be the input to the IC.

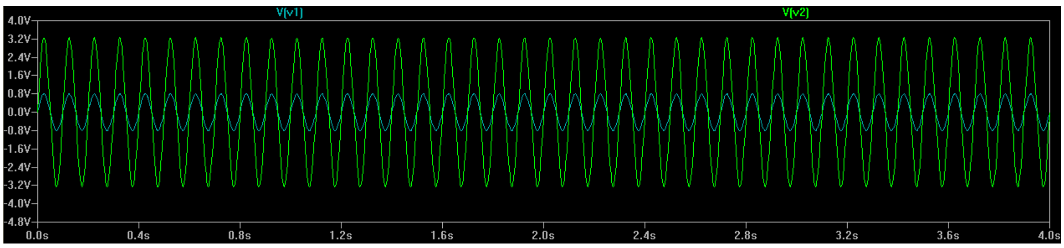

Figure 5.6: Comparison of V_1 ande V_2

Now I had to check how the differences rates of the impedance of the transformer, that are possible to get in the market, and how this will affect to the result. In Figure 5.7, 5.8, 5.9 and 5.10 it is possible to discard this simulation because there is no difference when I change the values of the impedance.

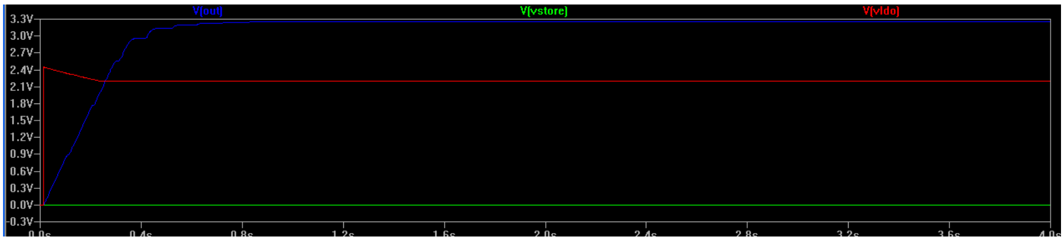

Figure 5.7: Circuit with transformer of 2,5H

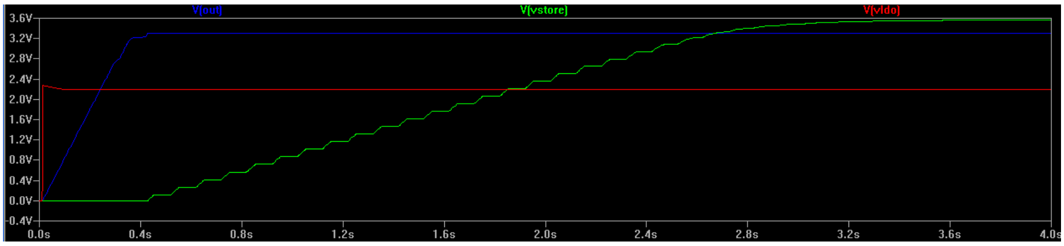

Figure 5.8: Circuit with transformer of 3H

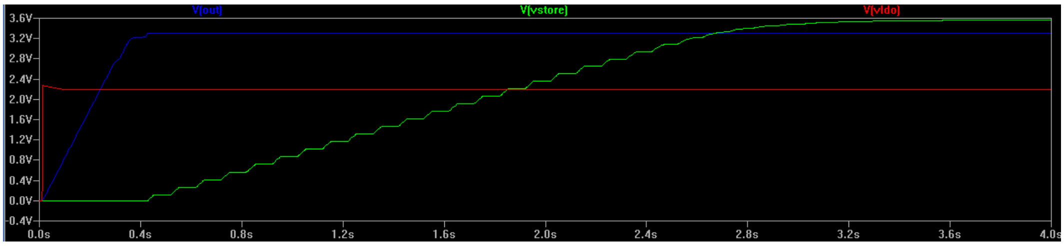

Figure 5.9: Circuit with transformer of 4H

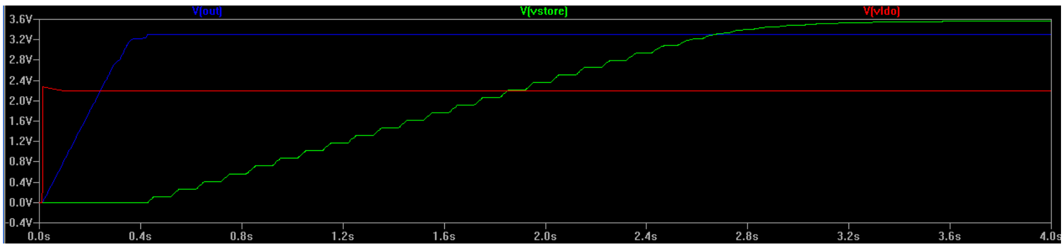

Figure 5.10: Circuit with transformer of 5H

The following step is to test if it is required to include a rectifier circuit on the input to have positive values of the signal or just positive and 0 value all the time. In Figure

5.11 and 5.12 there is a scheme of the simulation, where I included a capacitor, resistor and a diode.

Also, I tried this kind of rectifier without resistor to see the difference. This circuit is a rectifier of half wave, this means that the negative part will be 0. I made some simulation with a 4 diode bridge that would rectify the whole wave, which gave me positive value of the signal in the total time. I don't include the Figures of the bridge because there was no result on the V_{out} with such a circuit.

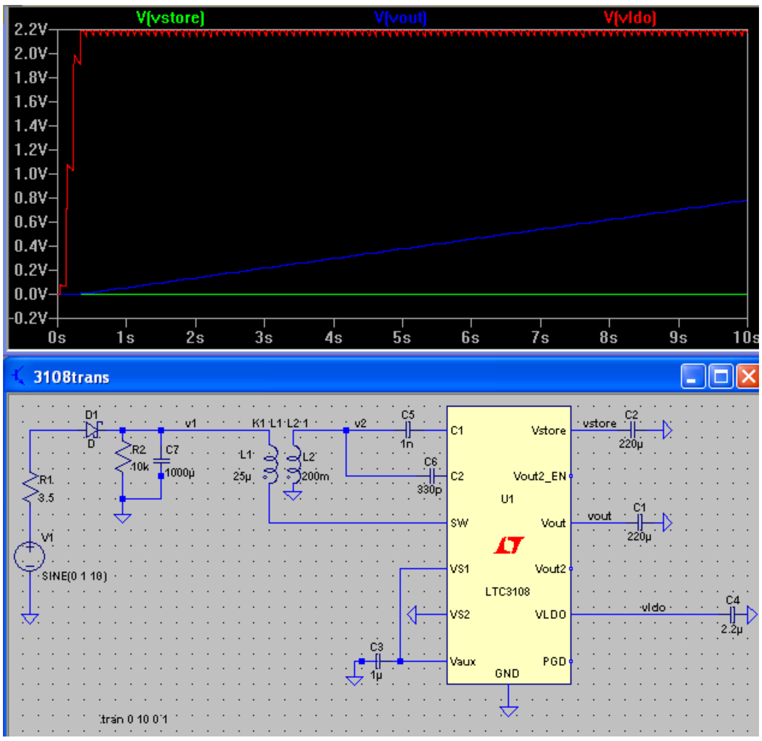

Figure 5.11: Half Wave Rectifier Circuit 1

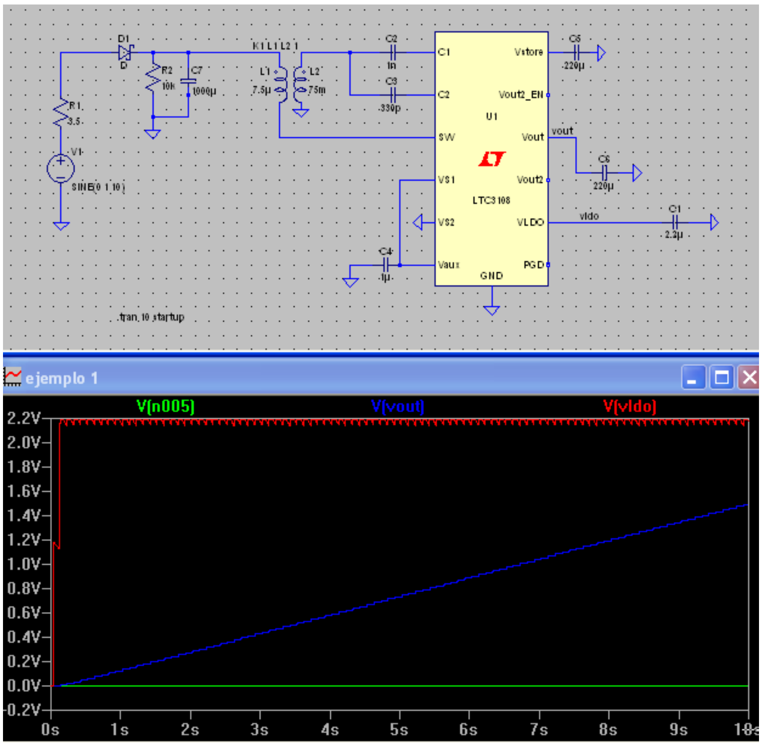

Figure 5.12: Half Wave Rectifier Circuit 2

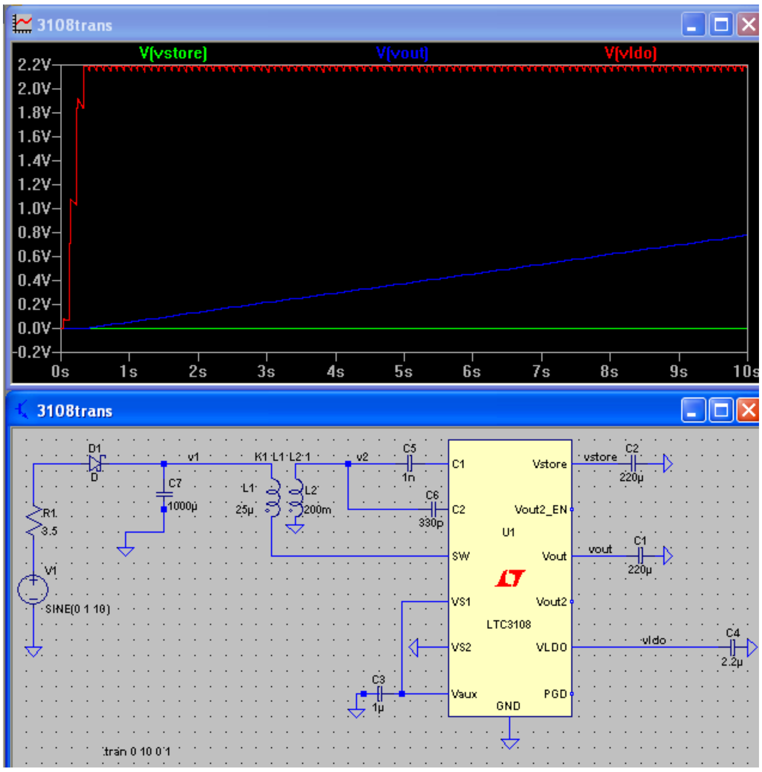

Figure 5.13: Half Wave Rectifier Circuit 5

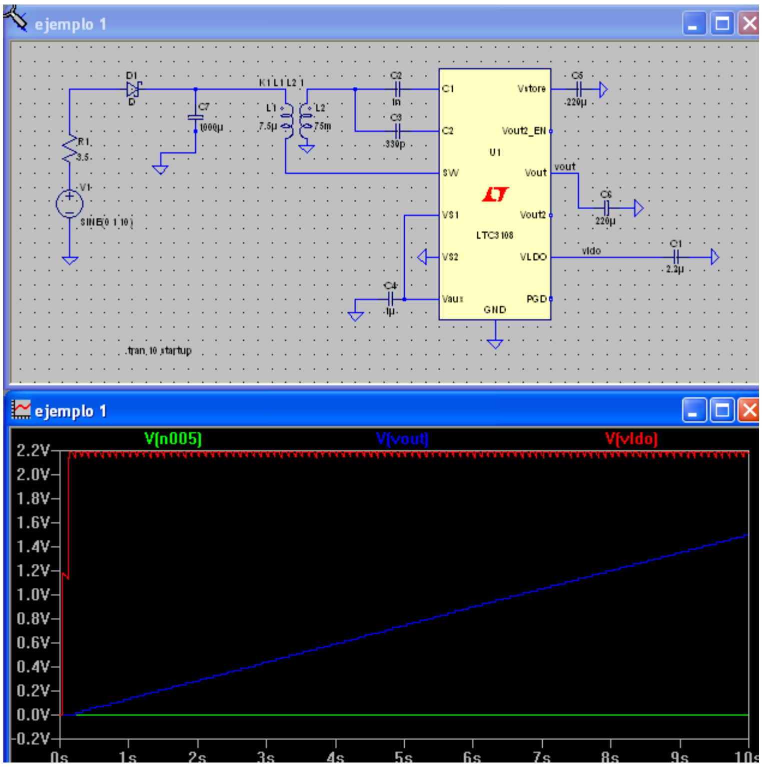

Figure 5.14: Half Wave Rectifier Circuit 4

The rectifier circuit doesn't work well on this IC circuit in 10 second V_{out} doesn't reach the expected 3.3V. Because the operation configuration of the LTC3108 is in Charge Pump and Rectifier mode. So I can conclude that it is not necessary to apply a rectifier circuit, because the IC do this part of the problem.

At this moment I have a good configuration of LTC3108 that can be used for the prototype. I was requested from my tutor to take a look also at LTC3109, so I started some simulation with this IC. In the circuit from Figure 4.24 there was no result on V_{out}. With these simulations of LTC3109 I had big problems due to the duration of the simulations, which took between three or four days to simulate 5 seconds. This is the reason why from this point I only had few simulation of LTC3109.

Then, I realized that i needed to attach a big resistor in the circuit as it is shown on Figure 4.25. Also due to the length of the simulations they were not conducted until 3.3V in V_{out} is obtained, it is understood that when V_{ldo} manages to obtain a high value within a reasonable time, V_{out} will reach the expected value of 3.3V.

	LTC3108 circuit
Transformer ratio	1:100
C_1	2,2 μ F
C_2	1 n F
C_3	470p F
C_4	1 μ F
C_5	10 μ F
C_6	10 μ F

Table 5.2: LTC3108 Values

	LTC3109 circuit
Transformer ratio 1	1:100
Transformer ratio 2	1:100
C_1	1 n F
C_2	470p F
C_3	10 μ F
C_4	10 μ F
C_5	2,2 μ F
C_6	1 μ F
C_7	1 n F
C_8	470 p F
R_2	100M Ω

Table 5.3: LTC3109 Values

5.1 Final Simulation Results

I started to test both IC with different ranges of voltage on the V_{in} and with the values of resistor transformer and capacitor shown in Table 5.2 and 5.3.

5.1.1 Final Simulation Results for LTC3108

Figure 5.15: V_{in} = 0,5V

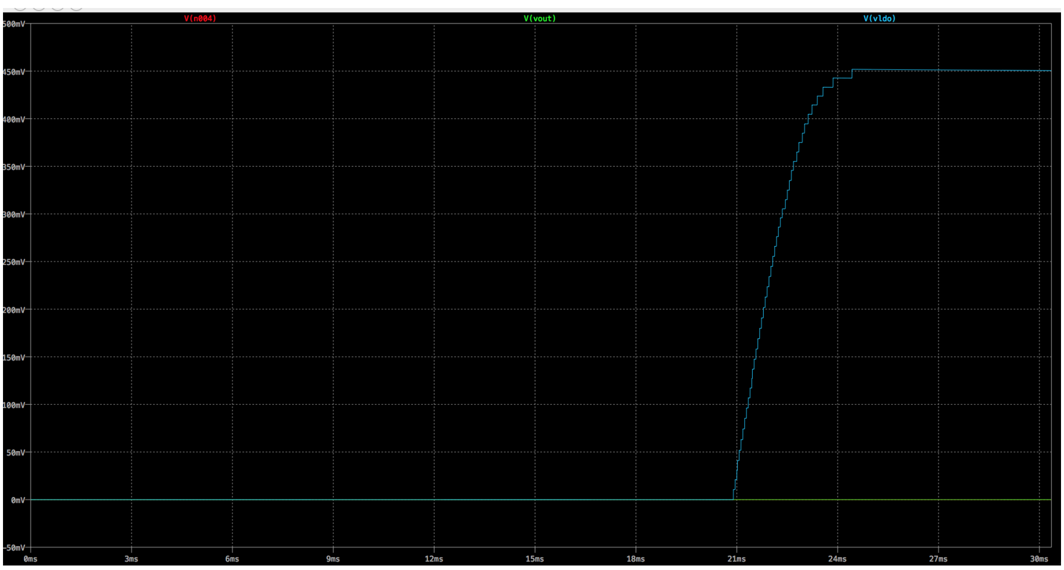

Figure 5.16: V_{in} = 0,3V

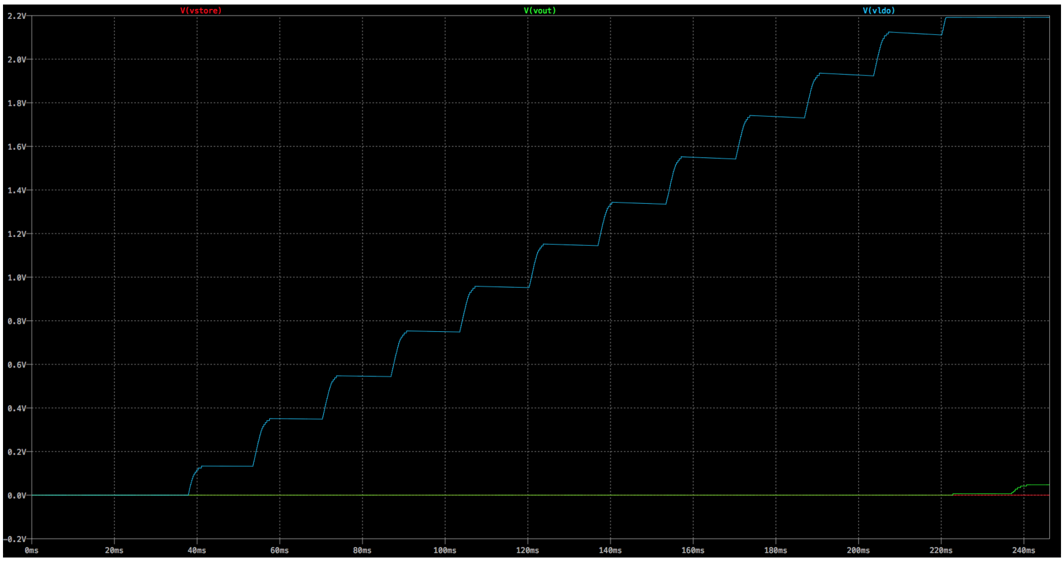

Figure 5.17: V_{in} = 0,2V

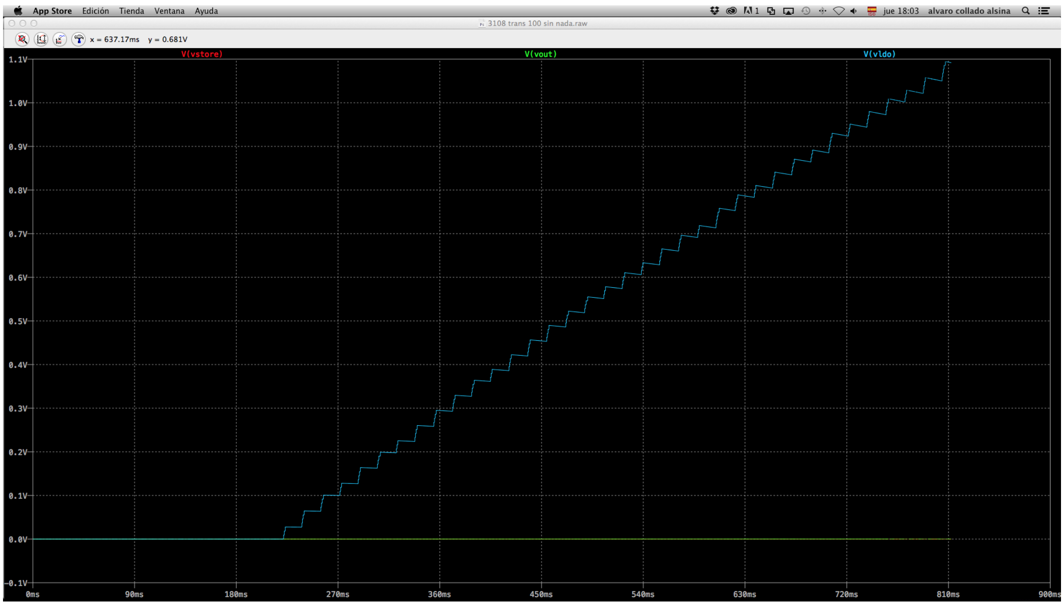

Figure 5.18: V_{in} = 0,1V

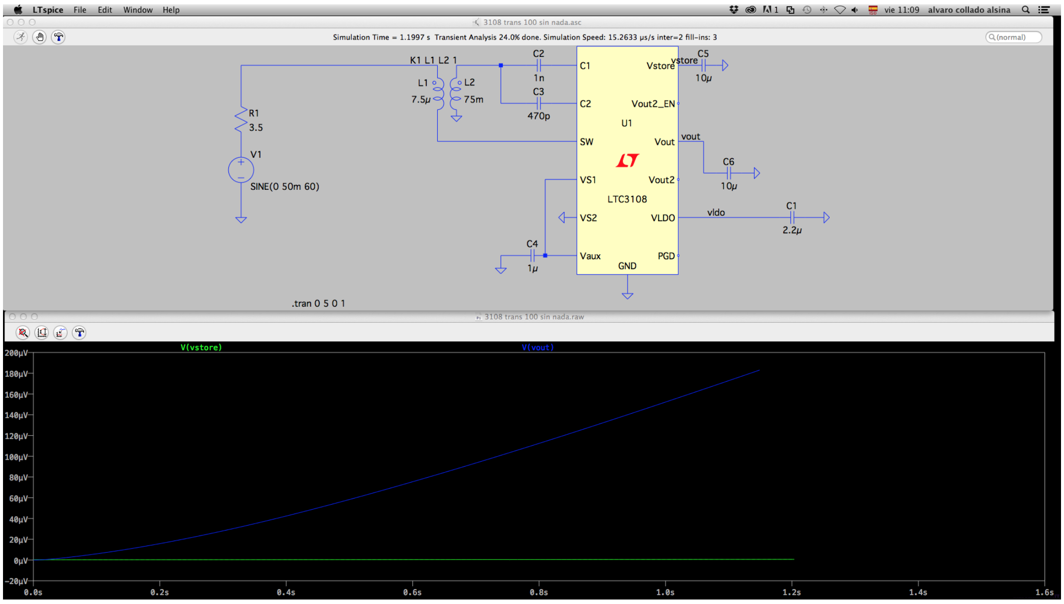

Figure 5.19: V_{in} = 50mV

Due to the duration of the simulation, these figures don't show the V_{out} result but I can guess that from 0.1V to higher value in small period of time V_{out} will get 3.3V. I can conclude that this circuit is valid for simulations in the prototype.

5.1.2 Final Simulation Results for LTC3109

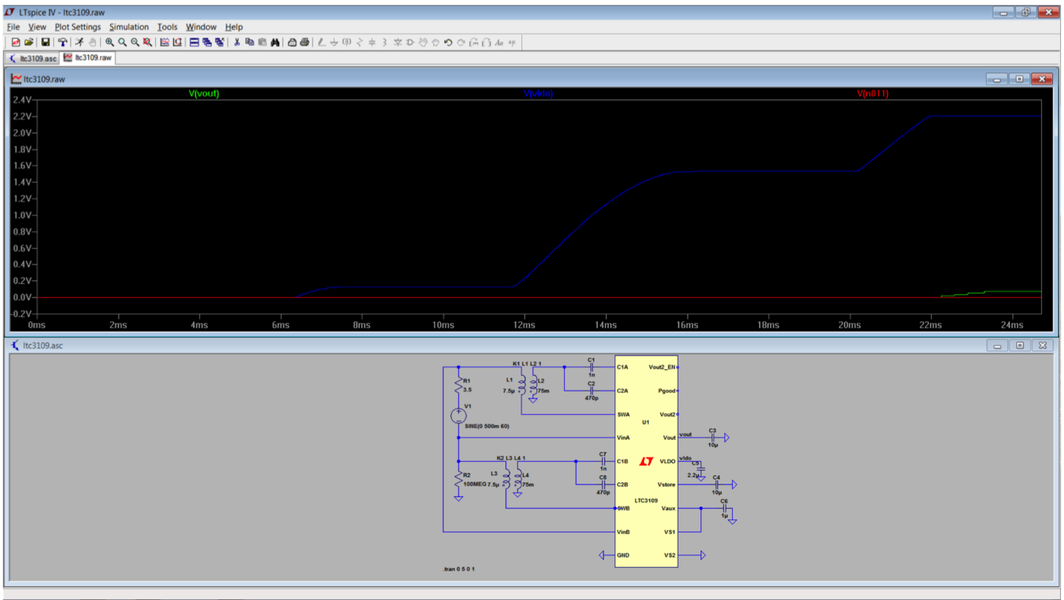

Figure 5.20: V_{in} = 0,5V

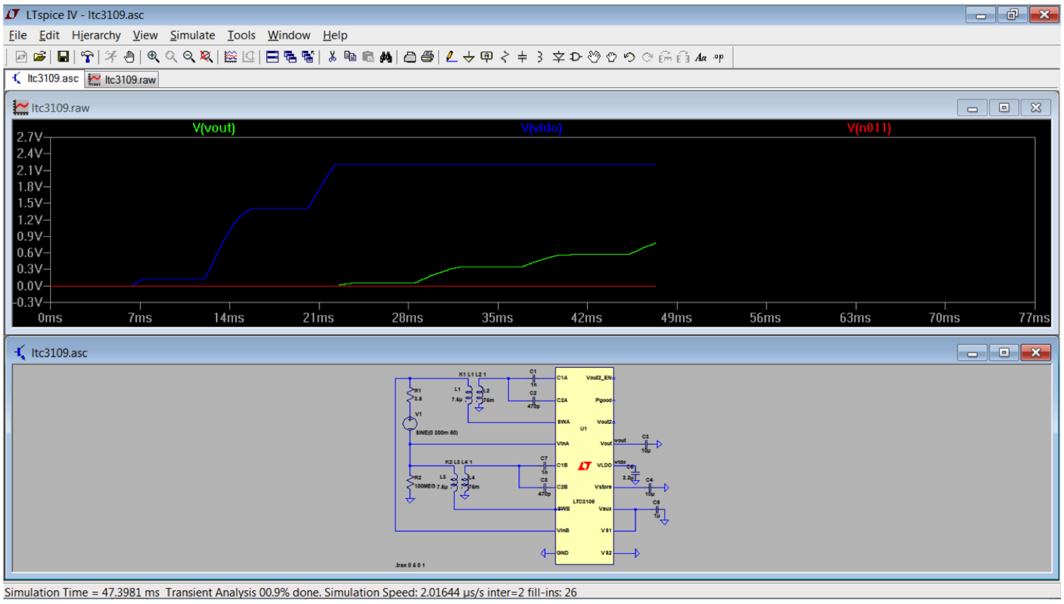

Figure 5.21: V_{in} = 0,3V

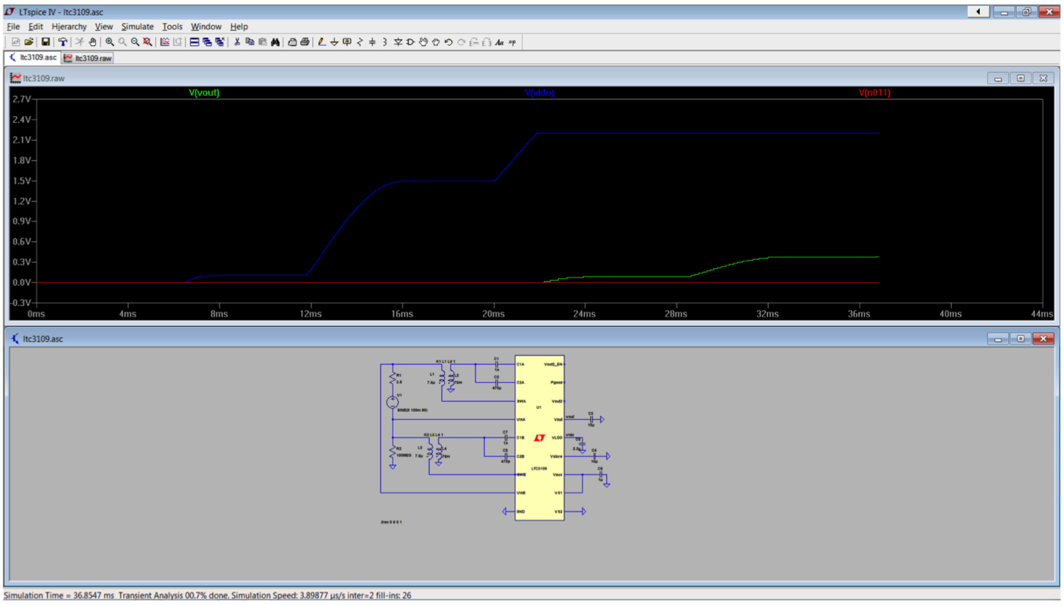

Figure 5.22: V_{in} = 0,1V

Although I have had many problems with simulations due to the time consuming and they were very heavy, I can say that LTC3109 it is a suitable circuit for the target of charging the battery with my prototype.

5.1.3 Circuit welding process

At this moment I know that LTC3109 and also LTC3108 can be suitable for my prototype. So now, I need to weld the IC and transformer to a board with all the values from table 5.2. and 5.3. Figure 4.27 and 4.29 will give us guidance of how the circuit will be welded.

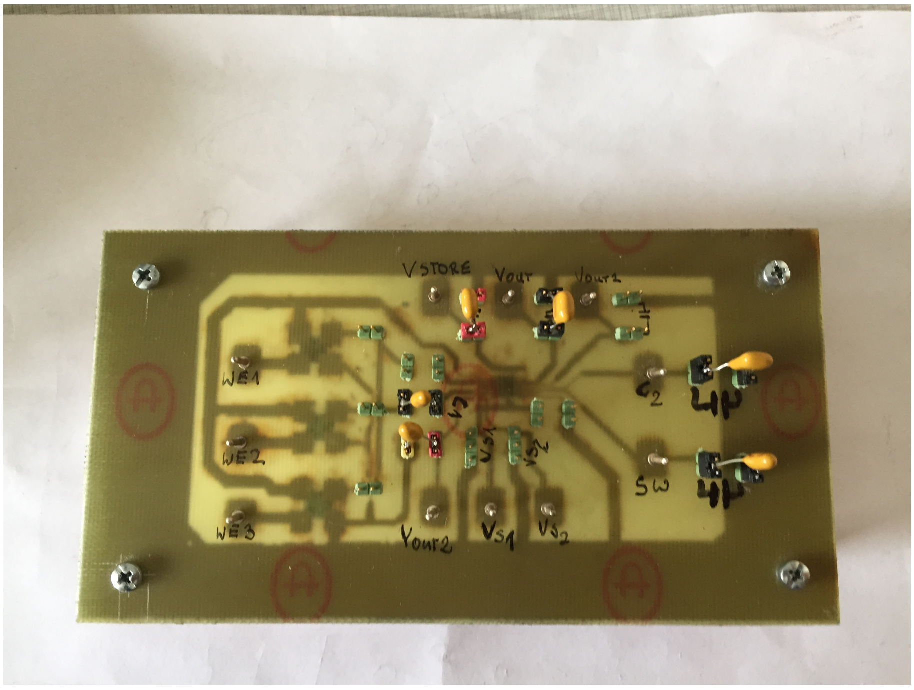

Figure 5.23: Welded Top Board for LTC3108

After some test on the prototype with the two welded board I made. I didn't get a huge difference between LTC3018 and LTC3109. Both of them are suitable for our objective to reach the value to charge a battery. As my tutor had a demo-board from Linear (see Figure 5.26) I decided to test the last part of the project with this demo-board.

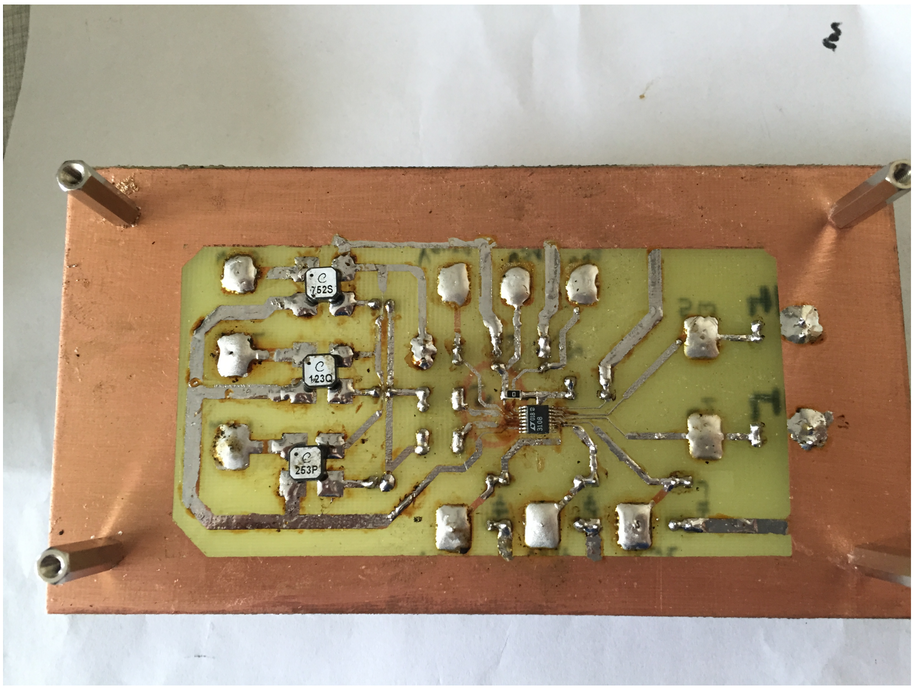

Figure 5.24: Welded Bottom Board for LTC3108

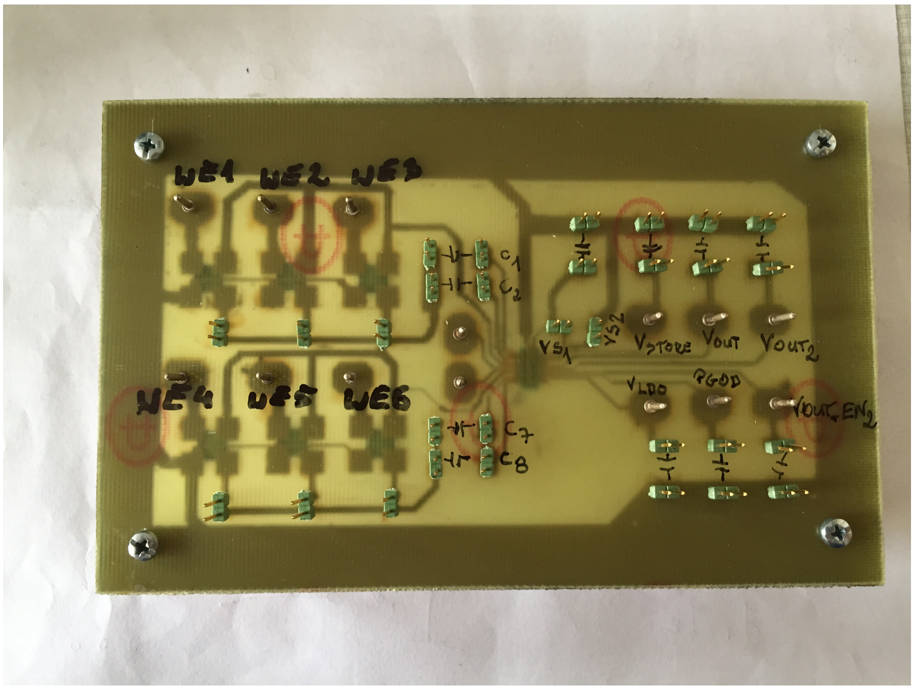

Figure 5.25: Welded Top Board for LTC3109

Figure 5.26: Welded Bottom Board for LTC3109

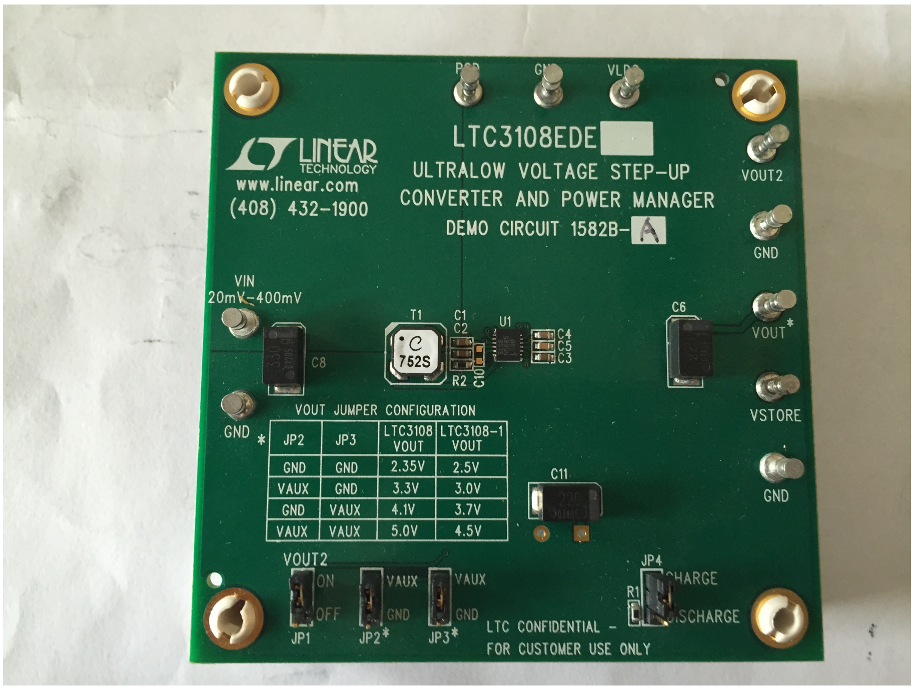

Figure 5.27: Linear Demo-Board

In Figure 5.28 is possible to see how the prototype is connected to the demo-board, to the Multimeter and also to the Power supply (which move the DC motor). So finally, I needed to check that V_{ldo} and V_{out} reach the expected values (Figure 5.27 and 5.28).

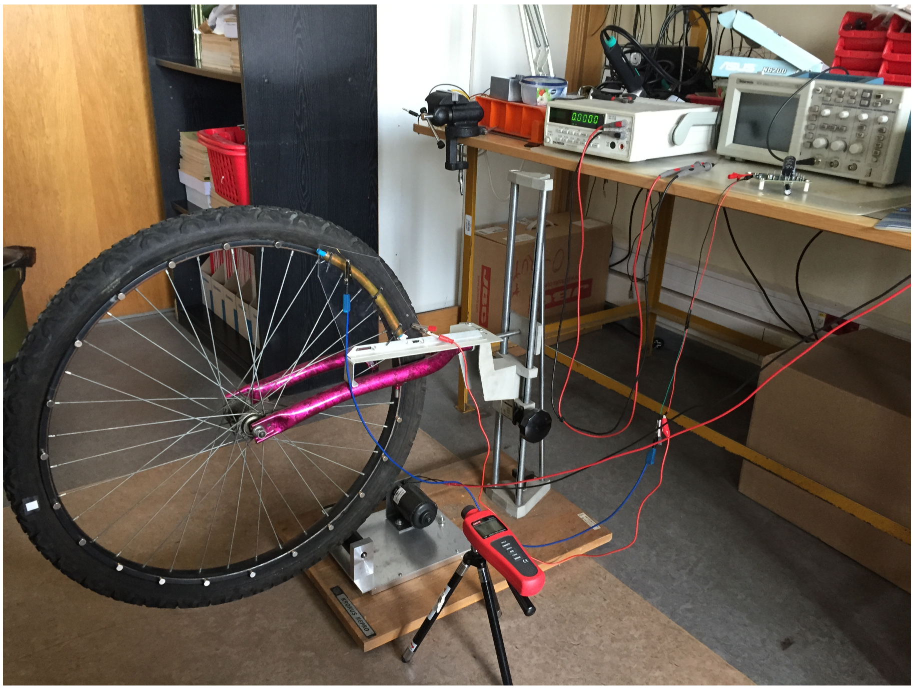

Figure 5.28: Final Laboratory Prototype

After checking the values of V_{ldo} and V_{out}, I apply to V_{store} a capacitor of 1 mili Farads and with the internal capacitor of the demo-board, I have a total capacitance of 1,22 mili Farads. With this capacitor what I get is that V_{store} goes up slower and I will be able to calculate how the speed of the wheel will affect to the V_{store} (see Table 5.4).

Speed	Time
31,79 rpm	484 sec
38,9 rpm	202 sec
43,7 rpm	166 sec
48,73 rpm	150
53,6 rpm	1115 sec
63,31 rpm	101 sec
70,1 rpm	69 sec
75,8 rpm	65 sec
81,8 rpm	55 sec

Table 5.4: Time from 1V to 5V of V_{store}

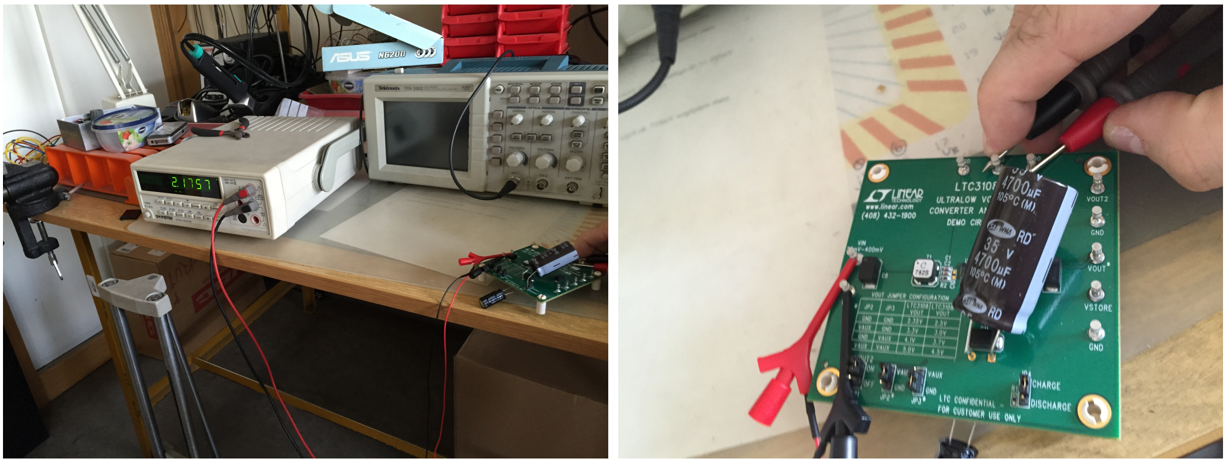

(a) Mutimeter (b) circuit

Figure 5.29: V_{ldo} Value

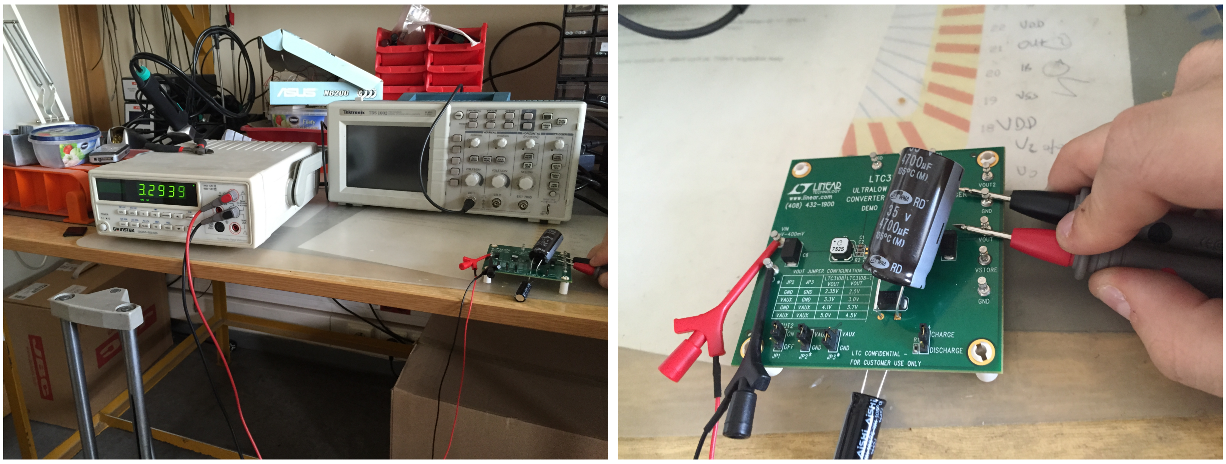

(a) Mutimeter (b) circuit

Figure 5.30: V_{out} Value

Chapter 6

Conclusions

6.1 Achievement of objectives

After all the research about Energy Harvesting, simulation with LTSpice and the subsequent testing of the prototype, it can be said that the objectives have been achieved. Finally the circuit I made reached the expected value for charging the battery at the output.

The time to reach the output value it is not big for a bicycle, it is around 1 second and also the speed is not an impediment to say that the whole prototype fulfills the expectations and objectives of the thesis.

6.2 Application of learning

During this thesis I applied all the knowledge gained during the degree on circuits, which was really useful for the simulation and preparation of the circuit for the prototype. Also it was really useful the knowledge on electromagnetic fields to know how this voltage is created by the coil and magnet and how the specification of the coil and more could change the results on the circuit.

1. Análisis y diseño de circuitos

2. Componentes eléctricos y medidas

3. Electronica analógica

4. Campos electromagnéticos

6.3 Lessons Learned

The most important lesson was to discover what is Energy harvesting, because I had never heard about it before. In my opinion it is a very interesting topic and really useful, that can create such a good things not to waste so much energy.

Also, it was quite new for me all this kind of software related with simulation and I found them very helpful for the realization of my thesis, because they helped me to understand how they worked the circuits and to choose the best option for the final prototype. This choice it was one of the most important part because if i had chosen the wrong IC the whole prototype maybe wouldn't have worked at all.

1. Energy harvesting
2. Circuit design software

6.4 Future works

The two main idea that I have right now after all this thesis are:

First, to attach a real USB port to the circuit and try charging a mobile phone.

Second, put all the prototype and circuit in a real bicycle to test it in a real life mode. Also its possible that there are some kind of different components, even values that can dwarf the whole circuit and can be more suitable for a day to day in a bicycle.

6.5 Personal Ratings

In my opinion I can assure that this thesis has opened my eyes as to renewable energy and green energy. For sure I will continue research in this area, because I find it very attractive for a better future and there are a lot of possibilities with different things not only electromagnetic.

Appendix A

Theoretical Calculation

A.1 Magnetic flux Generated by the Bar Magnet

The bar magnet is modeled as two point magnetic charges situated at $l_m/2$ on the y-axis. The magnitude of the magnetic point charges, q_m, is obtained by integrating the magnetization, μM, over the cross-sectional areas of the magnet ends. Thus,

$$q_m = \mu_o M \pi r_m^2 \tag{A.1}$$

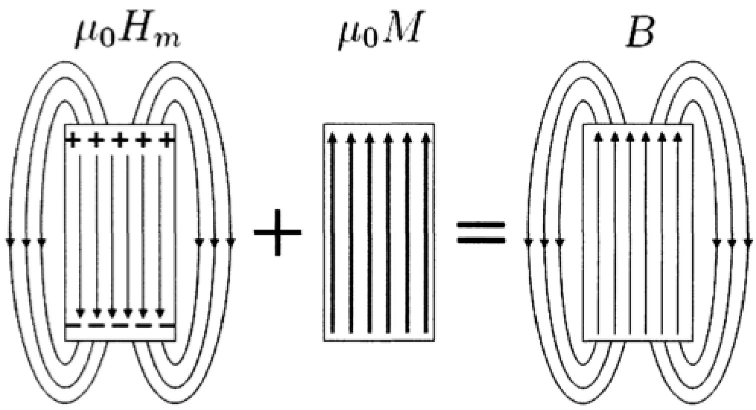

Figure A.1: Magnetic flux density from a bar magnet.

The magnetic flux density at a given point, B, depends on two terms: the magnetic field strength H_m; and the local magnetization. The local magnetization is M inside the magnet and 0 outside. Figure A.1 shows how the contributions from these two terms add up to the magnetic flux density:

$$B = \mu_0(H_m + M) \tag{A.2}$$

As shown in Figure A.1, a bar magnet has a uniform magnetic charge density on its ends at $x = + - l_m/2$. I make the simplifying assumption that the bar magnet can be modeled as two point magnetic charges located on the y-axis at $x = +-l_m/2$. Thus, while the μM term I calculate is exact, the μH term is an approximation because it comes from a point- charge assumption. I will concentrate on the calculation of $\mu_0 H_m$ and then add it to the simple $\mu_0 M$ term towards the end to arrive at B inside the magnet. Outside the magnet the $B = \mu_0 H$ alone.

The total flux emanating from the magnetic charge is q_m. The resultant flux through any given turn of wire is the fraction of the total flux that passes through the area enclosed by the wire turn; and this flux is numerically equal to the same fraction of q_n. If a sphere is imagined around the point charge, and a single wire turn intersects the sphere to delineate a spherical cap (Figure A.2),

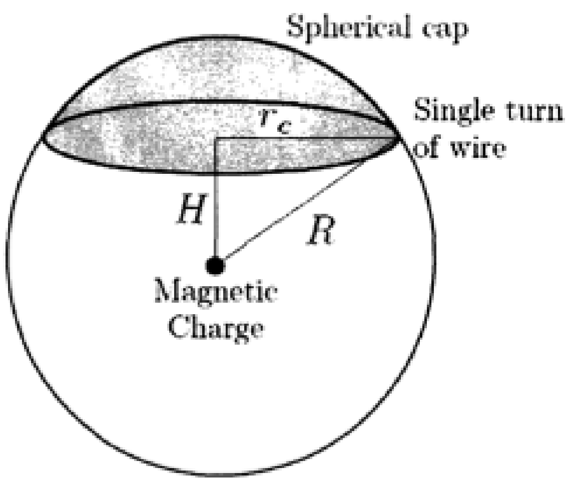

Figure A.2: Point charge and single wire turn geometry

then it follows from Gauss' Law that the magnetic flux through the wire turn is equal to the magnetic flux escaping through the cap. Thus, the magnetic flux through the wire turn is proportional to the ratio of the surface area of the cap to the surface area of the entire sphere. For a sphere of radius R, with a distance H from its center to the plane of the coil, the surface area of the cap formed is

$$A_{cap} = 2\pi R(R - H) \tag{A.3}$$

Therefore, the magnetic flux through a single wire turn of radius r_c at a height H above a point charge q_m is given by

$$\phi = q_m 2\pi R(R - H)/4\pi R^2 \tag{A.4}$$

The magnetic flux through a wire turn in the induction system depends on contributions from the magnetic charges at both ends of the bar magnet. The labeled geometry of the magnetic charges and a single wire turn is shown in Figure A.3. The magnetic charges have opposite signs to represent the North and South poles of the magnet, with q_1 positive and q_2 negative. In addition, the direction of the magnetic flux through the wire turn changes when a magnetic charge passes from one side of the wire turn to the other. Sign functions are added to Equation A.4 to account for these changes in the magnetic flux directions. The magnetic flux contributions and from the magnetic charges ϕ_1 and ϕ_2 respectively are

$$\phi_1 = sign(h - \frac{l_m}{2})\frac{-q_m(\sqrt{r_c^2 + (h - \frac{l_m}{2})^2} - |h - \frac{l_m}{2}|)}{2\sqrt{r_c^2 + (h - \frac{l_m}{2})^2}} \tag{A.5}$$

$$\phi_2 = sign(h + \frac{l_m}{2})\frac{q_m(\sqrt{r_c^2 + (h + \frac{l_m}{2})^2} - |h + \frac{l_m}{2}|)}{2\sqrt{r_c^2 + (h + \frac{l_m}{2})^2}} \tag{A.6}$$

ϕ_1 and ϕ_2 are the fluxes from the point charges at the ends of the bar magnet; when they are divided by the area of the wire turn, they sum up to the $\mu_0 H_m$ component of B. In addition, there is magnetic flux inside the bar magnet due to its magnetization; the magnitude of this flux is $\mu_0 M \pi r_m^2$, which from Equation A.1 is equal to q_m. Therefore the

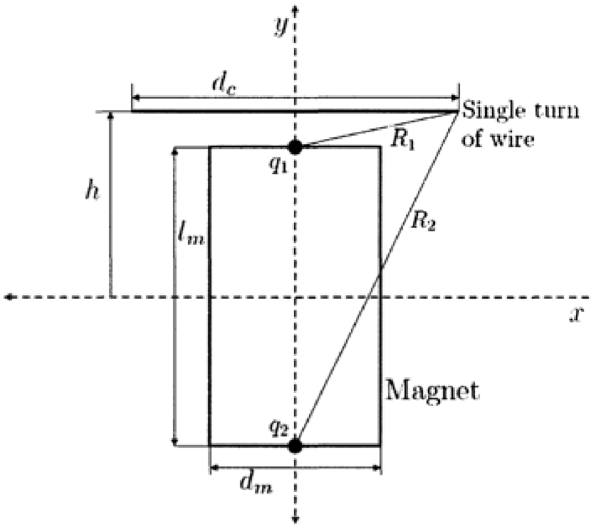

Figure A.3: Magnetic dipole and single wire turn geometry.

flux due to μ_0; term can be expressed as:

$$\phi_M = \begin{cases} q_m \quad si \quad -l_m/2 < y < l_m/2 \\ \\ 0 \quad si \quad y < -l_m/2 U l_m/2 < y \end{cases} \tag{A.7}$$

The total magnetic flux through a single wire turn at height h is the sum of ϕ_1, ϕ_2 and ϕ_M from Equation A.5 , A.6 and A.7 respectively. This sum is multiplied by the number of turns of wire per unit height, N/l_c, and a small incremental height, dy, to obtain the magnetic flux through all the wires coiled at height h. The total magnetic flux through the coil of length l_c is the integral of the magnetic flux over the height of the coil:

$$\phi_{Total} = \int_h^{h+l_c} \frac{N(\phi_1 + \phi_2 + \phi_M)}{l_c} d_y \tag{A.8}$$

A.1.1 Coil Inductance and Resistance

The inductance of the coil, L_C, is a function of the number of turns, cross-sectional area, and height of the coil. The inductance for a long thin coil, where $l_c > \sqrt{A_c}$, is given by:

$$L_c = \frac{\mu_0 N^2 A_c}{l_c} = \frac{\mu_0 \pi N^2 r_c^2}{l_c} \tag{A.9}$$

The resistance of the coil, R_c, depends on the resistivity of the wire material, ρ, the length of the coiled wire, I_w,, and the cross-sectional area of the wire, A_w,. If the radius of the wire is r_w, I have

$$l_w = N\pi d_c \tag{A.10}$$

$$A_w = \pi r_w^2 \tag{A.11}$$

$$R_c = \frac{\rho l_w}{A_w} = \frac{\rho(N2\pi r_c}{\pi r_c^2} = \frac{2N\rho r_c}{r_w^2} \tag{A.12}$$

If $R_c >> 2\pi f L_C$, the effects of the system inductance are negligible in comparison to those of the system resistance. Since this relation often holds true in real systems, the subsequent analysis assumes that the resistance effects dominate the system

A.2 Voltage and Power Generation

Faraday's Law states that the open-circuit voltage induced across a turn of wire is the negative integral of the time-change in magnetic flux over the cross-sectional area of the turn. By the chain rule of differentiation, the time-change in magnetic flux can be separated into two multiplicative terms - the change in magnetic flux over height, and the change in coil height over time (in other words, the velocity of the coil). Thus,

$$V = \int \frac{d\phi_total)}{dt} d_A = \int \frac{d\phi_total)}{dh} \frac{dh)}{dt} d_A \tag{A.13}$$

The formula for $\frac{d\phi_total)}{dh}$ can be calculated by differentiating Equation A.8 to arrive at

$$\frac{d\phi_total}{dh} = \frac{d}{dh} \int_h^{h+l_c} \frac{N(\phi_1 + \phi_2)}{l_c} d_h \tag{A.14}$$

Given the velocity of the coil, v, the open-circuit voltage induced across the coil can be calculated:

$$V = \int_h^{h+l_c} \frac{vN(\phi_1 + \phi_2)}{l_c} d_A \tag{A.15}$$

P is the power delivered by the system to a load, modeled here as a resistor R_I. Since the system inductance is assumed to be negligible, the open-circuit voltage generated across the ends of the coil is now applied across the resistances R_c, and R_L in series. Then, Kirchhoff's Voltage Law implies that

$$V = V_c + V_L \tag{A.16}$$

where V_c, and V_L are the voltages across the coil and load resistor respectively. I is the resultant current flowing through the circuit. Ohm's Law states that the voltage across a resistor is the product of the resistance and the current flowing through it; applying this to Equation A.16 allows us to solve for the value of I:

$$V = I(R_C + R_L) \tag{A.17}$$

$$I = \frac{V}{(R_C + R_L)} \tag{A.18}$$

The instantaneous power dissipated across the load resistance is the product of the current flowing through it and the voltage across it. This gives

$$P = V_l I = (R_l I^2) \tag{A.19}$$

and substituting the value for I from Equation A.18,

$$P = \frac{R_L V^2}{(R_C + R_L)^2} \tag{A.20}$$

Since R_L is fixed, I differentiate P with respect to R_L to find the maximum:

$$\frac{dP}{dR_l} = \frac{V^2}{(R_c + R_l)^2} - \frac{2R_l V^2}{(R_c + R_l)^3} = 0; (R_c + R_l) - 2R_l = 0; R_l = R_c \tag{A.21}$$

Hence, the load resistance should be matched to the coil resistance in order to extract the maximum possible power from the system.

A.2.1 Magnetic Field Generated by the Magnets

Within the system with magnets, there are two regions: Region A, between $x = 0$ and $x = X_A$, with the magnets; and Region B, between $x = 0$ and $x = -X_B$, with the air gap and coils. These regions have distinct magnetic fields, H_A and H_B respectively. The interface between the magnetic region and the air gap provides the boundary conditions on the fields in these two regions. The x-axis is defined such that $x = 0$ at the interface between the magnets and air. The magnetic charge is concentrated on the planes at the ends of the magnets at $x = 0$. The magnetic charge density on the z-axis is represented by $\phi_M(z)$. Figure A.4 shows a schematic of the magnet placement and the resulting graph of $\phi_M(z)$ as a function of z. The charge density function from Figure A.4 can be represented by a Fourier series. Then I can solve for the magnetic field caused by a sine wave charge distribution, and use superposition to get the total field.

The charge density waveform can be represented by

$$\sigma_M = a_{0(\phi_M} + \sum_{k=1}^{\infty}(a_{k(\phi M)}cos(\frac{2\pi kz}{Z}) + b_{k(\phi M)}sin(\frac{2\pi kz}{Z})) \tag{A.22}$$

where Z is the spatial period of the magnetic charge density function and the Fourier coefficients are:

$$a_{0(\sigma_M)} = 0 \tag{A.23}$$

$$a_{k(\sigma_M)} = 0 \tag{A.24}$$

$$b_{k(\sigma_M)} = \begin{cases} \frac{4|sigma_{max}}{k\pi} cos\frac{\pi kd}{l+2d} & si \quad \text{for odd k.} \\ \\ 0 & si \quad \text{for even k.} \end{cases} \tag{A.25}$$

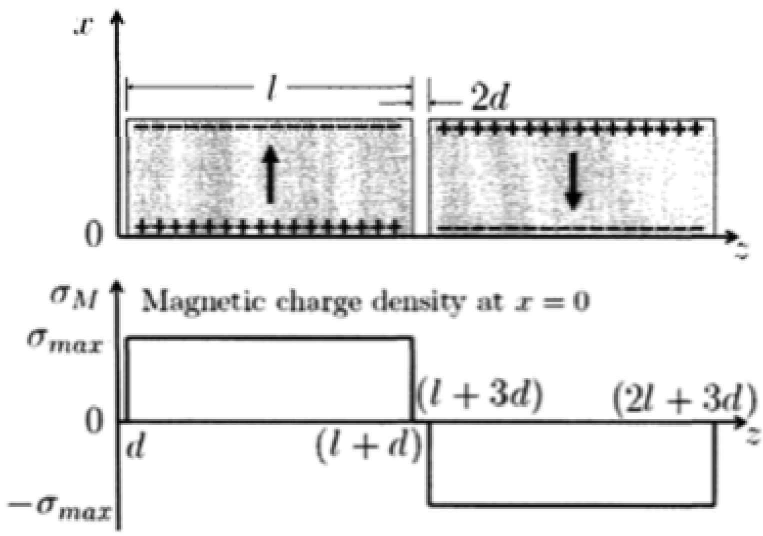

Figure A.4: Schematic of the magnet placement and the resulting charge density on the z-axis.

Since the magnetic charge density waveform is reducible to a sum of sines, I solve for the magnetic fields resulting from a sinusoidal charge density ($\sigma_{Mk} = b_{k(\sigma_M)} sin(\frac{2\pi kz}{Z})$) on the z-axis. For a system with current J, Maxwell's Equations state that:

$$\nabla \times H = J \tag{A.26}$$

$$\nabla * B = 0 \tag{A.27}$$

Since I are solving the part of the superposition that only considers the fields due to the magnets, there is no current in the system and J in Equation A.26 is zero. This means that the curl of H is zero, which implies that H is the negative gradient of some scalar magnetic potential function ψ.

$$\nabla \times H = 0 \tag{A.28}$$

$$\Rightarrow H = -\nabla_{\psi} \tag{A.29}$$

From Equations A.2, A.27, A.28 and A.29 I get

$$\nabla * \mu(-a\nabla\psi + M) = 0 \tag{A.30}$$

Because the magnetization M of a magnet is a constant, and M of air is zero, in both cases $\nabla * M$ vanishes. Thus I get the simplified equation

$$\nabla^2 \psi = 0 \tag{A.31}$$

This equation must be solved for regions A and B to obtain the corresponding magnetic potentials (ψA and ψB) in those regions. To satisfy Equation A.31, the solutions must be of the form $\psi_A = [\alpha_1 sin\frac{2\pi kz}{Z} + \alpha_2 cos\frac{2\pi kz}{Z}]x[\alpha_3 sinh\frac{2\pi kz}{Z} + \alpha_4 cosh\frac{2\pi kz}{Z}]$ $\psi_B = [\beta_1 sin\frac{2\pi kz}{Z} + \beta_2 cos\frac{2\pi kz}{Z}]x[\beta_3 sinh\frac{2\pi kz}{Z} + \beta_4 cosh\frac{2\pi kz}{Z}]$

The values of the constants in these equations are obtained by applying the boundary conditions on the regions. The first two boundary conditions arise at the interfaces with the magnetically permeable backings at $x = x_A$ and $x = -x_B$. Given the absence of surface currents at these interfaces, the tangential magnetic field, H_z is conserved.

I have assumed that the materials have $\mu = \infty$; therefore $B = \mu H$ dictates that $H = 0$ in order for B to be finite. Since $H = 0$, the tangential field H_z must be zero at these interfaces. The interface between the magnets and air at $x = 0$ is considered next. The conservation of the tangential magnetic field, Hz, (given the absence of surface currents at x = 0), and the conservation of the normal magnetic flux, B_x, yield two more boundary conditions for the system. In conclusion, the boundary conditions applicable are :

1. $H_{A_z} = 0$ at $x = x_A$
2. $H_{B_Z} = 0$ at $x = -x_B$.
3. $H_{A_z} = H_{B_z}$ at $x = 0$
4. $\mu_0 H_{A_z} = H_{B_z}$ at $x = 0$

Solving for the values of the constants is now a matter of algebraic manipulation. Boundary conditions (1) and (2) state that H_{A_z} and H_{B_z}, are zero-valued at x_A and $-x_B$ respectively. H_{A_z} and H_{B_z}, are the partial derivatives of $-\psi_A$ and ψ_B with respect to z, so for them to be zero at x_A and $-x_B$ respectively, the x-dependent components of $-\psi_A$ and ψ_B must be zero.

This means that the x-dependent components of the magnetic potentials must be sinh functions, since cosh functions cannot be zero-valued at any points. This means that the constants α_2, α_4 , β_2 and β_4 are zero. Constants α_1 and α_3 can be combined into α, and

β_1 and β_3 into β.

$$\psi_A = \alpha sin(\frac{2\pi kz}{Z})sinh(\frac{2\pi(x - x_A)}{Z}) \tag{A.32}$$

$$\psi_B = \beta sin(\frac{2\pi kz}{Z})sinh(\frac{2\pi(x + x_B)}{Z}) \tag{A.33}$$

Now I have two equations (boundary conditions (3) and (4)) and two unknowns (the values of the two constants α and β); the following steps show the rearrangement of variables to arrive at the answer.

$$\alpha = \frac{b_{k(\alpha_M)}sinh(\frac{2\pi kzx_B}{Z})}{\frac{2\pi kz\mu_0}{Z}(sinh(\frac{2\pi kzx_A}{Z})cosh(\frac{2\pi kzx_B}{Z}) + sinh(\frac{2\pi kzx_B}{Z})cosh(\frac{2\pi kzx_A}{Z}))} \tag{A.34}$$

$$\beta = \frac{-b_{k(\alpha_M)}sinh(\frac{2\pi kzx_A}{Z})}{\frac{2\pi kz\mu_0}{Z}(sinh(\frac{2\pi kzx_A}{Z})cosh(\frac{2\pi kzx_B}{Z}) + sinh(\frac{2\pi kzx_B}{Z})cosh(\frac{2\pi kzx_A}{Z}))} \tag{A.35}$$

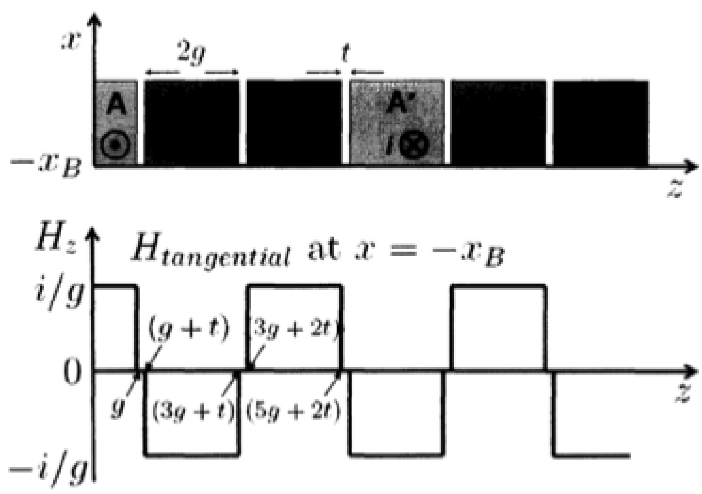

Figure A.5: Schematic of the coil placement and the tangential magnetic field at $-x_B$ resulting from current i flowing through all three phases of coils.

From equations A.22, A.32 and A.33, the total magnetic potential due to the magnets is :

$$\psi_{A_{(magnets)}} = \sum_{k=1}^{\infty} \alpha sinh(\frac{2\pi k(x - x_A)}{2(l+2d)}) sin(\frac{2\pi kz}{2(l+2d)}) \tag{A.36}$$

$$\psi_{B_{(magnets)}} = \sum_{k=1}^{\infty} \beta sinh(\frac{2\pi k(x + x_B)}{2(l+2d)}) sin(\frac{2\pi kz}{2(l+2d)}) \tag{A.37}$$

A.2.2 Magnetic Field Generated by Coil Current

For the calculation of the fields due to current flowing through the coils, the magnets are ignored. The current through the coils is approximated as a surface current at $x = -x_B$. This means that there is no difference between Region A and Region B for this calculation. Thus I solve for the magnetic fields from the coils in the region bounded by x_A and $-x_B$. Figure A.5 shows a graph of the tangential magnetic field H_z, at $-x_B$ that would result from a current i flowing through all three phases of coils.

The tangential magnetic field at the surface of the magnetic backing is the sum of the contributions from the three phases A, B and C. The width of each phase is $2g$, and the gap between phases is t. Since the three phases are symmetric, I can solve for one phase and then use superposition to add in the effects from the other two phases. In particular, I will solve for the contribution from current i flowing through the phase A coils. The tangential magnetic field, H_z, at plane $x = -x_B$, due to the current i passing through the phase A coils, can be expressed as

$$H_z = a_{0(H_z)} + \sum_{k=1}^{\infty} [a_{k(H_z)} cos(\frac{2\pi kz}{Z}) + b_{k(H_z)} sin(\frac{2\pi kz}{Z})] \tag{A.38}$$

where Z, the spatial period of the tangential magnetic field function, is 6(2g + t), and the Fourier coefficients are

$$a_{0(H_z)} = 0 \tag{A.39}$$

$$a_{k(H_z)} = \begin{cases} \frac{4i}{gk\pi} sin(\frac{\pi kg}{3(2t+g)}) & \text{for odd k} \\ \\ 0 & \text{for even k} \end{cases} \tag{A.40}$$

$$b_{k(H_z)} = 0 \tag{A.41}$$

Since Hz can be expressed as a sum of cosines, I can solve for the contribution from a single harmonic ($H_{zk} = a_{k(Hz)} cos(\frac{2\pi kz}{Z})$ and then use superposition to obtain the complete solution. Similarly to the case of the magnets, the boundary conditions on the magnetic field due to coil current are:

1. $H_z = 0$ at $x = x_A$
2. $H_z = a_{k(Hz)} cos(\frac{2\pi kz}{Z})$ at $x = -x_B$.

Within the region, similar to the case with the magnets,

$\nabla \times H = 0 \Rightarrow H = -\nabla\psi \Rightarrow \nabla^2\psi = 0$

The solution of this equation is the magnetic potential (0) due to the current in the coils, and must be of the form

$\psi = [D_1 sin(\frac{}{2\pi kz} Z) + D_2 cos(\frac{}{2\pi kz} Z)] \times [D_3 sinh(\frac{}{2\pi kx} Z) + D_4 cosh(\frac{}{2\pi kx} Z)]$.

Since boundary condition (1) states that H_z, must be zero at x_A, the x-dependent component of the magnetic potential must be a sinh function.

$\psi = Dsin(\frac{2\pi kz}{Z}) sinh(\frac{2\pi k(x-x_A)}{Z})$

$\Rightarrow H_z \mid_{x=x_A} = -\frac{2\pi kD}{Z} cos(\frac{2\pi kz}{Z}) sinh(\frac{2\pi k(x-x_A)}{Z}) \mid_{x=x_A} = 0$

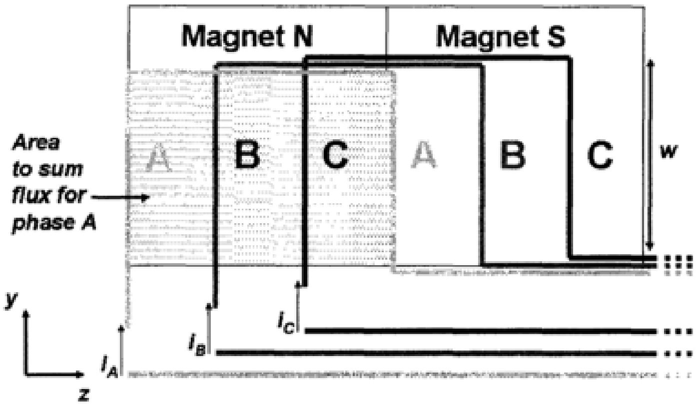

Figure A.6: Three-phase coil arrangement geometry.

From boundary condition (2), H_z is $a_{k(H_z)}cos(\frac{2\pi kz}{Z})$ at $-x_B$.

$$H_z \mid_{x=-x_B} = -\frac{2\pi kD}{Z}cos(\frac{2\pi kz}{Z})sinh(\frac{2\pi k(x-x_A)}{Z}) \mid_{x=x_A} = a_{k(H_z)}cos(\frac{2\pi kz}{Z})$$
$$D = \frac{a_{k(H_z)}Z}{2\pi k sinh(\frac{2\pi k(x_A+x_B)}{Z})} \tag{A.42}$$

$$\psi_{coils} = \sum_{k=1}^{\infty} Dsinh(\frac{2\pi k(x-x_A)}{6(2g+t)})sin(\frac{2\pi kz}{6(2g+t)}) \tag{A.43}$$

A.2.3 Coil Self-Inductance, Mutual Inductance, and Resistance

Equation A.43 allows us to calculate the magnetic potential created by the flow of current through the coils; the magnetic flux density generated can be obtained from this magnetic potential.

$B_{coils} = \mu_0 H_{coils} = -\mu_0 \nabla \psi_{coils}$

The magnetic fluxes through the coils due to current through them are $\lambda_{c(A)}$, $\lambda_{c(B)}$ and $\lambda_{c(C)}$ through phase A, B and C respectively, and can be calculated by multiplying the magnetic flux density and the area of the coils. Figure A.6 shows the geometry of the three phases. For example, the magnetic flux through phase A coils is:

$\lambda_{c(A)} = B_{coils} \cdot A_A$

where A_A is the area of the phase A coils. Since the coils lie in the $x = -x_B$ plane, only he x-component of the magnetic flux density will pass through them; hence $B_{coils}\Delta A_A = B_{x(coils)}A_A$.

The self-inductance, L, of a coil is defined as the magnetic flux generated through the coil due to the flow of a unit current through it. The mutual inductance between a pair of coils, M, is defined as the magnetic flux generated through one coil due to the flow of a unit current through the other. The magnetic flux through each phase is influenced by the current flowing through every phase. Since everything is symmetric across phases, the self-inductance of each phase and the mutual inductance between each pair of phases is the same. Equation defines the dependence of the magnetic fluxes and the current through the coils.

$$\begin{bmatrix} \lambda_{c(A)} \\ \lambda_{c(B)} \\ \lambda_{c(C)} \end{bmatrix} = \begin{bmatrix} L & -M & -M \\ -M & L & -M \\ -M & -M & L \end{bmatrix} \begin{bmatrix} i_A \\ i_B \\ i_C \end{bmatrix} \tag{A.44}$$

To calculate the value of L and M, I consider the flux linked by a phase A coil and a phase B coil due to a current i flowing through the phase A coil (when i_B and i_C are 0):

$\lambda_{c(A)} = B_{x(coils)}A_A = nN \int \frac{-l}{2}\frac{l}{2}\mu_0 H_{x(coils)} w dz = Li$

$\lambda_{c(B)} = B_{x(coils)}A_B = nN \int \frac{2g+t-l}{2}\frac{2g+t+l}{2}\mu_0 H_{x(coils)} w dz = Li$

The integrals are the flux through one coil and one turn of wire; to get the total flux they are multiplied by the number of coils (which should be the same as the number of magnetic poles, n), and the number of turns of wire (N) in each coil. The turns of wire in the coil are approximated into a point-wise lumped distribution; therefore I just multiply by the number of wire turns instead of integrating over the physical width of the turns ($2g$ for each phase). Rearranging the terms, I get:

$$L = \frac{nN}{i} \int \frac{-l}{2} \frac{l}{2} \mu_0 H_{x(coils)} w dz. \tag{A.45}$$

$$M = \frac{nN}{i} \int \frac{-l}{2} \frac{l}{2} \mu_0 H_{x(coils)} w dz. \tag{A.46}$$

Since $H_{x(coils)}$ as a function of i can be calculated from Equation A-43, the values of L and M can be found.

The resistance of all the coil phases should be the same since they are the same pattern displaced in space. The resistance of each phase depends on the resistivity of the wire material, ρW, the cross-sectional area of the wire, A_W, and the total length of the wire, l_w. The length of wire used will depend on the number of turns of wire and on the pattern of winding.

$$R = \frac{\rho_w l_w}{A_w} \tag{A.47}$$

A.2.4 Voltage and Power Generation

The magnetic fields in the system are linear; therefore superposition can be used and the total magnetic field is the sum of the magnetic fields from the magnets and the coils.

$$H_{total} = \begin{cases} -\nabla(\psi_{A(magnets)} + \psi_{coils}) & 0 \leqslant x \leqslant x_A \\ \\ -\nabla(\psi_{B(coils)} + \psi_{magnets}) & 0 \geqslant x \geqslant -x_B \end{cases} \quad B_{total} = \mu H_{total}. \tag{A.48}$$

The magnetic fluxes through the coils due to the magnets,$\lambda_{m(A)}$, $\lambda_{m(B)}$) and $\lambda_{m(C)}$ through phases A, B and C respectively, are calculated by multiplying the magnetic flux density and the area of the coils.

$$\begin{bmatrix} \lambda_{m(A)} \\ \lambda_{m(B)} \\ \lambda_{m(C)} \end{bmatrix} = \begin{bmatrix} B_{x(magnets)}A_A \\ B_{x(magnets)}A_B \\ B_{x(magnets)}A_C \end{bmatrix} \tag{A.49}$$

By superposition, the total magnetic flux through the coils is the sum of the fluxes generated by the magnets and by the flow of current through the coils.

$$\begin{bmatrix} \lambda_A \\ \lambda_B \\ \lambda_C \end{bmatrix} = \begin{bmatrix} \lambda_{c(A)} \\ \lambda_{c(B)} \\ \lambda_{c(C)} \end{bmatrix} + \begin{bmatrix} \lambda_{m(A)} \\ \lambda_{m(B)} \\ \lambda_{m(C)} \end{bmatrix} = \begin{bmatrix} L & -M & -M \\ -M & L & -M \\ -M & -M & L \end{bmatrix} \begin{bmatrix} i_A \\ i_B \\ i_C \end{bmatrix} + \begin{bmatrix} B_{x(magnets)}A_A \\ B_{x(magnets)}A_B \\ B_{x(magnets)}A_C \end{bmatrix} \tag{A.50}$$

In order for these equations to hold true, it is important that the magnetic backing of the coils does not saturate due to the magnetic flux through it. Figure A.7 shows the path of the flux through the magnetically permeable backings. $B \cdot A$ should be calculated for the area under half a magnet, and should be equated to $B_{new} \cdot A_{new}$, where A_{new} is the cross-sectional area of the magnetic backing through which the flux will pass. A BH chart of the backing material should be consulted to confirm that B_{new} will not cause it to saturate. A similar check should be conducted for the backing of the magnets.

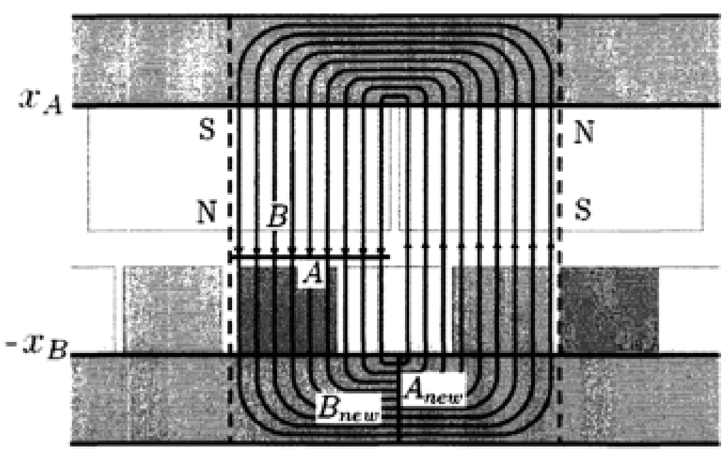

Figure A.7: Path of the magnetic flux in a magnet-across-coils system.

Faraday's law is invoked again in order to calculate the voltage generated across the coils. λ_A, λ_B and λ_C are known as a function of position, so $\frac{d\lambda}{dz}$ can be calculated for each phase. These values, when multiplied by the velocity of the coil ($\frac{dz}{dt}$) , give $\frac{d\lambda}{dt}$ for each respective phrase. Since the phases are identical except for a displacement in space, the voltage through them will be identical except displaced in time.

$$\frac{d}{dt}\begin{bmatrix}\lambda_A\\ \lambda_B\\ \lambda_C\end{bmatrix} = \begin{bmatrix}V_A\\ V_B\\ V_C\end{bmatrix} - \begin{bmatrix}R & 0 & 0\\ 0 & R & 0\\ 0 & 0 & R\end{bmatrix}\begin{bmatrix}i_A\\ i_B\\ i_C\end{bmatrix} \tag{A.51}$$

Equations A.50 and A.51 give us a system of 9 equations and 9 variables: the variables are the magnetic fluxes, currents, and voltages for the three phases; the resistance, self-inductance, and mutual inductance of the coils are known.

Now that I can solve for the output voltage of the system, I consider the dissipation of the power produced. Applying Ohm's law to the system connected to a load resistor R_L gives:

$$\begin{bmatrix}V_A\\ V_B\\ V_C\end{bmatrix} = -\begin{bmatrix}R_L & 0 & 0\\ 0 & R_L & 0\\ 0 & 0 & R_L\end{bmatrix}\begin{bmatrix}i_A\\ i_B\\ i_C\end{bmatrix} \tag{A.52}$$

If $R \gg \omega L$, where w is the operating frequency of the system in rad/s, the effect of inductances L and M is negligible compared to that of the resistance R. In conclusion R_L should be equal to R in order to extract the maximum possible power from the system, the instantaneous power dissipated through R_L being:

$$\begin{bmatrix}P_A\\ P_B\\ P_C\end{bmatrix} = \frac{R_L}{(R+R_L)^2}\begin{bmatrix}V_A^2\\ V_B^2\\ V_C^2\end{bmatrix} \tag{A.53}$$

Appendix B

Datasheet LTC3108

Ultralow Voltage Step-Up Converter and Power Manager

FEATURES

- **Operates from Inputs of 20mV**
- **Complete Energy Harvesting Power Management System**
  - **- Selectable V_{OUT} of 2.35V, 3.3V, 4.1V or 5V**
  - **- LDO: 2.2V at 3mA**
  - **- Logic Controlled Output**
  - **- Reserve Energy Output**
- **Power Good Indicator**
- Uses Compact Step-Up Transformers
- Small 12-Lead (3mm × 4mm) DFN or 16-Lead SSOP Packages

APPLICATIONS

- Remote Sensors and Radio Power
- Surplus Heat Energy Harvesting
- HVAC Systems
- Industrial Wireless Sensing
- Automatic Metering
- Building Automation
- Predictive Maintenance

DESCRIPTION

The LTC®3108 is a highly integrated DC/DC converter ideal for harvesting and managing surplus energy from extremely low input voltage sources such as TEGs (thermoelectric generators), thermopiles and small solar cells. The step-up topology operates from input voltages as low as 20mV. The LTC3108 is functionally equivalent to the LTC3108-1 except for its unique fixed V_{OUT} options.

Using a small step-up transformer, the LTC3108 provides a complete power management solution for wireless sensing and data acquisition. The 2.2V LDO powers an external microprocessor, while the main output is programmed to one of four fixed voltages to power a wireless transmitter or sensors. The power good indicator signals that the main output voltage is within regulation. A second output can be enabled by the host. A storage capacitor provides power when the input voltage source is unavailable. Extremely low quiescent current and high efficiency design ensure the fastest possible charge times of the output reservoir capacitor.

The LTC3108 is available in a small, thermally enhanced 12-lead (3mm × 4mm) DFN package and a 16-lead SSOP package.

TYPICAL APPLICATION

Wireless Remote Sensor Application Powered From a Peltier Cell

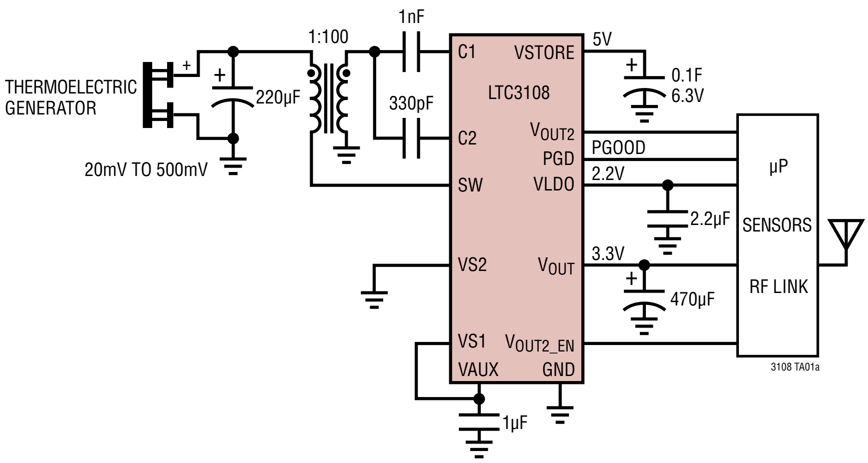

V_{OUT} Charge Time

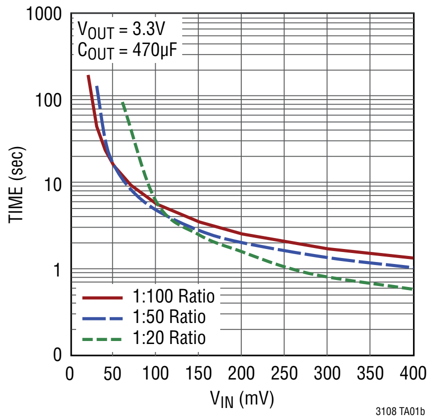

ABSOLUTE MAXIMUM RATINGS (Note 1)

SW Voltage ....–0.3V to 2V
C1 Voltage..–0.3V to 6V
C2 Voltage (Note 5)...–8V to 8V
V_{OUT2}, V_{OUT2_EN} ....–0.3V to 6V
VAUX..15mA into VAUX
VS1, VS2, VAUX, V_{OUT}, PGD.......................–0.3V to 6V
VLDO, VSTORE ....–0.3V to 6V
Operating Junction Temperature Range
(Note 2).. –40°C to 125°C
Storage Temperature Range.................. –65°C to 125°C

PIN CONFIGURATION

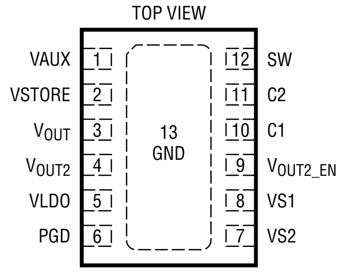

DE PACKAGE
12-LEAD (4mm × 3mm) PLASTIC DFN
T_{JMAX} = 125°C, θ_{JA} = 43°C/W
EXPOSED PAD (PIN 13) IS GND, MUST BE SOLDERED TO PCB (NOTE 4)

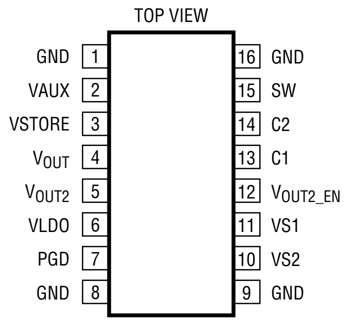

GN PACKAGE
16-LEAD PLASTIC SSOP NARROW
T_{JMAX} = 125°C, θ_{JA} = 110°C/W

ORDER INFORMATION

LEAD FREE FINISH	TAPE AND REEL	PART MARKING*	PACKAGE DESCRIPTION	TEMPERATURE RANGE
LTC3108EDE#PBF	LTC3108EDE#TRPBF	3108	12-Lead (4mm × 3mm) Plastic DFN	–40°C to 125°C
LTC3108IDE#PBF	LTC3108IDE#TRPBF	3108	12-Lead (4mm × 3mm) Plastic DFN	–40°C to 125°C
LTC3108EGN#PBF	LTC3108EGN#TRPBF	3108	16-Lead Plastic SSOP	–40°C to 125°C
LTC3108IGN#PBF	LTC3108IGN#TRPBF	3108	16-Lead Plastic SSOP	–40°C to 125°C

Consult LTC Marketing for parts specified for other fixed output voltages or wider operating temperature ranges.
*The temperature grade is identified by a label on the shipping container.

For more information on lead free part marking, go to: http://www.linear.com/leadfree/
For more information on tape and reel specifications, go to: http://www.linear.com/tapeandreel/

ELECTRICAL CHARACTERISTICS

The ● denotes the specifications which apply over the full operating junction temperature range, otherwise specifications are for T_A = 25°C (Note 2). VAUX = 5V, unless otherwise noted.

PARAMETER	CONDITIONS		MIN	TYP	MAX	UNITS
Minimum Start-Up Voltage	Using 1:100 Transformer Turns Ratio, VAUX = 0V			20	50	mV
No-Load Input Current	Using 1:100 Transformer Turns Ratio; V_{IN} = 20mV, V_{OUT2_EN} = 0V; All Outputs Charged and in Regulation			3		mA
Input Voltage Range	Using 1:100 Transformer Turns Ratio	●	$V_{STARTUP}$		500	mV

ELECTRICAL CHARACTERISTICS

The ● denotes the specifications which apply over the full operating junction temperature range, otherwise specifications are for T_A = 25°C (Note 2). VAUX = 5V, unless otherwise noted.

PARAMETER	CONDITIONS		MIN	TYP	MAX	UNITS
Output Voltage	VS1 = VS2 = GND VS1 = VAUX, VS2 = GND VS1 = GND, VS2 = VAUX VS1 = VS2 = VAUX	● ● ● ●	2.30 3.234 4.018 4.90	2.350 3.300 4.100 5.000	2.40 3.366 4.182 5.10	V V V V
V_{OUT} Quiescent Current	V_{OUT} = 3.3V, V_{OUT2_EN} = 0V			0.2		μA
VAUX Quiescent Current	No Load, All Outputs Charged			6	9	μA
LDO Output Voltage	0.5mA Load	●	2.134	2.2	2.266	V
LDO Load Regulation	For 0mA to 2mA Load			0.5	1	%
LDO Line Regulation	For VAUX from 2.5V to 5V			0.05	0.2	%
LDO Dropout Voltage	I_{LDO} = 2mA	●		100	200	mV
LDO Current Limit	V_{LDO} = 0V	●	4	11		mA
V_{OUT} Current Limit	V_{OUT} = 0V	●	2.8	4.5	7	mA
VSTORE Current Limit	VSTORE = 0V	●	2.8	4.5	7	mA
VAUX Clamp Voltage	Current into VAUX = 5mA	●	5	5.25	5.55	V
VSTORE Leakage Current	VSTORE = 5V			0.1	0.3	μA
V_{OUT2} Leakage Current	V_{OUT2} = 0V, V_{OUT2_EN} = 0V			0.1		μA
VS1, VS2 Threshold Voltage		●	0.4	0.85	1.2	V
VS1, VS2 Input Current	VS1 = VS2 = 5V			0.01	0.1	μA
PGOOD Threshold (Rising)	Measured Relative to the V_{OUT} Voltage			–7.5		%
PGOOD Threshold (Falling)	Measured Relative to the V_{OUT} Voltage			–9		%
PGOOD V_{OL}	Sink Current = 100μA			0.15	0.3	V
PGOOD V_{OH}	Source Current = 0		2.1	2.2	2.3	V
PGOOD Pull-Up Resistance				1		MΩ
V_{OUT2_EN} Threshold Voltage	V_{OUT2_EN} Rising	●	0.4	1	1.3	V
V_{OUT2_EN} Pull-Down Resistance				5		MΩ
V_{OUT2} Turn-On Time				5		μs
V_{OUT2} Turn-Off Time	(Note 3)			0.15		μs
V_{OUT2} Current Limit	V_{OUT} = 3.3V	●	0.15	0.3	0.45	A
V_{OUT2} Current Limit Response Time	(Note 3)			350		ns
V_{OUT2} P-Channel MOSFET On-Resistance	V_{OUT} = 3.3V (Note 3)			1.3		Ω
N-Channel MOSFET On-Resistance	C2 = 5V (Note 3)			0.5		Ω

Note 1: Stresses beyond those listed under Absolute Maximum Ratings may cause permanent damage to the device. Exposure to any Absolute Maximum Rating condition for extended periods may affect device reliability and lifetime.

Note 2: The LTC3108 is tested under pulsed load conditions such that $T_J \approx T_A$. The LTC3108E is guaranteed to meet specifications from 0°C to 85°C junction temperature. Specifications over the –40°C to 125°C operating junction temperature range are assured by design, characterization and correlation with statistical process controls. The LTC3108I is guaranteed over the full –40°C to 125°C operating junction temperature range. Note that the maximum ambient temperature is determined by specific operating conditions in conjunction with board layout, the rated thermal package thermal resistance and other environmental factors. The junction temperature (T_J) is calculated from the ambient temperature (T_A) and power dissipation (P_D) according to the formula: $T_J = T_A + (P_D \bullet \theta_{JA}°C/W)$, where θ_{JA} is the package thermal impedance.

Note 3: Specification is guaranteed by design and not 100% tested in production.

Note 4: Failure to solder the exposed backside of the package to the PC board ground plane will result in a thermal resistance much higher than 43°C/W.

Note 5: The absolute maximum rating is a DC rating. Under certain conditions in the applications shown, the peak AC voltage on the C2 pin may exceed ±8V. This behavior is normal and acceptable because the current into the pin is limited by the impedance of the coupling capacitor.

TYPICAL PERFORMANCE CHARACTERISTICS T_A = 25°C, unless otherwise noted.

I_{IN} vs V_{IN}, (V_{OUT} = 0V)

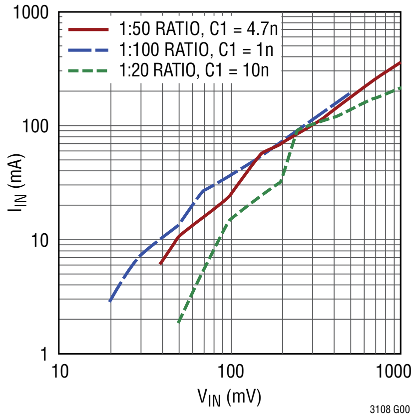

I_{VOUT} and Efficiency vs V_{IN}, 1:20 Ratio Transformer

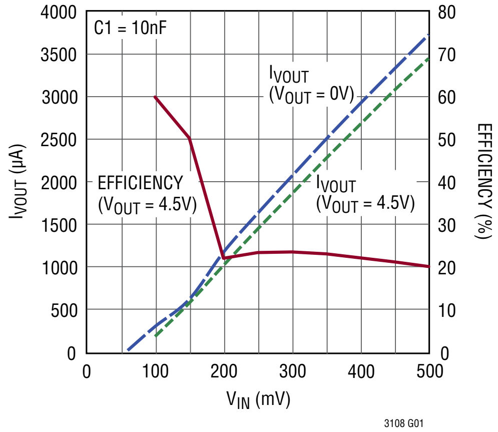

I_{VOUT} and Efficiency vs V_{IN}, 1:100 Ratio Transformer

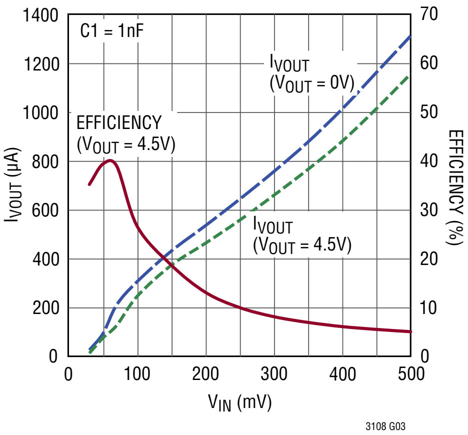

I_{VOUT} and Efficiency vs V_{IN}, 1:50 Ratio Transformer

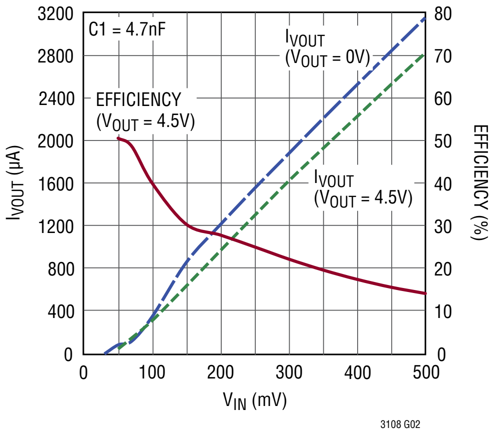

Input Resistance vs V_{IN} (V_{OUT} Charging)

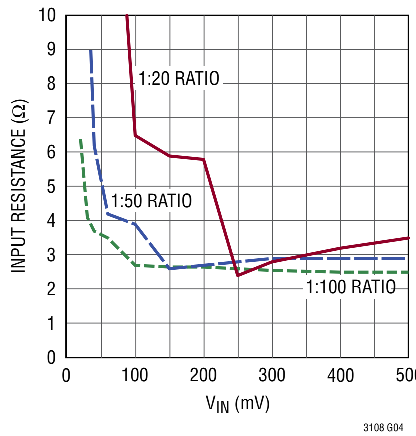

I_{VOUT} vs V_{IN} and Source Resistance, 1:20 Ratio

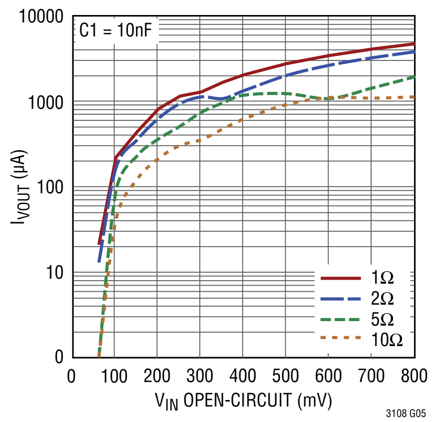

TYPICAL PERFORMANCE CHARACTERISTICS $T_A = 25°C$, unless otherwise noted.

I_{VOUT} vs V_{IN} and Source Resistance, 1:50 Ratio

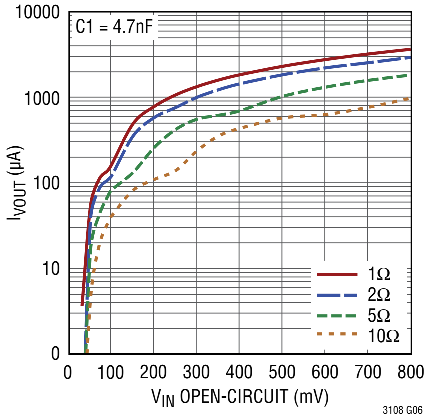

I_{VOUT} vs V_{IN} and Source Resistance, 1:100 Ratio

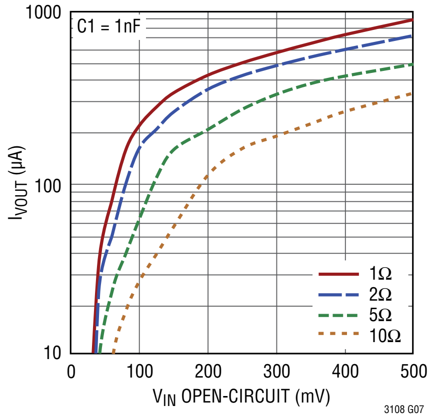

I_{VOUT} vs dT and TEG Size, 1:100 Ratio

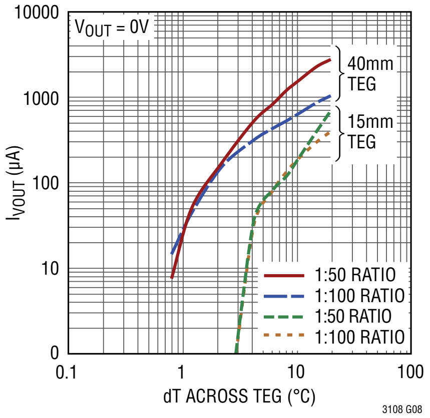

Resonant Switching Waveforms

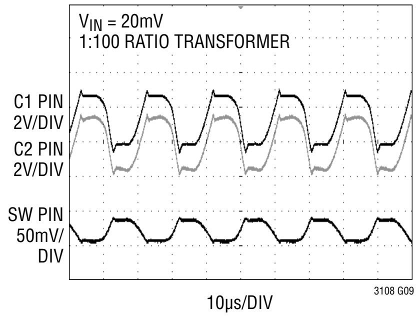

LDO Load Regulation

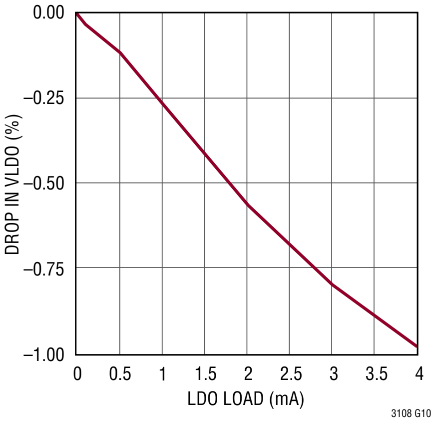

LDO Dropout Voltage

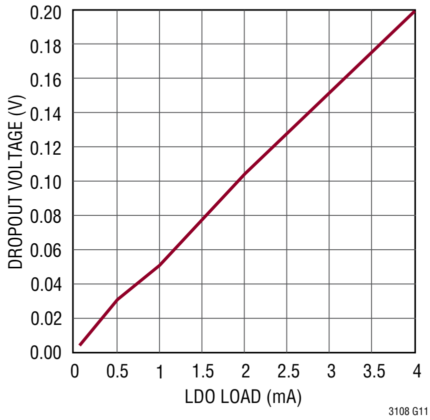

TYPICAL PERFORMANCE CHARACTERISTICS T_A = 25°C, unless otherwise noted.

Start-Up Voltage Sequencing

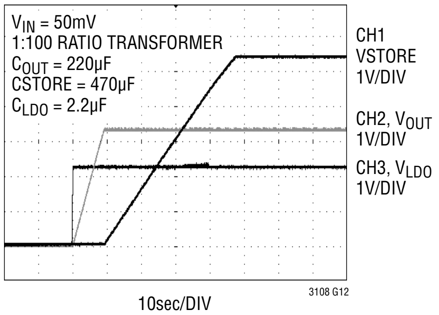

V_{OUT} and PGD Response During a Step Load

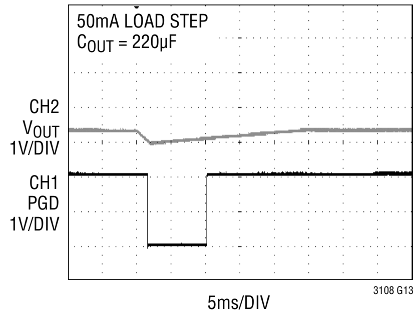

V_{OUT} Ripple

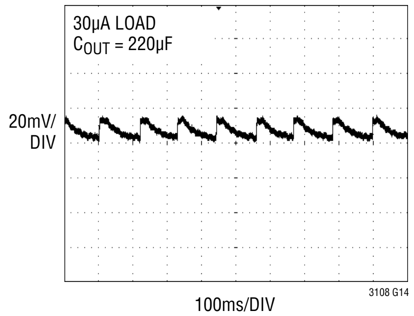

LDO Step Load Response

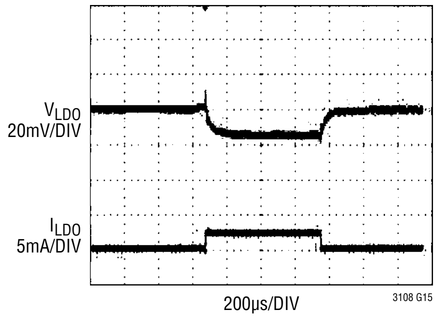

0mA TO 3mA LOAD STEP
C_{LDO} = 2.2µF

Enable Input and V_{OUT2}

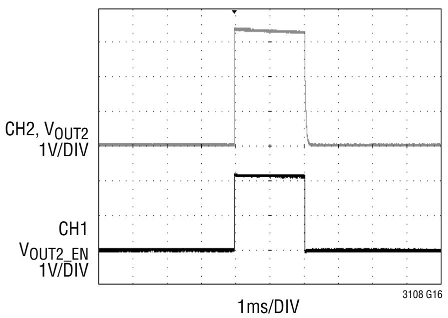

10mA LOAD ON V_{OUT2}
C_{OUT} = 220µF

Running on Storage Capacitor

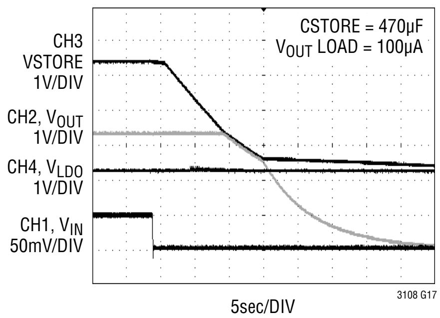

PIN FUNCTIONS (DFN/SSOP)

VAUX (Pin 1/Pin 2): Output of the Internal Rectifier Circuit and V_{CC} for the IC. Bypass VAUX with at least 1µF of capacitance. An active shunt regulator clamps VAUX to 5.25V (typical).

VSTORE (Pin 2/Pin 3): Output for the Storage Capacitor or Battery. A large capacitor may be connected from this pin to GND for powering the system in the event the input voltage is lost. It will be charged up to the maximum VAUX clamp voltage. If not used, this pin should be left open or tied to VAUX.

V_{OUT} (Pin 3/Pin 4): Main Output of the Converter. The voltage at this pin is regulated to the voltage selected by VS1 and VS2 (see Table 1). Connect this pin to an energy storage capacitor or to a rechargeable battery.

V_{OUT2} (Pin 4/Pin 5): Switched Output of the Converter. Connect this pin to a switched load. This output is open until V_{OUT2_EN} is driven high, then it is connected to V_{OUT} through a 1.3Ω P-channel switch. If not used, this pin should be left open or tied to V_{OUT}. The peak current in this output is limited to 0.3A typical.

VLDO (Pin 5/Pin 6): Output of the 2.2V LDO. Connect a 2.2µF or larger ceramic capacitor from this pin to GND. If not used, this pin should be tied to VAUX.

PGD (Pin 6/Pin 7): Power Good Output. When V_{OUT} is within 7.5% of its programmed value, PGD will be pulled up to VLDO through a 1MΩ resistor. If V_{OUT} drops 9% below its programmed value PGD will go low. This pin can sink up to 100µA.

VS2 (Pin 7/Pin 10): V_{OUT} Select Pin 2. Connect this pin to ground or VAUX to program the output voltage (see Table 1).

VS1 (Pin 8/Pin 11): V_{OUT} Select Pin 1. Connect this pin to ground or VAUX to program the output voltage (see Table 1).

V_{OUT2_EN} (Pin 9/Pin 12): Enable Input for V_{OUT2}. V_{OUT2} will be enabled when this pin is driven high. There is an internal 5M pull-down resistor on this pin. If not used, this pin can be left open or grounded.

C1 (Pin 10/Pin 13): Input to the Charge Pump and Rectifier Circuit. Connect a capacitor from this pin to the secondary winding of the step-up transformer.

C2 (Pin 11/Pin 14): Input to the N-Channel Gate Drive Circuit. Connect a capacitor from this pin to the secondary winding of the step-up transformer.

SW (Pin 12/Pin 15): Drain of the Internal N-Channel Switch. Connect this pin to the primary winding of the transformer.

GND (Pins 1, 8, 9, 16) SSOP Only: Ground

GND (Exposed Pad Pin 13) DFN Only: Ground. The DFN exposed pad must be soldered to the PCB ground plane. It serves as the ground connection, and as a means of conducting heat away from the die.

Table 1. Regulated Voltage Using Pins VS1 and VS2

VS2	VS1	V_{OUT}
GND	GND	2.35V
GND	VAUX	3.3V
VAUX	GND	4.1V
VAUX	VAUX	5V

BLOCK DIAGRAM

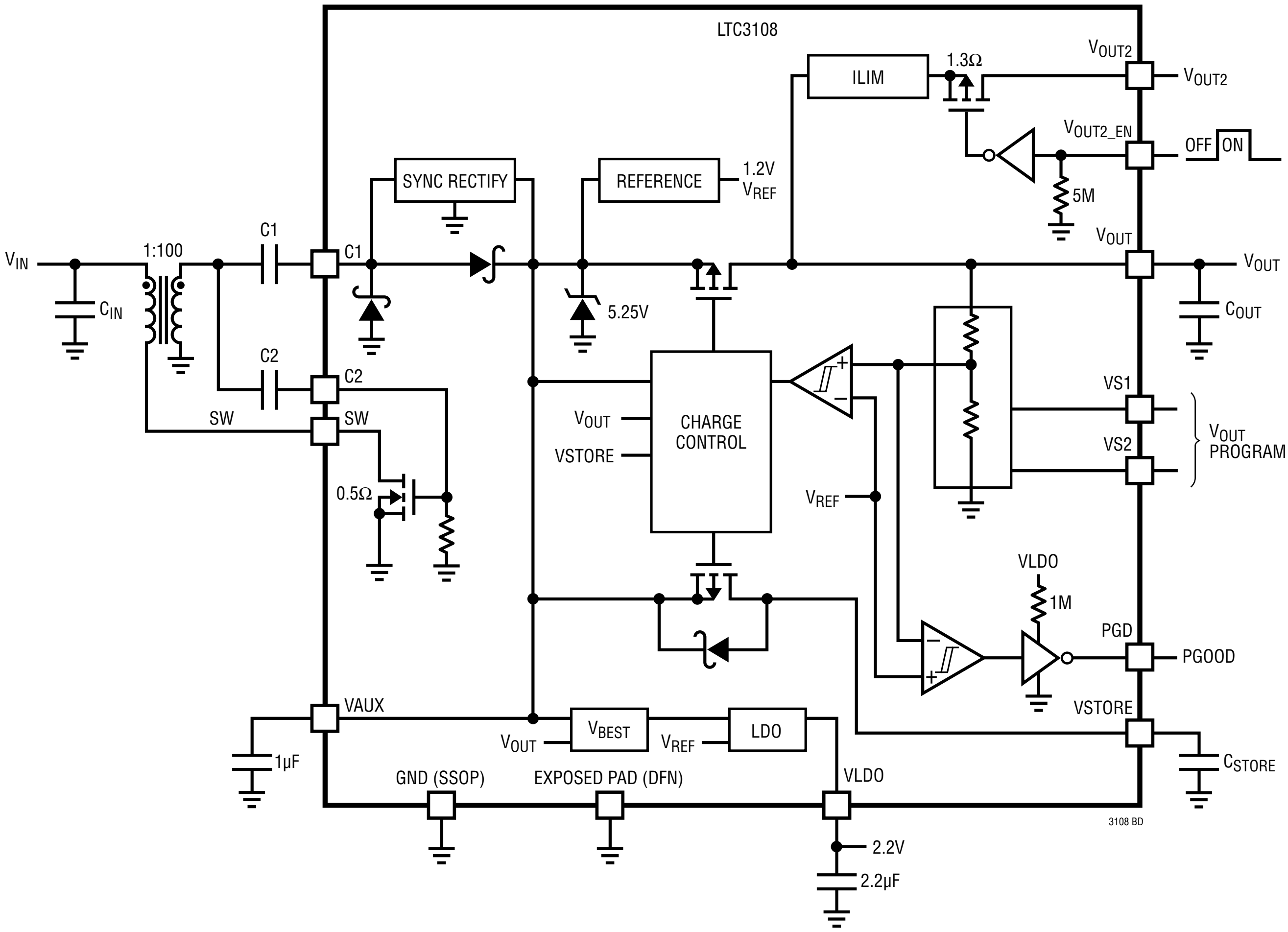

OPERATION (Refer to the Block Diagram)

The LTC3108 is designed to use a small external step-up transformer to create an ultralow input voltage step-up DC/DC converter and power manager. It is ideally suited for low power wireless sensors and other applications in which surplus energy harvesting is used to generate system power because traditional battery power is inconvenient or impractical.

The LTC3108 is designed to manage the charging and regulation of multiple outputs in a system in which the average power draw is very low, but there may be periodic pulses of higher load current required. This is typical of wireless sensor applications, where the quiescent power draw is extremely low most of the time, except for transmit bursts when circuitry is powered up to make measurements and transmit data.

The LTC3108 can also be used to trickle charge a standard capacitor, supercapacitor or rechargeable battery, using energy harvested from a Peltier or photovoltaic cell.

OPERATION

Oscillator

The LTC3108 utilizes a MOSFET switch to form a resonant step-up oscillator using an external step-up transformer and a small coupling capacitor. This allows it to boost input voltages as low as 20mV high enough to provide multiple regulated output voltages for powering other circuits. The frequency of oscillation is determined by the inductance of the transformer secondary winding and is typically in the range of 10kHz to 100kHz. For input voltages as low as 20mV, a primary-secondary turns ratio of about 1:100 is recommended. For higher input voltages, this ratio can be lower. See the Applications Information section for more information on selecting the transformer.

Charge Pump and Rectifier

The AC voltage produced on the secondary winding of the transformer is boosted and rectified using an external charge pump capacitor (from the secondary winding to pin C1) and the rectifiers internal to the LTC3108. The rectifier circuit feeds current into the VAUX pin, providing charge to the external VAUX capacitor and the other outputs.

VAUX

The active circuits within the LTC3108 are powered from VAUX, which should be bypassed with a 1µF capacitor. Larger capacitor values are recommended when using turns ratios of 1:50 or 1:20 (refer to the Typical Application examples). Once VAUX exceeds 2.5V, the main V_{OUT} is allowed to start charging.

An internal shunt regulator limits the maximum voltage on VAUX to 5.25V typical. It shunts to GND any excess current into VAUX when there is no load on the converter or the input source is generating more power than is required by the load.

Voltage Reference

The LTC3108 includes a precision, micropower reference, for accurate regulated output voltages. This reference becomes active as soon as VAUX exceeds 2V.

Synchronous Rectifiers

Once VAUX exceeds 2V, synchronous rectifiers in parallel with each of the internal diodes take over the job of rectifying the input voltage, improving efficiency.

Low Dropout Linear Regulator (LDO)

The LTC3108 includes a low current LDO to provide a regulated 2.2V output for powering low power processors or other low power ICs. The LDO is powered by the higher of VAUX or V_{OUT}. This enables it to become active as soon as VAUX has charged to 2.3V, while the V_{OUT} storage capacitor is still charging. In the event of a step load on the LDO output, current can come from the main V_{OUT} capacitor if VAUX drops below V_{OUT}. The LDO requires a 2.2µF ceramic capacitor for stability. Larger capacitor values can be used without limitation, but will increase the time it takes for all the outputs to charge up. The LDO output is current limited to 4mA minimum.

V_{OUT}

The main output voltage on V_{OUT} is charged from the VAUX supply, and is user programmed to one of four regulated voltages using the voltage select pins VS1 and VS2, according to Table 2. Although the logic threshold voltage for VS1 and VS2 is 0.85V typical, it is recommended that they be tied to ground or VAUX.

Table 2. Regulated Voltage Using Pins VS1 and VS2

VS2	VS1	V_{OUT}
GND	GND	2.35V
GND	VAUX	3.3V
VAUX	GND	4.1V
VAUX	VAUX	5V

When the output voltage drops slightly below the regulated value, the charging current will be enabled as long as VAUX is greater than 2.5V. Once V_{OUT} has reached the proper value, the charging current is turned off.

The internal programmable resistor divider sets V_{OUT}, eliminating the need for very high value external resistors that are susceptible to board leakage.

OPERATION

In a typical application, a storage capacitor (typically a few hundred microfarads) is connected to V_{OUT}. As soon as VAUX exceeds 2.5V, the V_{OUT} capacitor will be allowed to charge up to its regulated voltage. The current available to charge the capacitor will depend on the input voltage and transformer turns ratio, but is limited to about 4.5mA typical.

PGOOD

A power good comparator monitors the V_{OUT} voltage. The PGD pin is an open-drain output with a weak pull-up (1MΩ) to the LDO voltage. Once V_{OUT} has charged to within 7.5% of its regulated voltage, the PGD output will go high. If V_{OUT} drops more than 9% from its regulated voltage, PGD will go low. The PGD output is designed to drive a microprocessor or other chip I/O and is not intended to drive a higher current load such as an LED. Pulling PGD up externally to a voltage greater than VLDO will cause a small current to be sourced into VLDO. PGD can be pulled low in a wire-OR configuration with other circuitry.

V_{OUT2}

V_{OUT2} is an output that can be turned on and off by the host, using the V_{OUT2_EN} pin. When enabled, V_{OUT2} is connected to V_{OUT} through a 1.3Ω P-channel MOSFET switch. This output, controlled by a host processor, can be used to power external circuits such as sensors and amplifiers, that do not have a low power sleep or shutdown capability. V_{OUT2} can be used to power these circuits only when they are needed.

Minimizing the amount of decoupling capacitance on V_{OUT2} will allow it to be switched on and off faster, allowing shorter burst times and, therefore, smaller duty cycles in pulsed applications such as a wireless sensor/transmitter. A small V_{OUT2} capacitor will also minimize the energy that will be wasted in charging the capacitor every time V_{OUT2} is enabled.

V_{OUT2} has a soft-start time of about 5µs to limit capacitor charging current and minimize glitching of the main output when V_{OUT2} is enabled. It also has a current limiting circuit that limits the peak current to 0.3A typical.

The V_{OUT2} enable input has a typical threshold of 1V with 100mV of hysteresis, making it logic-compatible. If V_{OUT2_EN} (which has an internal pull-down resistor) is low, V_{OUT2} will be off. Driving V_{OUT2_EN} high will turn on the V_{OUT2} output.

Note that while V_{OUT2_EN} is high, the current limiting circuitry for V_{OUT2} draws an extra 8µA of quiescent current from V_{OUT}. This added current draw has a negligible effect on the application and capacitor sizing, since the load on the V_{OUT2} output, when enabled, is likely to be orders of magnitude higher than 8µA.

VSTORE

The VSTORE output can be used to charge a large storage capacitor or rechargeable battery after V_{OUT} has reached regulation. Once V_{OUT} has reached regulation, the VSTORE output will be allowed to charge up to the VAUX voltage. The storage element on VSTORE can be used to power the system in the event that the input source is lost, or is unable to provide the current demanded by the V_{OUT}, V_{OUT2} and LDO outputs. If VAUX drops below VSTORE, the LTC3108 will automatically draw current from the storage element. Note that it may take a long time to charge a large capacitor, depending on the input energy available and the loading on V_{OUT} and VLDO.

Since the maximum current from VSTORE is limited to a few milliamps, it can safely be used to trickle-charge NiCd or NiMH rechargeable batteries for energy storage when the input voltage is lost. Note that the VSTORE capacitor cannot supply large pulse currents to V_{OUT}. Any pulse load on V_{OUT} must be handled by the V_{OUT} capacitor.

Short-Circuit Protection

All outputs of the LTC3108 are current limited to protect against short-circuits to ground.

Output Voltage Sequencing

A timing diagram showing the typical charging and voltage sequencing of the outputs is shown in Figure 1. Note: time not to scale.

OPERATION

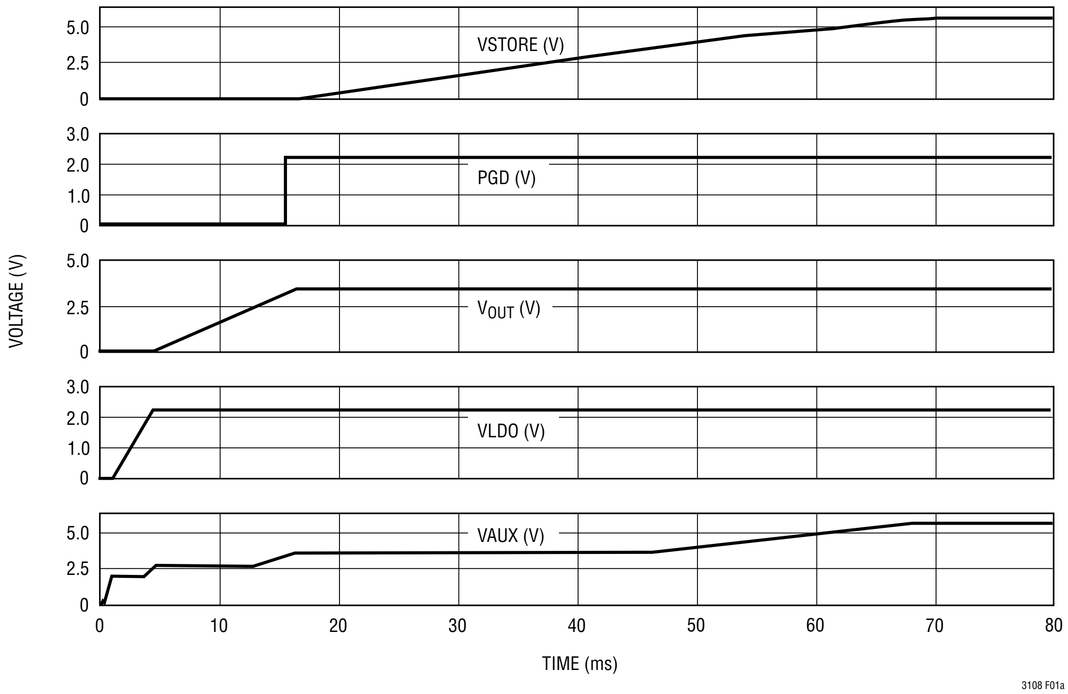

Figure 1. Output Voltage Sequencing with V_{OUT} Programmed for 3.3V (Time Not to Scale)

APPLICATIONS INFORMATION

Introduction

The LTC3108 is designed to gather energy from very low input voltage sources and convert it to usable output voltages to power microprocessors, wireless transmitters and analog sensors. Such applications typically require much more peak power, and at higher voltages, than the input voltage source can produce. The LTC3108 is designed to accumulate and manage energy over a long period of time to enable short power bursts for acquiring and transmitting data. The bursts must occur at a low enough duty cycle such that the total output energy during the burst does not exceed the average source power integrated over the accumulation time between bursts. For many applications, this time between bursts could be seconds, minutes or hours.

The PGD signal can be used to enable a sleeping microprocessor or other circuitry when V_{OUT} reaches regulation, indicating that enough energy is available for a burst.

Input Voltage Sources

The LTC3108 can operate from a number of low input voltage sources, such as Peltier cells, photovoltaic cells or thermopile generators. The minimum input voltage required for a given application will depend on the transformer turns ratio, the load power required, and the internal DC resistance (ESR) of the voltage source. Lower ESR will allow the use of lower input voltages, and provide higher output power capability.

Refer to the I_{IN} vs V_{IN} curves in the Typical Performance Characteristics section to see what input current is required from the source for a given input voltage.

For a given transformer turns ratio, there is a maximum recommended input voltage to avoid excessively high secondary voltages and power dissipation in the shunt regulator. It is recommended that the maximum input voltage times the turns ratio be less than 50.

Note that a low ESR bulk decoupling capacitor will usually be required across the input source to prevent large voltage droop and ripple caused by the source's ESR and the peak primary switching current (which can reach hundreds of milliamps). The time constant of the filter capacitor and the ESR of the voltage source should be much longer than the period of the resonant switching frequency.

Peltier Cell (Thermoelectric Generator)

A Peltier cell (also known as a thermoelectric cooler) is made up of a large number of series-connected P-N junctions, sandwiched between two parallel ceramic plates. Although Peltier cells are often used as coolers by applying a DC voltage to their inputs, they will also generate a DC output voltage, using the Seebeck effect, when the two plates are at different temperatures. The polarity of the output voltage will depend on the polarity of the temperature differential between the plates. The magnitude of the output voltage is proportional to the magnitude of the temperature differential between the plates. When used in

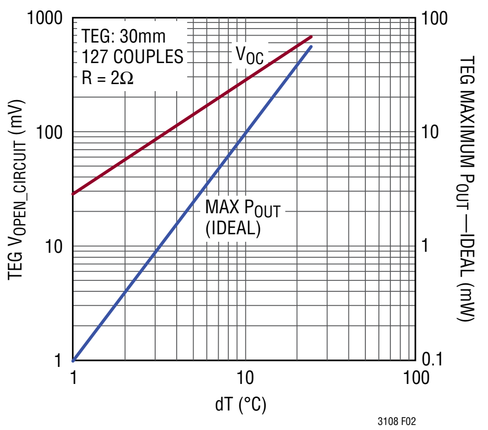

Figure 2. Typical Performance of a Peltier Cell Acting as a Thermoelectric Generator

APPLICATIONS INFORMATION

this manner, a Peltier cell is referred to as a thermoelectric generator (TEG).

The low voltage capability of the LTC3108 design allows it to operate from a TEG with temperature differentials as low as 1°C, making it ideal for harvesting energy in applications in which a temperature difference exists between two surfaces or between a surface and the ambient temperature. The internal resistance (ESR) of most cells is in the range of 1Ω to 5Ω, allowing for reasonable power transfer. The curves in Figure 2 show the open-circuit output voltage and maximum power transfer for a typical Peltier cell (with an ESR of 2Ω) over a 20°C range of temperature differential.

TEG Load Matching

The LTC3108 was designed to present a minimum input resistance (load) in the range of 2Ω to 10Ω, depending on input voltage and transformer turns ratio (as shown in the Typical Performance Characteristics curves). For a given turns ratio, as the input voltage drops, the input resistance increases. This feature allows the LTC3108 to optimize power transfer from sources with a few ohms of source resistance, such as a typical TEG. Note that a lower source resistance will always provide more output current capability by providing a higher input voltage under load.

Peltier Cell (TEG) Suppliers

Peltier cells are available in a wide range of sizes and power capabilities, from less than 10mm square to over 50mm square. They are typically 2mm to 5mm in height. A list of Peltier cell manufacturers is given in Table 3.

Table 3. Peltier Cell Manufacturers

CUI, Inc. www.cui.com (Distributor)
Fujitaka www.fujitaka.com/pub/peltier/english/thermoelectric_power.html
Ferrotec www.ferrotec.com/products/thermal/modules
Kryotherm www.kryothermusa.com
Laird Technologies www.lairdtech.com
Marlow Industries www.marlow.com
Micropelt www.micropelt.com
Nextreme www.nextreme.com
TE Technology www.tetech.com/Peltier-Thermoelectric-Cooler-Modules.html
Tellurex www.tellurex.com

Table 4. Recommended TEG Part Numbers by Size

MANUFACTURER	15mm × 15mm	20mm × 20mm	30mm × 30mm	40mm × 40mm
CUI Inc. (Distributor)	CP60133	CP60233	CP60333	CP85438
Ferrotec	9501/031/030 B	9501/071/040 B	9500/097/090 B	9500/127/100 B
Fujitaka	FPH13106NC	FPH17106NC	FPH17108AC	FPH112708AC
Kryotherm			TGM-127-1.0-0.8	LCB-127-1.4-1.15
Laird Technology			PT6.7.F2.3030.W6	PT8.12.F2.4040.TA.W6
Marlow Industries		RC3-8-01	RC6-6-01	RC12-8-01LS
Tellurex	C2-15-0405	C2-20-0409	C2-30-1505	C2-40-1509
TE Technology	TE-31-1.0-1.3	TE-31-1.4-1.15	TE-71-1.4-1.15	TE-127-1.4-1.05

APPLICATIONS INFORMATION

Thermopile Generator

Thermopile generators (also called powerpile generators) are made up of a number of series-connected thermocouples enclosed in a metal tube. They are commonly used in gas burner applications to generate a DC output of hundreds of millivolts when exposed to the high temperature of a flame. Typical examples are the Honeywell CQ200 and Q313. These devices have an internal series resistance of less than 3Ω, and can generate as much as 750mV open-circuit at their highest rated temperature. For applications in which the temperature rise is too high for a solid-state thermoelectric device, a thermopile can be used as an energy source to power the LTC3108. Because of the higher output voltages possible with a thermopile generator, a lower transformer turns ratio can be used (typically 1:20, depending on the application).

Photovoltaic Cell

The LTC3108 converter can also operate from a single photovoltaic cell (also known as a PV or solar cell) at light levels too low for other low input voltage boost converters to operate. However, many variables will affect the performance in these applications. Light levels can vary over several orders of magnitude and depend on lighting conditions (the type of lighting and indoor versus outdoor). Different types of light (sunlight, incandescent, fluorescent) also have different color spectra, and will produce different output power levels depending on which type of photovoltaic cell is being used (monocrystalline, polycrystalline or thin-film). Therefore, the photovoltaic cell must be chosen for the type and amount of light available. Note that the short-circuit output current from the cell must be at least a few milliamps in order to power the LTC3108 converter

Non-Boost Applications

The LTC3108 can also be used as an energy harvester and power manager for input sources that do not require boosting. In these applications the step-up transformer can be eliminated.

Any source whose peak voltage exceeds 2.5V AC or 5V DC can be connected to the C1 input through a current-limiting resistor where it will be rectified/peak detected. In these applications the C2 and SW pins are not used and can be grounded or left open.

Examples of such input sources would be piezoelectric transducers, vibration energy harvesters, low current generators, a stack of low current solar cells or a 60Hz AC input.

A series resistance of at least 100Ω/V should be used to limit the maximum current into the VAUX shunt regulator.

COMPONENT SELECTION

Step-Up Transformer

The step-up transformer turns ratio will determine how low the input voltage can be for the converter to start. Using a 1:100 ratio can yield start-up voltages as low as 20mV. Other factors that affect performance are the DC resistance of the transformer windings and the inductance of the windings. Higher DC resistance will result in lower efficiency. The secondary winding inductance will determine the resonant frequency of the oscillator, according to the following formula.

$$\text{Frequency} = \frac{1}{2 \bullet \pi \bullet \sqrt{L(\text{sec}) \bullet C}} \text{ Hz}$$

Where L is the inductance of the transformer secondary winding and C is the load capacitance on the secondary winding. This is comprised of the input capacitance at pin C2, typically 30pF, in parallel with the transformer secondary winding's shunt capacitance. The recommended resonant frequency is in the range of 10kHz to 100kHz. See Table 5 for some recommended transformers.

Table 5. Recommended Transformers

VENDOR	PART NUMBER
Coilcraft www.coilcraft.com	LPR6235-752SML (1:100 Ratio) LPR6235-253PML (1:20 Ratio) LPR6235-123QML (1:50 Ratio)
Würth www.we-online	74488540070 (1:100 Ratio) 74488540120 (1:50 Ratio) 74488540250 (1:20 Ratio)

APPLICATIONS INFORMATION

C1 Capacitor

The charge pump capacitor that is connected from the transformer's secondary winding to the C1 pin has an effect on converter input resistance and maximum output current capability. Generally, a minimum value of 1nF is recommended when operating from very low input voltages using a transformer with a ratio of 1:100. Too large a capacitor value can compromise performance when operating at low input voltage or with high resistance sources. For higher input voltages and lower turns ratios, the value of the C1 capacitor can be increased for higher output current capability. Refer to the Typical Applications schematic examples for the recommended value for a given turns ratio.

Squegging

Certain types of oscillators, including transformer-coupled oscillators such as the resonant oscillator of the LTC3108, can exhibit a phenomenon called squegging. This term refers to a condition that can occur which blocks or stops the oscillation for a period of time much longer than the period of oscillation, resulting in bursts of oscillation. An example of this is the blocking oscillator, which is designed to squegg to produce bursts of oscillation. Squegging is also encountered in RF oscillators and regenerative receivers.

In the case of the LTC3108, squegging can occur when a charge builds up on the C2 gate coupling capacitor, such that the DC bias point shifts and oscillation is extinguished for a certain period of time, until the charge on the capacitor bleeds off, allowing oscillation to resume. It is difficult to predict when and if squegging will occur in a given application. While squegging is not harmful, it reduces the average output current capability of the LTC3108.

Squegging can easily be avoided by the addition of a bleeder resistor in parallel with the coupling capacitor on the C2 pin. Resistor values in the range of 100k to 1MΩ are sufficient to eliminate squegging without having any negative impact on performance. For the 330pF capacitor used for C2 in most applications, a 499k bleeder resistor is recommended. See the Typical Applications schematics for an example.

Using External Charge Pump Rectifiers

The synchronous charge pump rectifiers in the LTC3108 (connected to the C1 pin) are optimized for operation from very low input voltage sources, using typical transformer step-up ratios between 1:100 and 1:50, and typical C1 charge pump capacitor values less than 10nF.

Operation from higher input voltage sources (typically 250mV or greater, under load), allows the use of lower transformer step-up ratios (such as 1:20 and 1:10) and larger C1 capacitor values to provide higher output current capability from the LTC3108. However, due to the resulting increase in rectifier currents and resonant oscillator frequency in these applications, the use of external charge pump rectifiers is recommended for optimal performance.

In applications where the step-up ratio is 1:20 or less, and the C1 capacitor is 10nF or greater, the C1 pin should be grounded and two external rectifiers (such as 1N4148 or 1N914 diodes) should be used. These are available as dual diodes in a single package. Avoid the use of Schottky rectifiers, as their lower forward voltage drop increases the minimum start-up voltage. See the Typical Applications schematics for an example.

V_{OUT} and VSTORE Capacitor

For pulsed load applications, the V_{OUT} capacitor should be sized to provide the necessary current when the load is pulsed on. The capacitor value required will be dictated by the load current, the duration of the load pulse, and the amount of voltage droop the circuit can tolerate. The capacitor must be rated for whatever voltage has been selected for V_{OUT} by VS1 and VS2.

$$C_{OUT}(\mu F) \geq \frac{I_{LOAD}(mA) \bullet t_{PULSE}(ms)}{V_{OUT}(V)}$$

Note that there must be enough energy available from the input voltage source for V_{OUT} to recharge the capacitor during the interval between load pulses (to be discussed in the next example). Reducing the duty cycle of the load pulse will allow operation with less input energy.

APPLICATIONS INFORMATION

The VSTORE capacitor may be of very large value (thousands of microfarads or even Farads), to provide holdup at times when the input power may be lost. Note that this capacitor can charge all the way to 5.25V (regardless of the settings for V_{OUT}), so ensure that the holdup capacitor has a working voltage rating of at least 5.5V at the temperature for which it will be used. The VSTORE capacitor can be sized using the following:

$$C_{STORE} \geq \frac{[6\mu A + I_Q + I_{LDO} + (I_{BURST} \bullet t \bullet f)] \bullet TSTORE}{5.25 - V_{OUT}}$$

Where 6µA is the quiescent current of the LTC3108, I_Q is the load on V_{OUT} in between bursts, I_{LDO} is the load on the LDO between bursts, I_{BURST} is the total load during the burst, t is the duration of the burst, f is the frequency of the bursts, TSTORE is the storage time required and V_{OUT} is the output voltage required. Note that for a programmed output voltage of 5V, the VSTORE capacitor cannot provide any beneficial storage time.

To minimize losses and capacitor charge time, all capacitors used for V_{OUT} and VSTORE should be low leakage. See Table 6 for recommended storage capacitors.

Table 6. Recommended Storage Capacitors

VENDOR	PART NUMBER/SERIES
AVX www.avx.com	BestCap Series TAJ and TPS Series Tantalum
Cap-XX www.cap-xx.com	GZ Series
Cooper/Bussmann www.bussmann.com/3/PowerStor.html	KR Series P Series
Vishay/Sprague www.vishay.com/capacitors	Tantamount 592D 595D Tantalum 150CRZ/153CRV Aluminum 013 RLC (Low Leakage)

Storage capacitors requiring voltage balancing are not recommended due to the current draw of the balancing resistors.

PCB Layout Guidelines

Due to the rather low switching frequency of the resonant converter and the low power levels involved, PCB layout is not as critical as with many other DC/DC converters. There are, however, a number of things to consider.

Due to the very low input voltage the circuit may operate from, the connections to V_{IN}, the primary of the transformer and the SW and GND pins of the LTC3108 should be designed to minimize voltage drop from stray resistance and able to carry currents as high as 500mA. Any small voltage drop in the primary winding conduction path will lower efficiency and increase capacitor charge time.

Also, due to the low charge currents available at the outputs of the LTC3108, any sources of leakage current on the output voltage pins must be minimized. An example board layout is shown in Figure 3.

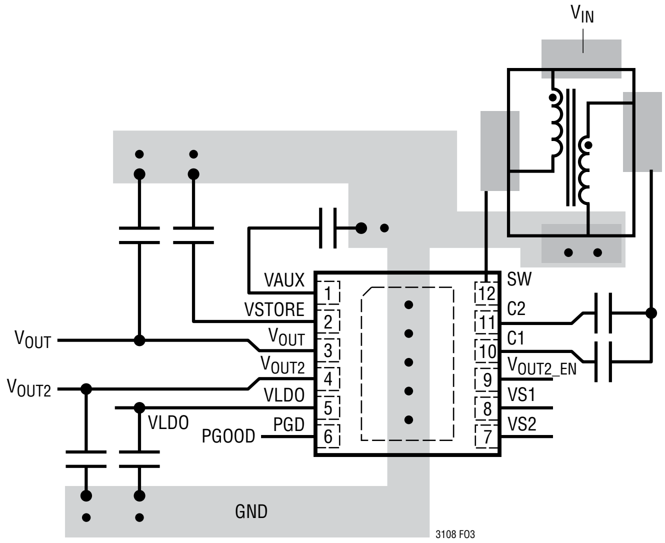

● VIAS TO GROUND PLANE

Figure 3. Example Component Placement for Two-Layer PC Board (DFN Package)

Design Example 1

This design example will explain how to calculate the necessary storage capacitor value for V_{OUT} in pulsed load applications, such as a wireless sensor/transmitter. In these types of applications, the load is very small for a majority of the time (while the circuitry is in a low power sleep state), with bursts of load current occurring periodically during a transmit burst. The storage capacitor on V_{OUT} supports the load during the transmit burst, and the long sleep time between bursts allows the LTC3108 to recharge the capacitor. A method for calculating the maximum rate

APPLICATIONS INFORMATION

at which the load pulses can occur for a given output current from the LTC3108 will also be shown.

In this example, V_{OUT} is set to 3.3V, and the maximum allowed voltage droop during a transmit burst is 10%, or 0.33V. The duration of a transmit burst is 1ms, with a total average current requirement of 40mA during the burst. Given these factors, the minimum required capacitance on V_{OUT} is:

$$C_{OUT}(\mu F) \geq \frac{40mA \bullet 1ms}{0.33V} = 121\mu F$$

Note that this equation neglects the effect of capacitor ESR on output voltage droop. For most ceramic or low ESR tantalum capacitors, the ESR will have a negligible effect at these load currents.

A standard value of 150µF or larger could be used for C_{OUT} in this case. Note that the load current is the total current draw on V_{OUT}, V_{OUT2} and VLDO, since the current for all of these outputs must come from V_{OUT} during a burst. Current contribution from the holdup capacitor on VSTORE is not considered, since it may not be able to recharge between bursts. Also, it is assumed that the charge current from the LTC3108 is negligible compared to the magnitude of the load current during the burst.

To calculate the maximum rate at which load bursts can occur, determine how much charge current is available from the LTC3108 V_{OUT} pin given the input voltage source being used. This number is best found empirically, since there are many factors affecting the efficiency of the converter. Also determine what the total load current is on V_{OUT} during the sleep state (between bursts). Note that this must include any losses, such as storage capacitor leakage.

Assume, for instance, that the charge current from the LTC3108 is 50µA and the total current drawn on V_{OUT} in the sleep state is 17µA, including capacitor leakage. In addition, use the value of 150µF for the V_{OUT} capacitor. The maximum transmit rate (neglecting the duration of the transmit burst, which is typically very short) is then given by:

$$t = \frac{150\mu F \bullet 0.33V}{(50\mu A - 17\mu A)} = 1.5\text{sec or } f_{MAX} = 0.666Hz$$

Therefore, in this application example, the circuit can support a 1ms transmit burst every 1.5 seconds.

It can be determined that for systems that only need to transmit every few seconds (or minutes or hours), the average charge current required is extremely small, as long as the sleep current is low. Even if the available charge current in the example above was only 10µA and the sleep current was only 5µA, it could still transmit a burst every ten seconds.

The following formula enables the user to calculate the time it will take to charge the LDO output capacitor and the V_{OUT} capacitor the first time, from 0V. Here again, the charge current available from the LTC3108 must be known. For this calculation, it is assumed that the LDO output capacitor is 2.2µF.

$$t_{LDO} = \frac{2.2V \bullet 2.2\mu F}{I_{CHG} - I_{LDO}}$$

If there were 50µA of charge current available and a 5µA load on the LDO (when the processor is sleeping), the time for the LDO to reach regulation would be 107ms.

If V_{OUT} were programmed to 3.3V and the V_{OUT} capacitor was 150µF, the time for V_{OUT} to reach regulation would be:

$$t_{VOUT} = \frac{3.3V \bullet 150\mu F}{I_{CHG} - I_{VOUT} - I_{LDO}} + t_{LDO}$$

If there were 50µA of charge current available and 5µA of load on V_{OUT}, the time for V_{OUT} to reach regulation after the initial application of power would be 12.5 seconds.

Design Example 2

In many pulsed load applications, the duration, magnitude and frequency of the load current bursts are known and fixed. In these cases, the average charge current required from the LTC3108 to support the average load must be calculated, which can be easily done by the following:

$$I_{CHG} \geq I_Q + \frac{I_{BURST} \bullet t}{T}$$

Where I_Q is the sleep current on V_{OUT} required by the external circuitry in between bursts (including cap leakage), I_{BURST} is the total load current during the burst, t is the

APPLICATIONS INFORMATION

duration of the burst and T is the period of the transmit burst rate (essentially the time between bursts).

In this example, I_Q = 5µA, I_{BURST} = 100mA, t = 5ms and T = one hour. The average charge current required from the LTC3108 would be:

$$I_{CHG} \geq 5\mu A + \frac{100mA \bullet 0.005sec}{3600sec} = 5.14\mu A$$

Therefore, if the LTC3108 has an input voltage that allows it to supply a charge current greater than 5.14µA, the application can support 100mA bursts lasting 5ms every hour. It can be determined that the sleep current of 5µA is the dominant factor because the transmit duty cycle is so small (0.00014%). Note that for a V_{OUT} of 3.3V, the average power required by this application is only 17µW (not including converter losses).

Note that the charge current available from the LTC3108 has no effect on the sizing of the V_{OUT} capacitor (if it is assumed that the load current during a burst is much larger than the charge current), and the V_{OUT} capacitor has no effect on the maximum allowed burst rate.

TYPICAL APPLICATIONS

Peltier-Powered Energy Harvester for Remote Sensor Applications

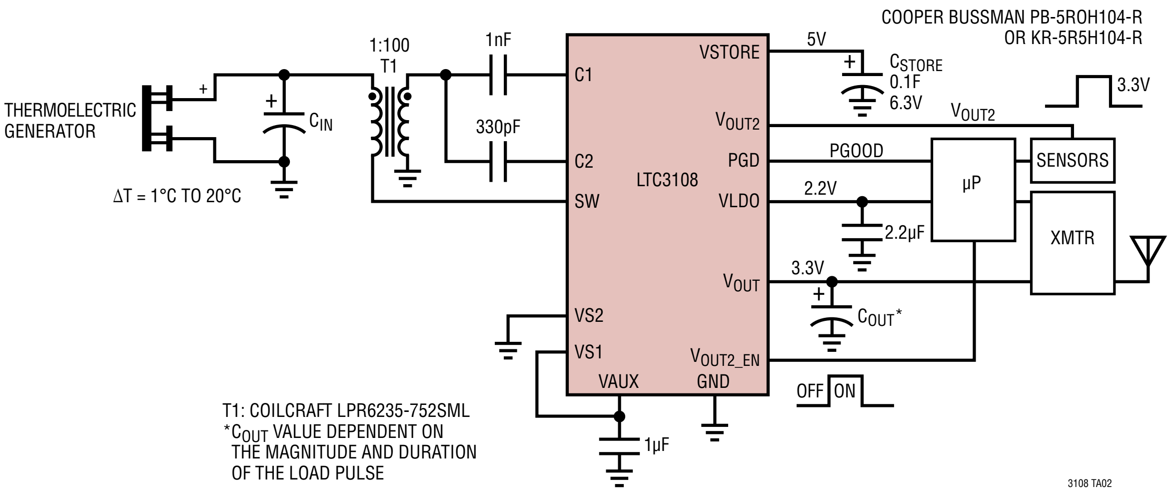

TYPICAL APPLICATIONS

Li-Ion Battery Charger and LDO Powered by a Solar Cell

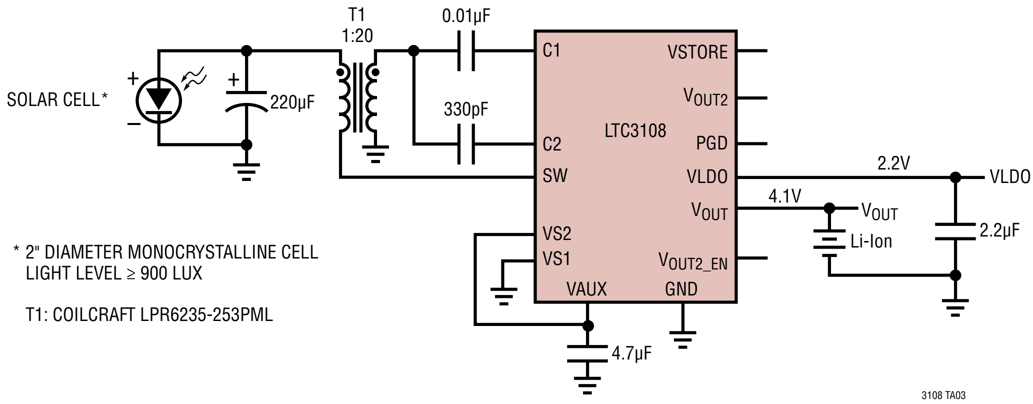

Supercapacitor Charger and LDO Powered by a Thermopile Generator

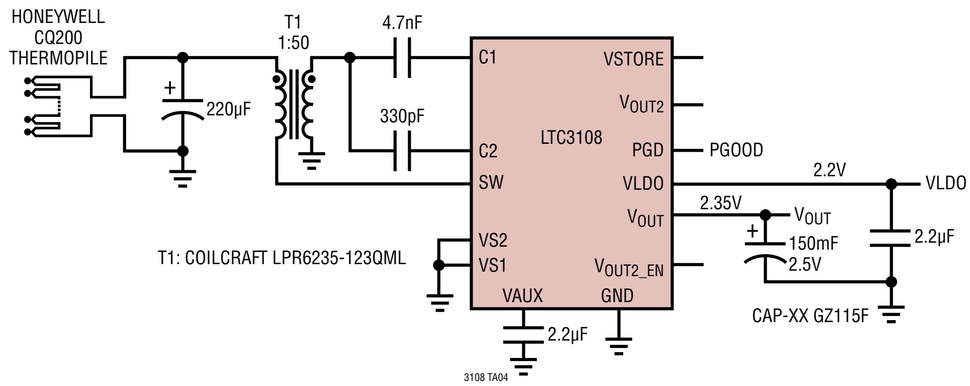

DC Input Energy Harvester and Power Manager

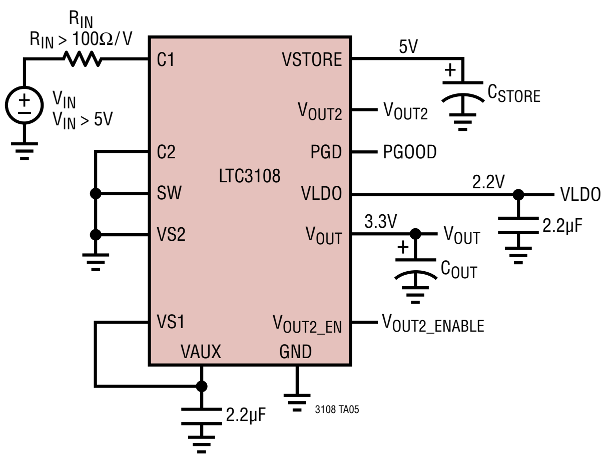

AC Input Energy Harvester and Power Manager

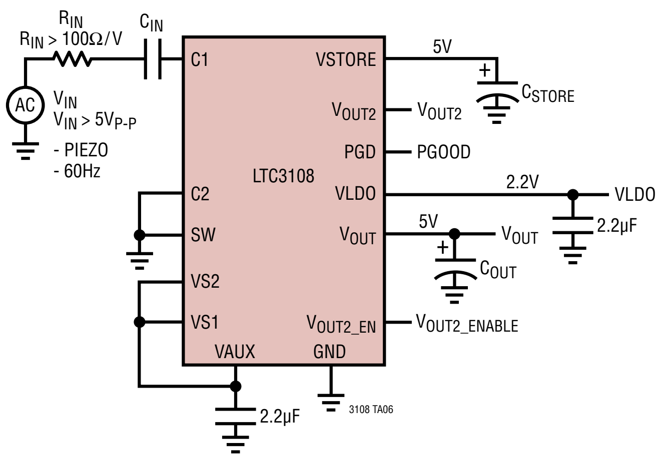

PACKAGE DESCRIPTION

Please refer to http://www.linear.com/designtools/packaging/ for the most recent package drawings.

GN Package
16-Lead Plastic SSOP (Narrow .150 Inch)
(Reference LTC DWG # 05-08-1641 Rev B)

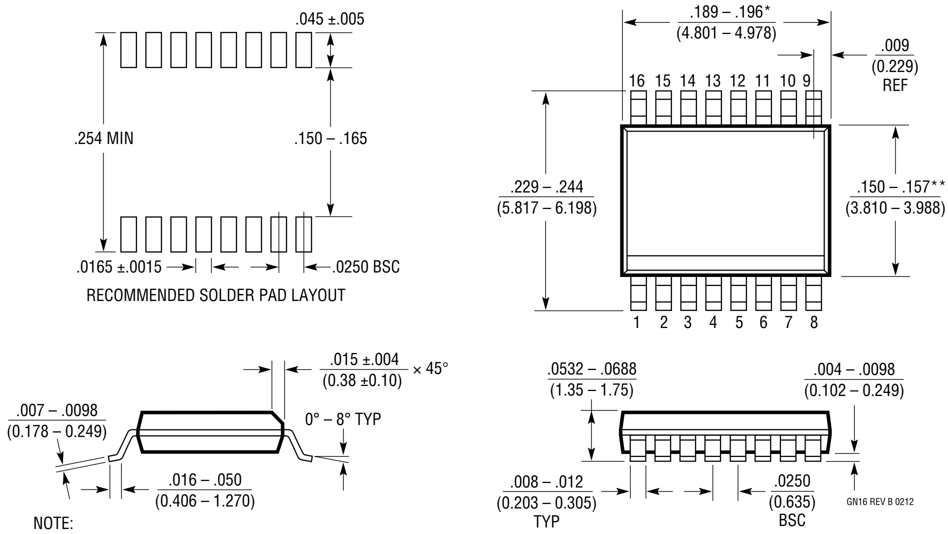

NOTE:
1. CONTROLLING DIMENSION: INCHES
2. DIMENSIONS ARE IN $\frac{\text{INCHES}}{\text{(MILLIMETERS)}}$
3. DRAWING NOT TO SCALE
4. PIN 1 CAN BE BEVEL EDGE OR A DIMPLE

*DIMENSION DOES NOT INCLUDE MOLD FLASH. MOLD FLASH SHALL NOT EXCEED 0.006" (0.152mm) PER SIDE
**DIMENSION DOES NOT INCLUDE INTERLEAD FLASH. INTERLEAD FLASH SHALL NOT EXCEED 0.010" (0.254mm) PER SIDE

DE/UE Package
12-Lead Plastic DFN (4mm × 3mm)
(Reference LTC DWG # 05-08-1695 Rev D)

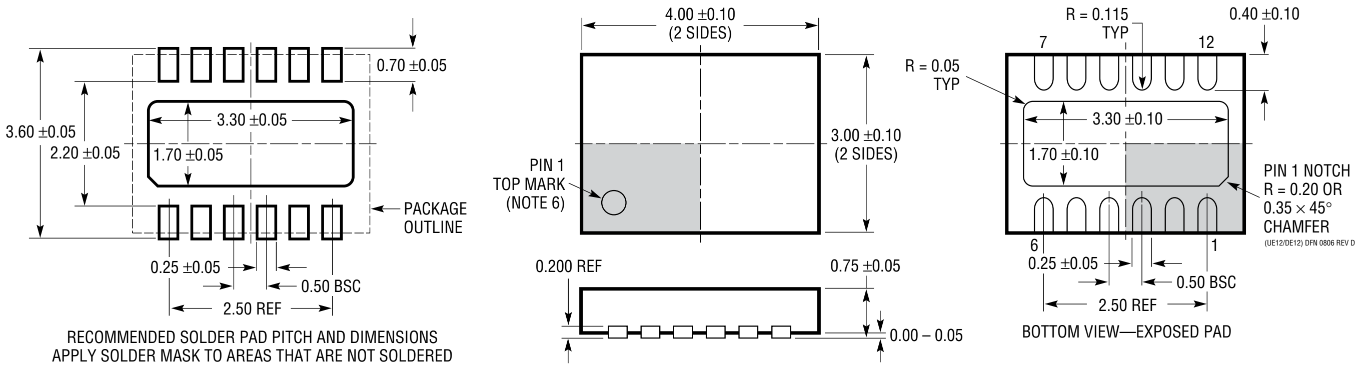

RECOMMENDED SOLDER PAD PITCH AND DIMENSIONS
APPLY SOLDER MASK TO AREAS THAT ARE NOT SOLDERED

NOTE:
1. DRAWING PROPOSED TO BE A VARIATION OF VERSION (WGED) IN JEDEC PACKAGE OUTLINE M0-229
2. DRAWING NOT TO SCALE
3. ALL DIMENSIONS ARE IN MILLIMETERS
4. DIMENSIONS OF EXPOSED PAD ON BOTTOM OF PACKAGE DO NOT INCLUDE MOLD FLASH. MOLD FLASH, IF PRESENT, SHALL NOT EXCEED 0.15mm ON ANY SIDE
5. EXPOSED PAD SHALL BE SOLDER PLATED
6. SHADED AREA IS ONLY A REFERENCE FOR PIN 1 LOCATION ON THE TOP AND BOTTOM OF PACKAGE

REVISION HISTORY

REV	DATE	DESCRIPTION	PAGE NUMBER
A	04/10	Updated front page text and Typical Appliction	1
		Updated Absolute Maximum Ratings and Order Information sections	2
		Updated Electrical Characteristics	3
		Added graph (3108 G00) to Typical Performance Characteristics	4
		Updated Block Diagram	8
		Text added to Operation section	9
		Changes to Applications Information section	12-18
		Updated Typical Applications	18, 19, 22
		Updated Related Parts	22
B	06/13	Added vendor information to Table 5	14
C	08/13	Changed Würth transformer part numbers	14

TYPICAL APPLICATION

Dual TEG Energy Harvester Operates from Temperature Differentials of Either Polarity

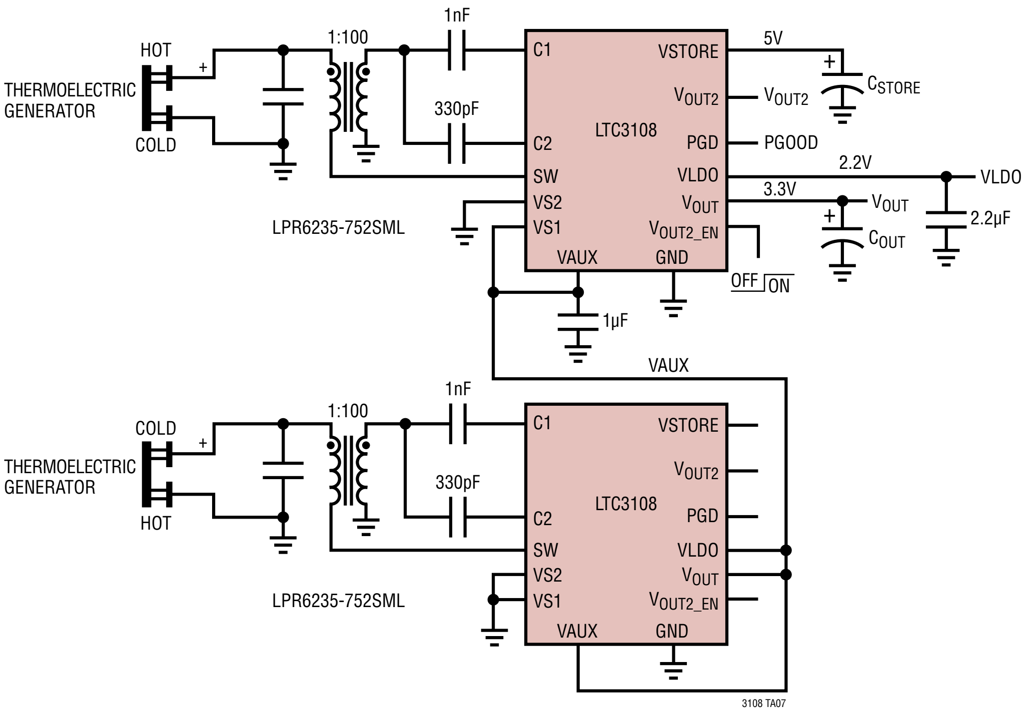

RELATED PARTS

PART NUMBER	DESCRIPTION	COMMENTS
LTC1041	Bang-Bang Controller	V_{IN}: 2.8V to 16V; I_Q = 1µA; SO-8 Package
LTC1389	Nanopower Precision Shunt Voltage Reference	$V_{OUT(MIN)}$ = 1.25V; I_Q = 0.8µA; SO-8 Package
LT1672/LT1673/ LT1674	Single-/Dual-/Quad-Precision 2µA Rail-to-Rail Op Amps	SO-8, SO-14 and MSOP-8 Packages
LT3009	3µA I_Q, 20mA Linear Regulator	V_{IN}: 1.6V to 20V; $V_{OUT(MIN)}$: 0.6V to Adj, 1.2V, 1.5V, 1.8V, 2.5V, 3.3V, 5V to Fixed; I_Q = 3µA; I_{SD} < 1µA; 2mm × 2mm DFN-8 and SC70 Packages
LTC3108-1	Ultralow Voltage Step-Up Converter and Power Manager	V_{IN}: 0.02V to 1V; V_{OUT} = 2.5V, 3V, 3.7V, 4.5V Fixed; I_Q = 6µA; 3mm × 4mm DFN-12 and SSOP-16 Packages
LTC3525L-3/ LTC3525L-3.3/ LTC3525L-5	400mA (I_{SW}), Synchronous Step-Up DC/DC Converter with Output Disconnect	V_{IN}: 0.7V to 4V; $V_{OUT(MIN)}$ = 5V_{MAX}; I_Q = 7µA; I_{SD} < 1µA; SC70 Package
LTC3588-1	Piezoelectric Energy Generator with Integrated High Efficiency Buck Converter	V_{IN}: 2.7V to 20V; $V_{OUT(MIN)}$: Fixed to 1.8V, 2.5V, 3.3V, 3.6V; I_Q = 0.95µA; 3mm × 3mm DFN-10 and MSOP-10E Packages
LTC3642	45V, 50mA Synchronous MicroPower Buck Converter	V_{IN}: 4.5V to 45V, 60V_{MAX}; $V_{OUT(MIN)}$: 0.8V to Adj, 3.3V Fixed, 5V Fixed; I_Q = 12µA; I_{SD} < 1µA; 3mm × 3mm DFN-8 and MSOP-8E Packages
LTC6656	850mA Precision Reference	Series Low Dropout Precision
LT8410/ LT8410-1	MicroPower 25mA/8mA Low Noise Boost Converter with Integrated Schottky Diode and Output Disconnect	V_{IN}: 2.6V to 16V; $V_{OUT(MIN)}$ = 40V_{MAX}; I_Q = 8.5µA; I_{SD} < 1µA; 2mm × 2mm DFN-8 Package
LTC4070	Micropower Shunt Li-Ion Charge	Controls Charging with µA Source

Linear Technology Corporation
1630 McCarthy Blvd., Milpitas, CA 95035-7417
(408) 432-1900 • FAX: (408) 434-0507 • www.linear.com/LTC3108

LT 0813 REV C • PRINTED IN USA

Appendix C

Datasheet LTC3109

Auto-Polarity, Ultralow Voltage Step-Up Converter and Power Manager

FEATURES

- **Operates from Inputs as Low as ±30mV**
- **Less Than ±1°C Needed Across TEG to Harvest Energy**
- **Proprietary Auto-Polarity Architecture**
- **Complete Energy Harvesting Power Management System**
  - **Selectable V_{OUT} of 2.35V, 3.3V, 4.1V or 5V**
  - **2.2V, 5mA LDO**
  - **Logic-Controlled Output**
  - **Energy Storage Capability for Operation During Power Interruption**
- **Power Good Indicator**
- Uses Compact Step-up Transformers
- Small, 20-lead (4mm × 4mm) QFN Package or 20-Lead SSOP

APPLICATIONS

- Remote Sensor and Radio Power
- HVAC Systems
- Automatic Metering
- Building Automation
- Predictive Maintenance
- Industrial Wireless Sensing

DESCRIPTION

The LTC®3109 is a highly integrated DC/DC converter ideal for harvesting surplus energy from extremely low input voltage sources such as TEGs (thermoelectric generators) and thermopiles. Its unique, proprietary autopolarity topology* allows it to operate from input voltages as low as 30mV, regardless of polarity.

Using two compact step-up transformers and external energy storage elements, the LTC3109 provides a complete power management solution for wireless sensing and data acquisition. The 2.2V LDO can power an external microprocessor, while the main output can be programmed to one of four fixed voltages. The power good indicator signals that the main output is within regulation. A second output can be enabled by the host. A storage capacitor (or battery) can also be charged to provide power when the input voltage source is unavailable. Extremely low quiescent current and high efficiency maximizes the harvested energy available for the application.

The LTC3109 is available in a small, thermally enhanced 20-lead (4mm × 4mm) QFN package and a 20-lead SSOP package.

*Patent pending.

TYPICAL APPLICATION

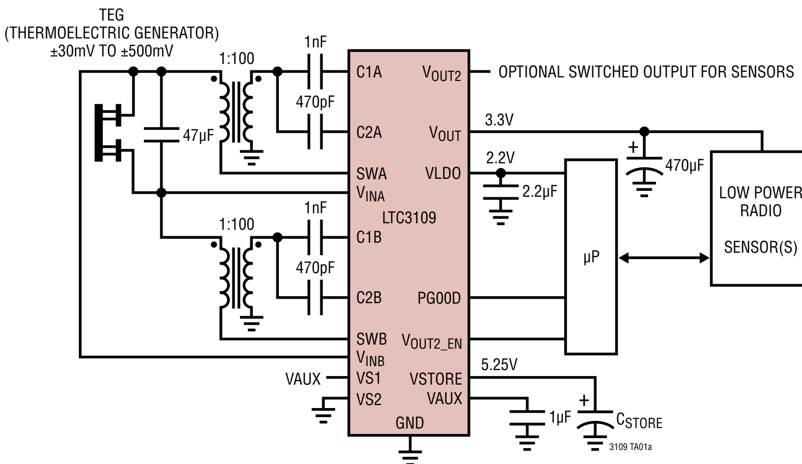

V_{OUT} Current vs TEG Voltage

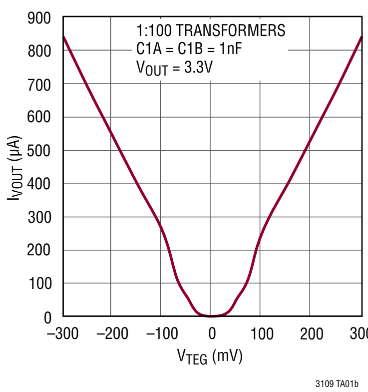

ABSOLUTE MAXIMUM RATINGS (Note 1)

SWA, SWB, V_{INA}, V_{INB} Voltage .... –0.3V to 2V
C1A, C1B Voltage .... –0.3V to 6V
C2A, C2B Voltage (Note 6) .... –8V to 8V
V_{OUT2}, V_{OUT2_EN} .... –0.3V to 6V
VS1, VS2, V_{OUT}, PGOOD .... –0.3V to 6V
VLDO, VSTORE .... –0.3V to 6V
VAUX... 15mA Into V_{AUX}
Operating Junction Temperature Range
(Note 2).. –40°C to 125°C
Storage Temperature Range .... –65°C to 125°C

PIN CONFIGURATION

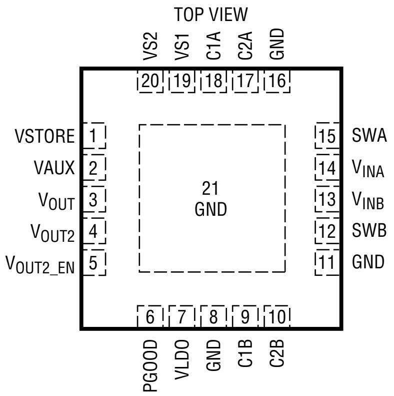

UF PACKAGE
20-LEAD (4mm × 4mm) PLASTIC QFN
T_{JMAX} = 125°C, θ_{JA} = 37°C/W
EXPOSED PAD (PIN 21) IS GND (Note 5)

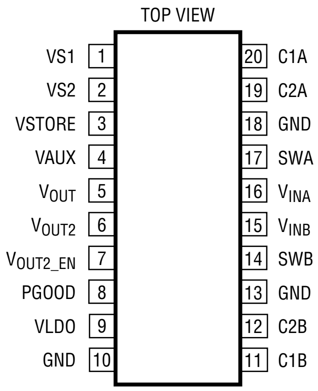

GN PACKAGE
20-LEAD PLASTIC SSOP
T_{JMAX} = 125°C, θ_{JA} = 90°C/W

ORDER INFORMATION

LEAD FREE FINISH	TAPE AND REEL	PART MARKING*	PACKAGE DESCRIPTION	TEMPERATURE RANGE
LTC3109EUF#PBF	LTC3109EUF#TRPBF	3109	20-Lead (4mm × 4mm) Plastic QFN	–40°C to 125°C
LTC3109IUF#PBF	LTC3109IUF#TRPBF	3109	20-Lead (4mm × 4mm) Plastic QFN	–40°C to 125°C
LTC3109EGN#PBF	LTC3109EGN#TRPBF	LTC3109GN	20-Lead Plastic SSOP	–40°C to 125°C
LTC3109IGN#PBF	LTC3109IGN#TRPBF	LTC3109GN	20-Lead Plastic SSOP	–40°C to 125°C

Consult LTC Marketing for parts specified with wider operating temperature ranges. *The temperature grade is identified by a label on the shipping container.
Consult LTC Marketing for information on non-standard lead based finish parts.

For more information on lead free part marking, go to: http://www.linear.com/leadfree/
For more information on tape and reel specifications, go to: http://www.linear.com/tapeandreel/

ELECTRICAL CHARACTERISTICS

The ● denotes the specifications which apply over the full operating junction temperature range, otherwise specifications are for T_A = 25°C (Note 2). VAUX = 5V unless otherwise noted.

PARAMETER	CONDITIONS		MIN	TYP	MAX	UNITS
Minimum Start-Up Voltage	Using 1:100 Transformer Turns Ratio, VAUX = 0V			±30	±50	mV
No-Load Input Current	Using 1:100 Transformer Turns Ratios, V_{IN} = 30mV, V_{OUT2_EN} = 0V, All Outputs Charged and in Regulation			6		mA
Input Voltage Range	Using 1:100 Transformer Turns Ratios	●	$V_{STARTUP}$		±500	mV
Output Voltage	VS1 = VS2 = GND VS1 = VAUX, VS2 = GND VS1 = GND, VS2 = VAUX VS1 = VS2 = VAUX	● ● ● ●	2.30 3.234 4.018 4.875	2.350 3.300 4.100 5.000	2.40 3.366 4.182 5.10	V V V V
VAUX Quiescent Current	No Load, All Outputs Charged			7	10	μA
VAUX Clamp Voltage	Current Into VAUX = 5mA	●	5.0	5.25	5.55	V
V_{OUT} Quiescent Current	V_{OUT} = 3.3V, V_{OUT2_EN} = 0V			0.2		μA
V_{OUT} Current Limit	V_{OUT} = 0V	●	6	15	26	mA
N-Channel MOSFET On-Resistance	C2B = C2A = 5V (Note 3) Measured from V_{INA} or SWA, V_{INB} or SWB to GND			0.35		Ω
LDO Output Voltage	0.5mA Load On V_{LDO}	●	2.134	2.2	2.30	V
LDO Load Regulation	For 0mA to 2mA Load			0.5	1	%
LDO Line Regulation	For V_{AUX} from 2.5V to 5V			0.05	0.2	%
LDO Dropout Voltage	I_{LDO} = 2mA	●		100	200	mV
LDO Current Limit	V_{LDO} = 0V	●	5	12		mA
VSTORE Leakage Current	VSTORE = 5V			0.1	0.3	μA
VSTORE Current Limit	VSTORE = 0V	●	6	15	26	mA
V_{OUT2} Leakage Current	V_{OUT2} = 0V, V_{OUT2_EN} = 0V			50		nA
VS1, VS2 Threshold Voltage		●	0.4	0.85	1.2	V
VS1, VS2 Input Current	V_{S1} = V_{S2} = 5V			1	50	nA
PGOOD Threshold (Rising)	Measured Relative to the V_{OUT} Voltage			–7.5		%
PGOOD Threshold (Falling)	Measured Relative to the V_{OUT} Voltage			–9		%
PGOOD V_{OL}	Sink Current = 100μA			0.12	0.3	V
PGOOD V_{OH}	Source Current = 0		2.1	2.2	2.3	V
PGOOD Pull-Up Resistance				1		MΩ
V_{OUT2_EN} Threshold Voltage	V_{OUT2_EN} Rising	●	0.4	1.0	1.3	V
V_{OUT2_EN} Threshold Hysteresis				100		mV
V_{OUT2_EN} Pull-Down Resistance				5		MΩ
V_{OUT2} Turn-On Time				0.5		μs
V_{OUT2} Turn-Off Time	(Note 3)			0.15		μs
V_{OUT2} Current Limit	V_{OUT} = 3.3V	●	0.2	0.3	0.5	A
V_{OUT2} Current Limit Response Time	(Note 3)			350		ns
V_{OUT2} P-Channel MOSFET On-Resistance	V_{OUT} = 5V (Note 3)			1.0		Ω

Note 1: Stresses beyond those listed under Absolute Maximum Ratings may cause permanent damage to the device. Exposure to any Absolute Maximum Rating condition for extended periods may affect device reliability and lifetime.

Note 2: The LTC3109 is tested under pulsed load conditions such that $T_J \approx T_A$. The LTC3109E is guaranteed to meet specifications from 0°C to 85°C junction temperature. Specifications over the –40°C to 125°C operating junction temperature range are assured by design, characterization and correlation with statistical process controls. The LTC3109I is guaranteed over the full –40°C to 125°C operating junction temperature range. Note that the maximum ambient temperature is determined by specific operating conditions in conjunction with

ELECTRICAL CHARACTERISTICS

board layout, the rated thermal package thermal resistance and other environmental factors. The junction temperature (T_J) is calculated from the ambient temperature (T_A) and power dissipation (P_D) according to the formula: $T_J = T_A + (P_D \bullet \theta_{JA}$°C/W), where θ_{JA} is the package thermal impedance.

Note 3: Specification is guaranteed by design and not 100% tested in production.

Note 4: Current measurements are made when the output is not switching.

Note 5: Failure to solder the exposed backside of the QFN package to the PC board ground plane will result in a thermal resistance much higher than 37°C/W.

Note 6: The Absolute Maximum Rating is a DC rating. Under certain conditions in the applications shown, the peak AC voltage on the C2A and C2B pins may exceed ±8V. This behavior is normal and acceptable because the current into the pin is limited by the impedance of the coupling capacitor.

TYPICAL PERFORMANCE CHARACTERISTICS $T_A = 25°C$, unless otherwise noted.

I_{IN} vs V_{IN}

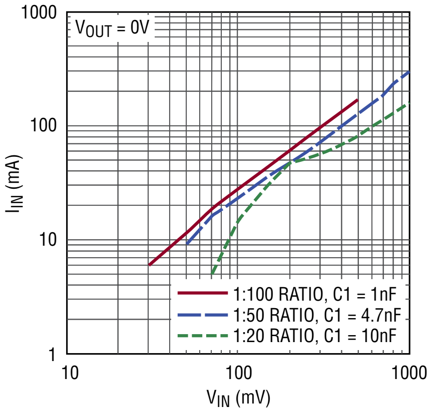

I_{VOUT} vs V_{IN}

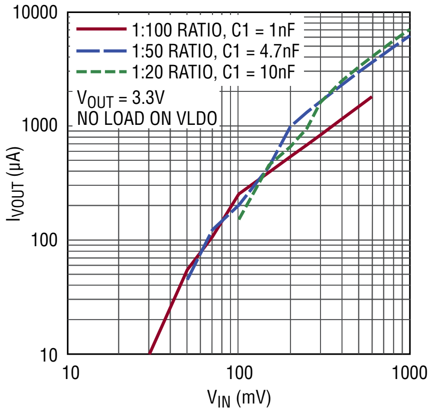

P_{VOUT} vs V_{IN}

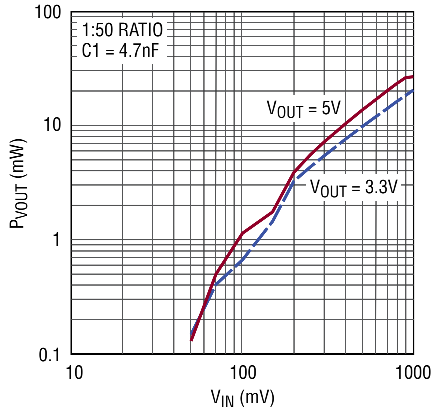

Input Resistance vs V_{IN}

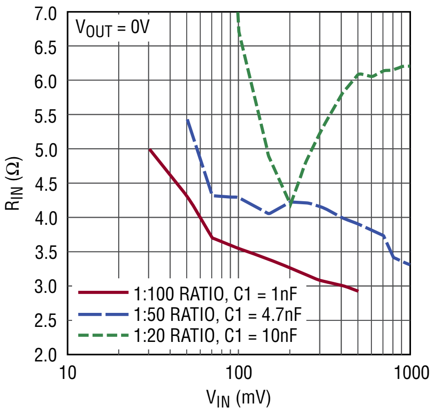

Efficiency vs V_{IN}

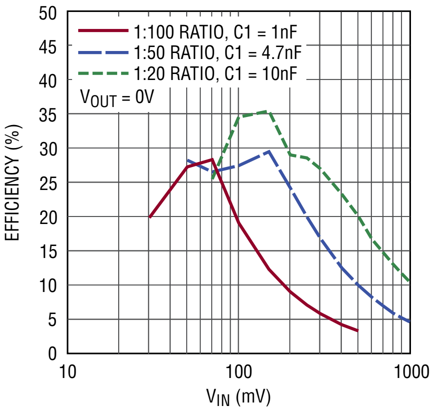

Open-Circuit Start-Up Voltage vs Source Resistance

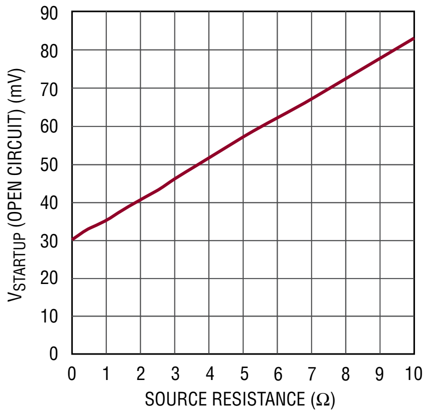

TYPICAL PERFORMANCE CHARACTERISTICS $T_A = 25°C$, unless otherwise noted.

V_{OUT} and VLDO vs Temperature

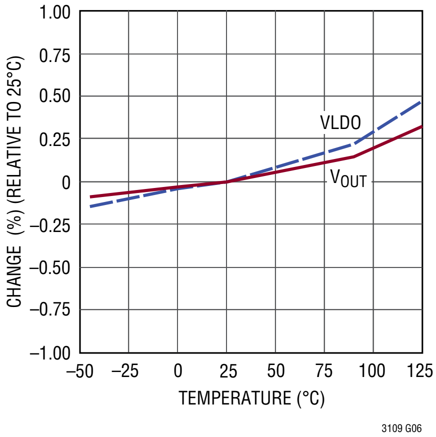

VAUX Clamp Voltage vs Shunt Current

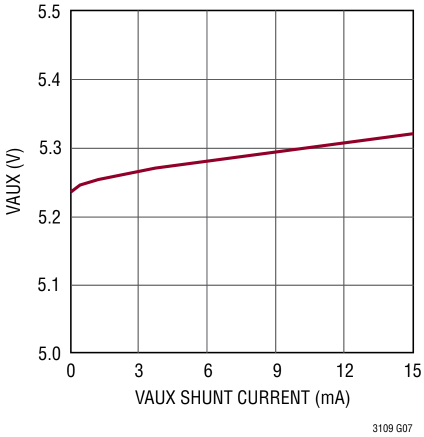

P_{VOUT} vs dT and TEG Size, 1:100 Ratio, V_{OUT} = 5V

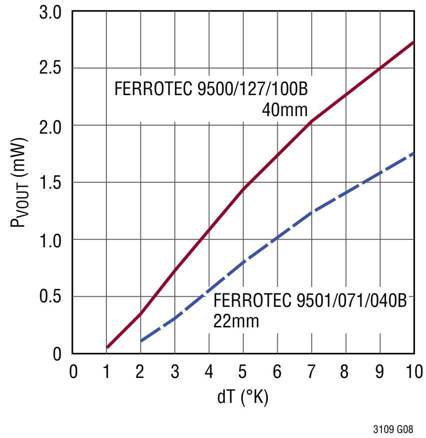

Resonant Switching Waveforms

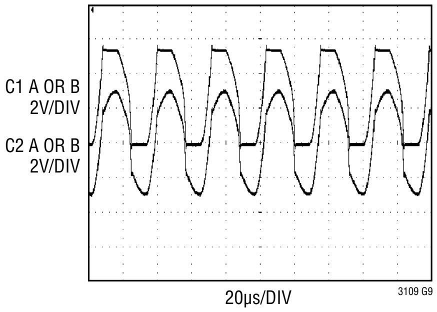

LDO Load Regulation

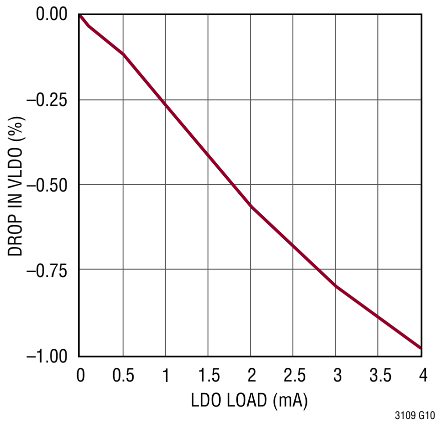

LDO Dropout Voltage

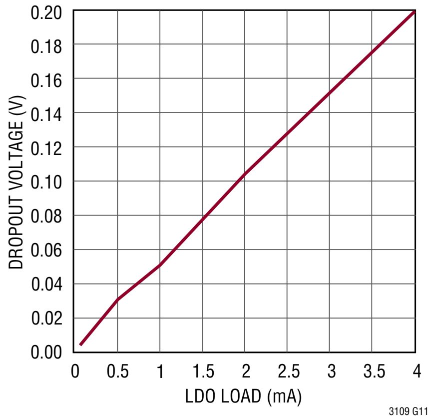

Start-Up Voltage Sequencing

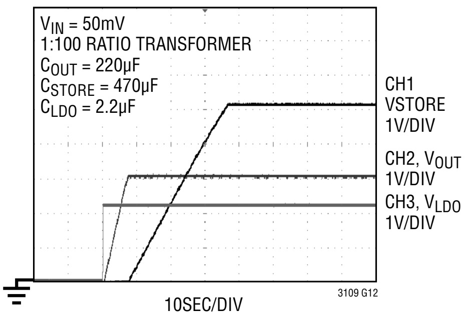

V_{OUT} and PGOOD Response During a Step Load

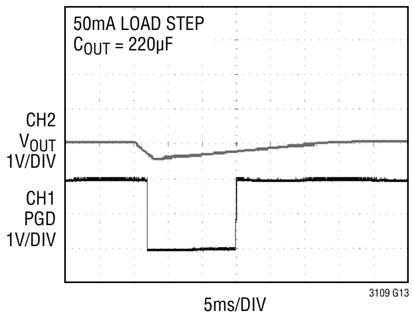

V_{OUT} Ripple

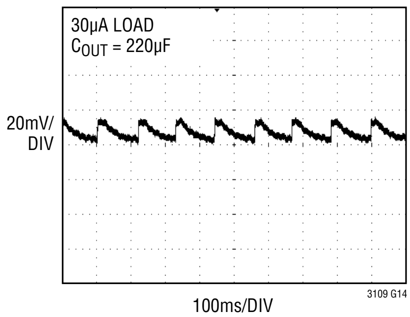

TYPICAL PERFORMANCE CHARACTERISTICS T_A = 25°C, unless otherwise noted.

LDO Step Load Response

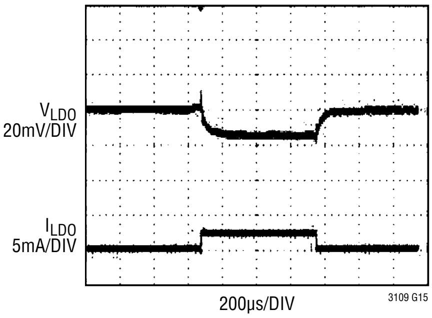

0mA TO 3mA LOAD STEP
C_{LDO} = 2.2µF

Enable Input and V_{OUT2}

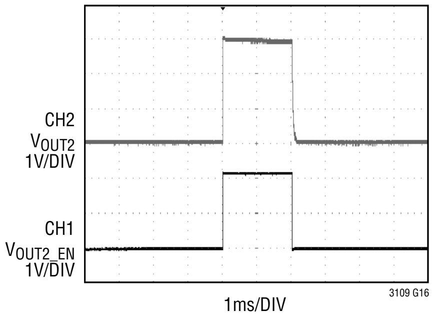

10mA LOAD ON V_{OUT2}
C_{OUT} = 220µF

Running on Storage Capacitor

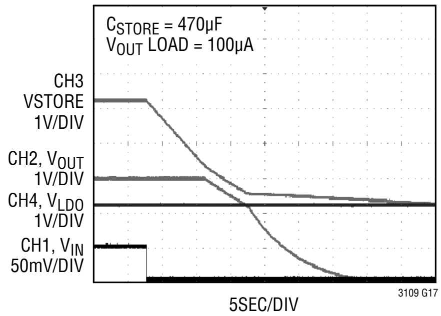

PIN FUNCTIONS (QFN/SSOP)

VSTORE (Pin 1/Pin 3): Output for the Storage Capacitor or Battery. A large storage capacitor may be connected from this pin to GND for powering the system in the event the input voltage is lost. It will be charged up to the maximum VAUX clamp voltage. If not used, this pin should be left open or tied to VAUX.

VAUX (Pin 2/Pin 4): Output of the Internal Rectifier Circuit and V_{CC} for the IC. Bypass VAUX with at least 1µF of capacitance to ground. An active shunt regulator clamps VAUX to 5.25V (typical).

V_{OUT} (Pin 3/Pin 5): Main Output of the Converter. The voltage at this pin is regulated to the voltage selected by VS1 and VS2 (see Table 1). Connect this pin to a reservoir capacitor or to a rechargeable battery. Any high current pulse loads must be fed by the reservoir capacitor on this pin.

V_{OUT2} (Pin 4/ Pin 6): Switched Output of the Converter. Connect this pin to a switched load. This output is open until V_{OUT_EN} is driven high, then it is connected to V_{OUT} through a 1Ω PMOS switch. If not used, this pin should be left open or tied to V_{OUT}.

V_{OUT2_EN} (Pin 5/Pin 7): Enable Input for V_{OUT2}. V_{OUT2} will be enabled when this pin is driven high. There is an internal 5M pull-down resistor on this pin. If not used, this pin can be left open or grounded.

PGOOD (Pin 6/Pin 8): Power Good Output. When V_{OUT} is within 7.5% of its programmed value, this pin will be pulled up to the LDO voltage through a 1M resistor. If V_{OUT} drops 9% below its programmed value PGOOD will go low. This pin can sink up to 100µA.

VLDO (Pin 7/Pin 9): Output of the 2.2V LDO. Connect a 2.2µF or larger ceramic capacitor from this pin to GND. If not used, this pin should be tied to VAUX.

GND (Pins 8, 11, 16, Exposed Pad Pin 21/Pins 10, 13, 18): Ground Pins. Connect these pins directly to the ground plane. The exposed pad serves as a ground connection and as a means of conducting heat away from the die.

VS2 (Pin 20/Pin 2): V_{OUT} Select Pin 2. Connect this pin to ground or VAUX to program the output voltage (see Table 1).

VS1 (Pin 19/Pin 1): V_{OUT} Select Pin 1. Connect this pin to ground or VAUX to program the output voltage (see Table 1).

Table 1. Regulated Output Voltage Using Pins VS1 and VS2

VS2	VS1	V_{OUT}
GND	GND	2.35V
GND	VAUX	3.3V
VAUX	GND	4.1V
VAUX	VAUX	5.0V

3109fb

PIN FUNCTIONS (DFN/SSOP)

C1B (Pin 9/Pin 11): Input to the Charge Pump and Rectifier Circuit for Channel B. Connect a capacitor from this pin to the secondary winding of the "B" step-up transformer. See the Applications Information section for recommended capacitor values.

C1A (Pin 18/Pin 20): Input to the Charge Pump and Rectifier Circuit for Channel A. Connect a capacitor from this pin to the secondary winding of the "A" step-up transformer. See the Applications Information section for recommended capacitor values.

C2B (Pin 10/Pin 12): Input to the Gate Drive Circuit for SWB. Connect a capacitor from this pin to the secondary winding of the "B" step-up transformer. See the Applications Information section for recommended capacitor values.

C2A (Pin 17/Pin 19): Input to the Gate Drive Circuit for SWA. Connect a capacitor from this pin to the secondary winding of the "A" step-up transformer. See the Applications Information section for recommended capacitor values.

SWA (Pin 15/Pin 17): Connection to the Internal N-Channel Switch for Channel A. Connect this pin to the primary winding of the "A" transformer.

SWB (Pin 12/Pin 14): Connection to the Internal N-Channel Switch for Channel B. Connect this pin to the primary winding of the "B" transformer.

V_{INA} (Pin 14/Pin 16): Connection to the Internal N-Channel Switch for Channel A. Connect this pin to one side of the input voltage source (see Typical Applications).

V_{INB} (Pin 13/Pin 15): Connection to the Internal N-Channel Switch for Channel B. Connect this pin to the other side of the input voltage source (see Typical Applications).

BLOCK DIAGRAM

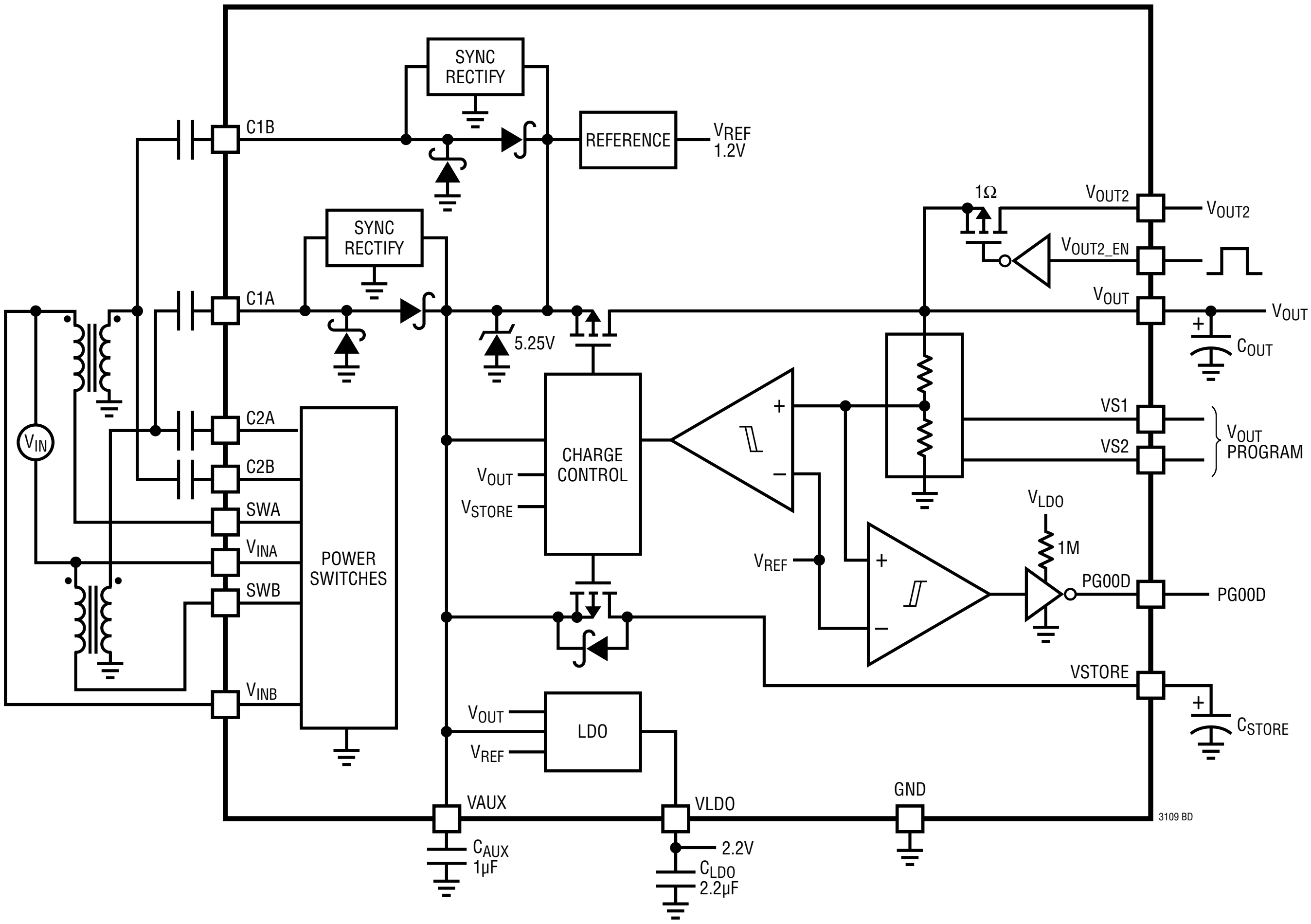

OPERATION (Refer to the Block Diagram)

The LTC3109 is designed to use two small external step-up transformers to create an ultralow input voltage step-up DC/DC converter and power manager that can operate from input voltages of either polarity. This unique capability enables energy harvesting from thermoelectric generators (TEGs) in applications where the temperature differential across the TEG may be of either (or unknown) polarity. It can also operate from low level AC sources. It is ideally suited for low power wireless sensors and other applications in which surplus energy harvesting is used to generate system power because traditional battery power is inconvenient or impractical.

The LTC3109 is designed to manage the charging and regulation of multiple outputs in a system in which the average power draw is very low, but where periodic pulses of higher load current may be required. This is typical of wireless sensor applications, where the quiescent power draw is extremely low most of the time, except for transmit pulses when circuitry is powered up to make measurements and transmit data.

The LTC3109 can also be used to trickle charge a standard capacitor, super capacitor or rechargeable battery, using energy harvested from a TEG or low level AC source.

Resonant Oscillator

The LTC3109 utilizes MOSFET switches to form a resonant step-up oscillator that can operate from an input of either polarity using external step-up transformers and small coupling capacitors. This allows it to boost input voltages as low as 30mV high enough to provide multiple regulated output voltages for powering other circuits. The frequency of oscillation is determined by the inductance of the transformer secondary winding, and is typically in the range of 10kHz to 100kHz. For input voltages as low as 30mV, transformers with a turns ratio of about 1:100 is recommended. For operation from higher input voltages, this ratio can be lower. See the Applications Information section for more information on selecting the transformers.

Charge Pump and Rectifier

The AC voltage produced on the secondary winding of the transformer is boosted and rectified using an external charge pump capacitor (from the secondary winding to pin C1A or C1B) and the rectifiers internal to the LTC3109. The rectifier circuit feeds current into the V_{AUX} pin, providing charge to the external VAUX capacitor and the other outputs.

VAUX

The active circuits within the LTC3109 are powered from VAUX, which should be bypassed with a 1µF minimum capacitor. Once VAUX exceeds 2.5V, the main V_{OUT} is allowed to start charging.

An internal shunt regulator limits the maximum voltage on VAUX to 5.25V typical. It shunts to ground any excess current into VAUX when there is no load on the converter or the input source is generating more power than is required by the load. This current should be limited to 15mA max.

Voltage Reference

The LTC3109 includes a precision, micropower reference, for accurate regulated output voltages. This reference becomes active as soon as VAUX exceeds 2V.

Synchronous Rectifiers

Once VAUX exceeds 2V, synchronous rectifiers in parallel with each of the internal rectifier diodes take over the job of rectifying the input voltage at pins C1A and C1B, improving efficiency.

Low Dropout Linear Regulator (LDO)

The LTC3109 includes a low current LDO to provide a regulated 2.2V output for powering low power processors or other low power ICs. The LDO is powered by the higher of VAUX or V_{OUT}. This enables it to become active as soon as VAUX has charged to 2.3V, while the

OPERATION (Refer to the Block Diagram)

V_{OUT} storage capacitor is still charging. In the event of a step load on the LDO output, current can come from the main V_{OUT} reservoir capacitor. The LDO requires a 2.2µF ceramic capacitor for stability. Larger capacitor values can be used without limitation, but will increase the time it takes for all the outputs to charge up. The LDO output is current limited to 5mA minimum.

V_{OUT}

The main output voltage on V_{OUT} is charged from the VAUX supply, and is user-programmed to one of four regulated voltages using the voltage select pins VS1 and VS2, according to Table 2. Although the logic-threshold voltage for VS1 and VS2 is 0.85V typical, it is recommended that they be tied to ground or VAUX.

Table 2

VS2	VS1	V_{OUT}
GND	GND	2.35V
GND	VAUX	3.3V
VAUX	GND	4.1V
VAUX	VAUX	5V

When the output voltage drops slightly below the regulated value, the charging current will be enabled as long as VAUX is greater than 2.5V. Once V_{OUT} has reached the proper value, the charging current is turned off. The resulting ripple on V_{OUT} is typically less than 20mV peak to peak.

The internal programmable resistor divider, controlled by VS1 and VS2, sets V_{OUT}, eliminating the need for very high value external resistors that are susceptible to noise pickup and board leakages.

In a typical application, a reservoir capacitor (typically a few hundred microfarads) is connected to V_{OUT}. As soon as VAUX exceeds 2.5V, the V_{OUT} capacitor will begin to charge up to its regulated voltage. The current available to charge the capacitor will depend on the input voltage and transformer turns ratio, but is limited to about 15mA typical. Note that for very low input voltages, this current may be in the range of 1µA to 1000µA.

PGOOD

A power good comparator monitors the V_{OUT} voltage. The PGOOD pin is an open-drain output with a weak pull-up (1MΩ) to the LDO voltage. Once V_{OUT} has charged to within 7.5% of its programmed voltage, the PGOOD output will go high. If V_{OUT} drops more than 9% from its programmed voltage, PGOOD will go low. The PGOOD output is designed to drive a microprocessor or other chip I/O and is not intended to drive a higher current load such as an LED. The PGOOD pin can also be pulled low in a wire-OR configuration with other circuitry.

V_{OUT2}

V_{OUT2} is an output that can be turned on and off by the host using the V_{OUT2_EN} pin. When enabled, V_{OUT2} is connected to V_{OUT} through a 1Ω P-channel MOSFET switch. This output, controlled by a host processor, can be used to power external circuits such as sensors and amplifiers, that don't have a low power "sleep" or shutdown capability. V_{OUT2} can be used to power these circuits only when they are needed.

Minimizing the amount of decoupling capacitance on V_{OUT2} enables it to be switched on and off faster, allowing shorter pulse times and therefore smaller duty cycles in applications such as a wireless sensor/transmitter. A small V_{OUT2} capacitor will also minimize the energy that will be wasted in charging the capacitor every time V_{OUT2} is enabled.

V_{OUT2} has a current limiting circuit that limits the peak current to 0.3A typical.

The V_{OUT2} enable input has a typical threshold of 1V with 100mV of hysteresis, making it logic compatible. If V_{OUT2_EN} (which has an internal 5M pull-down resistor) is low, V_{OUT2} will be off. Driving V_{OUT2_EN} high will turn on the V_{OUT2} output.

Note that while V_{OUT2_EN} is high, the current limiting circuitry for V_{OUT2} draws an extra 8µA of quiescent current from V_{OUT}. This added current draw has a negligible effect

OPERATION (Refer to the Block Diagram)

on the application and capacitor sizing, since the load on the V_{OUT2} output, when enabled, is likely to be orders of magnitude higher than 8µA.

VSTORE

The VSTORE output can be used to charge a large storage capacitor or rechargeable battery. Once V_{OUT} has reached regulation, the VSTORE output will be allowed to charge up to the clamped VAUX voltage (5.25V typical). The storage element on VSTORE can then be used to power the system in the event that the input source is lost, or is unable to provide the current demanded by the V_{OUT}, V_{OUT2} and LDO outputs.

If VAUX drops below VSTORE, the LTC3109 will automatically draw current from the storage element. Note that it may take a long time to charge a large storage capacitor, depending on the input energy available and the loading on V_{OUT} and VLDO.

Since the maximum charging current available at the VSTORE output is limited to about 15mA, it can safely be used to trickle charge NiCd or NiMH batteries for energy storage when the input voltage is lost.

Note that VSTORE is not intended to supply high pulse load currents to V_{OUT}. Any pulse load on V_{OUT} must be handled by the V_{OUT} reservoir capacitor.

Short-Circuit Protection

All outputs of the LTC3109 are current limited to protect against short circuits to ground.

Output Voltage Sequencing

A timing diagram showing the typical charging and voltage sequencing of the outputs is shown in Figure 1. Note that the horizontal (time) axis is not to scale, and is used for illustration purposes to show the relative order in which the output voltages come up.

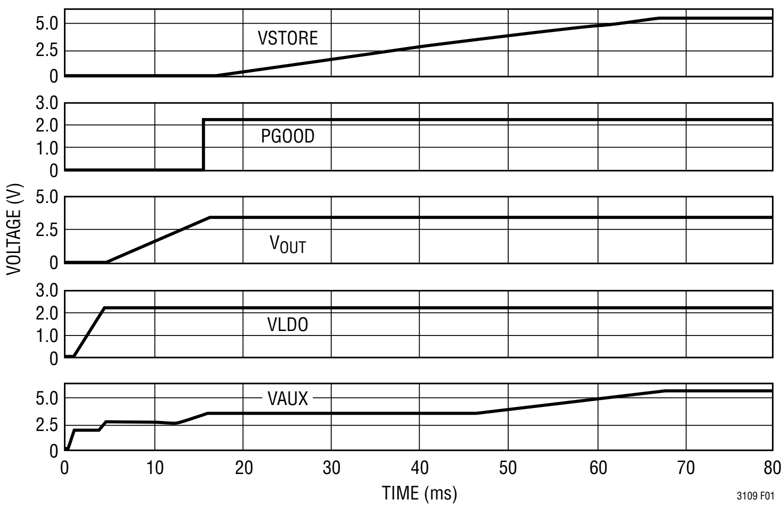

Figure 1. Output Voltage Sequencing (with V_{OUT} Programmed for 3.3V). Time Not to Scale

APPLICATIONS INFORMATION

INTRODUCTION

The LTC3109 is designed to gather energy from very low input voltage sources and convert it to usable output voltages to power microprocessors, wireless transmitters and analog sensors. Its architecture is specifically tailored to applications where the input voltage polarity is unknown, or can change. This "auto-polarity" capability makes it ideally suited to energy harvesting applications using a TEG whose temperature differential may be of either polarity.

Applications such as wireless sensors typically require much more peak power, and at higher voltages, than the input voltage source can produce. The LTC3109 is designed to accumulate and manage energy over a long period of time to enable short power pulses for acquiring and transmitting data. The pulses must occur at a low enough duty cycle that the total output energy during the pulse does not exceed the average source power integrated over the accumulation time between pulses. For many applications, this time between pulses could be seconds, minutes or hours.

The PGOOD signal can be used to enable a sleeping microprocessor or other circuitry when V_{OUT} reaches regulation, indicating that enough energy is available for a transmit pulse.

INPUT VOLTAGE SOURCES

The LTC3109 can operate from a number of low input voltage sources, such as Peltier cells (thermoelectric generators), or low level AC sources. The minimum input voltage required for a given application will depend on the transformer turns ratios, the load power required, and the internal DC resistance (ESR) of the voltage source. Lower ESR sources will allow operation from lower input voltages, and provide higher output power capability.

For a given transformer turns ratio, there is a maximum recommended input voltage to avoid excessively high secondary voltages and power dissipation in the shunt regulator. It is recommended that the maximum input voltage times the turns ratio be less than 50.

Note that a low ESR decoupling capacitor may be required across a DC input source to prevent large voltage droop and ripple caused by the source's ESR and the peak primary switching current (which can reach hundreds of milliamps). Since the input voltage may be of either polarity, a ceramic capacitor is recommended.

PELTIER CELL (THERMOELECTRIC GENERATOR)

A Peltier cell is made up of a large number of series-connected P-N junctions, sandwiched between two parallel ceramic plates. Although Peltier cells are often used as coolers by applying a DC voltage to their inputs, they will also generate a DC output voltage, using the Seebeck effect, when the two plates are at different temperatures.

When used in this manner, they are referred to as thermoelectric generators (TEGs). The polarity of the output voltage will depend on the polarity of the temperature differential between the TEG plates. The magnitude of the output voltage is proportional to the magnitude of the temperature differential between the plates.

The low voltage capability of the LTC3109 design allows it to operate from a typical TEG with temperature differentials as low as 1°C of either polarity, making it ideal for harvesting energy in applications where a temperature difference exists between two surfaces or between a surface and the ambient temperature. The internal resistance (ESR) of most TEGs is in the range of 1Ω to 5Ω, allowing for reasonable power transfer. The curves in Figure 2 show the open-circuit output voltage and maximum power transfer for a typical TEG with an ESR of 2Ω, over a 20°C range of temperature differential (of either polarity).

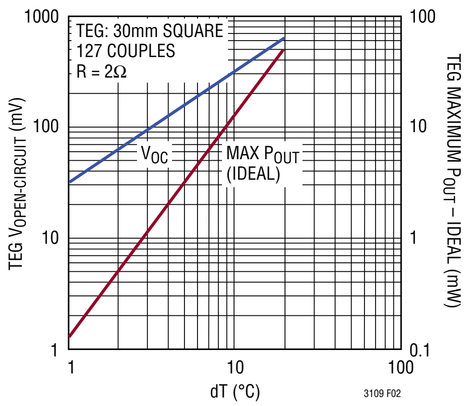

Figure 2. Typical Performance of a Peltier Cell Acting as a Power Generator (TEG)

APPLICATIONS INFORMATION

TEG LOAD MATCHING

The LTC3109 was designed to present an input resistance (load) in the range of 2Ω to 10Ω, depending on input voltage, transformer turns ratio and the C1A and C2A capacitor values (as shown in the Typical Performance curves). For a given turns ratio, as the input voltage drops, the input resistance increases. This feature allows the LTC3109 to optimize power transfer from sources with a few Ohms of source resistance, such as a typical TEG. Note that a lower source resistance will always provide more output current capability by providing a higher input voltage under load.

Table 3. Peltier Cell Manufacturers

CUI Inc www.cui.com
Ferrotec www.ferrotec.com/products/thermal/modules/
Fujitaka www.fujitaka.com/pub/peltier/english/thermoelectric_power.html
Hi-Z Technology www.hi-z.com
Kryotherm www.kryotherm
Laird Technologies www.lairdtech.com
Micropelt www.micropelt.com
Nextreme www.nextreme.com
TE Technology www.tetech.com/Peltier-Thermoelectric-Cooler-Modules.html
Tellurex www.tellurex.com/

UNIPOLAR APPLICATIONS

The LTC3109 can also be configured to operate from two independent unipolar voltage sources, such as two TEGs in different locations. In this configuration, energy can be harvested from either or both sources simultaneously. See the Typical Applications for an example.

The LTC3109 can also be configured to operate from a single unipolar source, using a single step-up transformer, by ganging its V_{IN} and SW pins together. In this manner, it can extract the most energy from very low resistance sources. See Figure 3 for an example of this configuration, along with the performance curves.

PELTIER CELL (TEG) SUPPLIERS

Peltier cells are available in a wide range of sizes and power capabilities, from less than 10mm square to over 50mm square. They are typically 2mm to 5mm in height. A list of some Peltier cell manufacturers is given in Table 3 and some recommended part numbers in Table 4.

COMPONENT SELECTION

Step-Up Transformer

The turns ratio of the step-up transformers will determine how low the input voltage can be for the converter to start. Due to the auto-polarity architecture, two identical step-up transformers should be used, unless the temperature drop across the TEG is significantly different in one polarity, in which case the ratios may be different.

Table 4. Recommended TEG Part Numbers by Size

MANUFACTURER	15mm	20mm	30mm	40mm
CUI Inc. (Distributor)	CP60133	CP60233	CP60333	CP85438
Ferrotec	9501/031/030 B	9501/071/040 B	9500/097/090 B	9500/127/100 B
Fujitaka	FPH13106NC	FPH17106NC	FPH17108AC	FPH112708AC
Kryotherm			TGM-127-1.0-0.8	LCB-127-1.4-1.15
Laird Technology			PT6.7.F2.3030.W6	PT8.12.F2.4040.TA.W6
Marlow Industries		RC3-8-01	RC6-6-01	RC12-8-01LS
Tellurex	C2-15-0405	C2-20-0409	C2-30-1505	C2-40-1509
TE Technology	TE-31-1.0-1.3	TE-31-1.4-1.15	TE-71-1.4-1.15	TE-127-1.4-1.05

APPLICATIONS INFORMATION

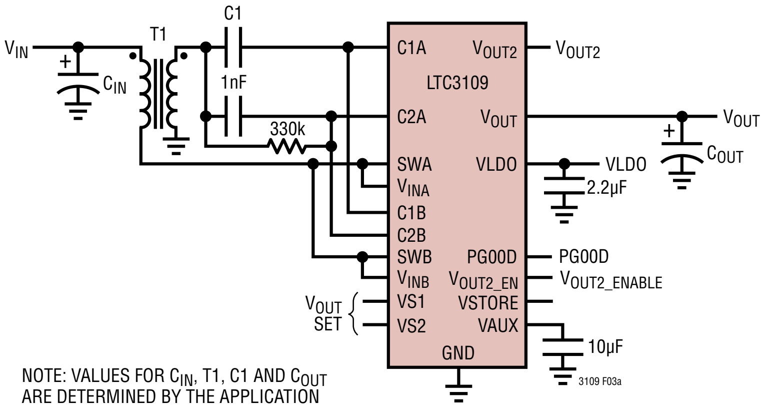

Figure 3. Unipolar Application

Typical P_{VOUT} vs dT for Unipolar Configuration

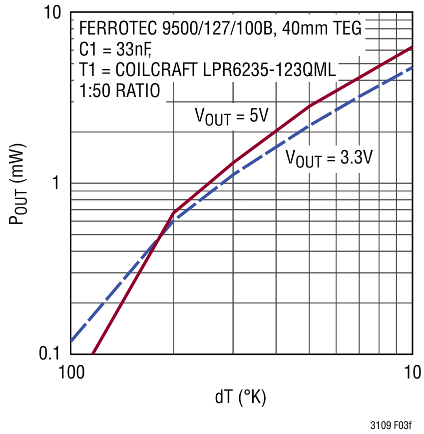

Typical I_{VOUT} vs V_{IN} for Unipolar Configuration

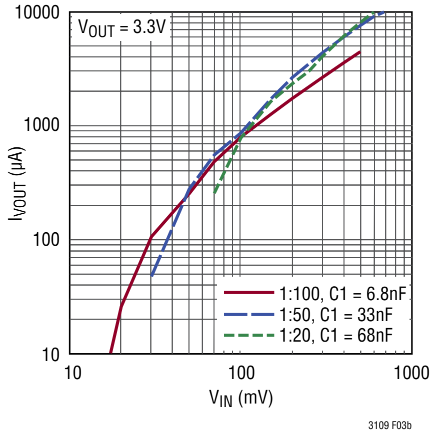

Typical Efficiency vs V_{IN} for Unipolar Configuration

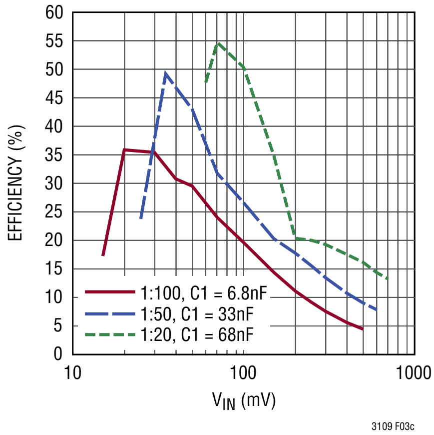

Typical Input Current vs V_{IN} for Unipolar Configuration

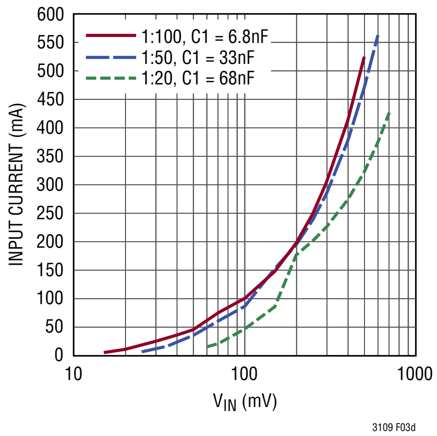

Typical R_{IN} vs V_{IN} for Unipolar Configuration

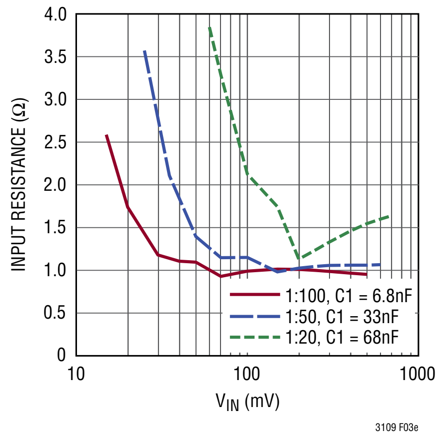

APPLICATIONS INFORMATION

Using a 1:100 primary-secondary ratio yields start-up voltages as low as 30mV. Other factors that affect performance are the resistance of the transformer windings and the inductance of the windings. Higher DC resistance will result in lower efficiency and higher start-up voltages. The secondary winding inductance will determine the resonant frequency of the oscillator, according to the formula below.

$$\text{Freq} = \frac{1}{2 \bullet \pi \bullet \sqrt{L_{SEC} \bullet C}}\ \text{Hz}$$

where L_{SEC} is the inductance of one of the secondary windings and C is the load capacitance on the secondary winding. This is comprised of the input capacitance at pin C2A or C2B, typically 70pF each, in parallel with the transformer secondary winding's shunt capacitance. The recommended resonant frequency is in the range of 10kHz to 100kHz. Note that loading will also affect the resonant frequency. See Table 5 for some recommended transformers.

Table 5. Recommended Transformers

VENDOR	TYPICAL START-UP VOLTAGE	PART NUMBER
Coilcraft www.coilcraft.com	25mV 35mV 85mV	LPR6235-752SML (1:100 ratio) LPR6235-123QML (1:50 ratio) LPR6235-253PML (1:20 ratio)
Würth www.we-online	25mV 35mV 85mV	74488540070 (1:100 Ratio) 74488540120 (1:50 Ratio) 74488540250 (1:20 Ratio)

USING EXTERNAL CHARGE PUMP RECTIFIERS

The synchronous rectifiers in the LTC3109 have been optimized for low frequency, low current operation, typical of low input voltage applications. For applications where the resonant oscillator frequency exceeds 100kHz, or a transformer turns ratio of less than 1:20 is used, or the C1A and C1B capacitor values are greater than 68nF, the use of external charge pump rectifiers (1N4148 or 1N914 or equivalent) is recommended. See the Typical Application circuits for an example. Avoid the use of Schottky rectifiers, as their low forward voltage increases the minimum start-up voltage.

C1 CAPACITOR

The charge pump capacitor that is connected from each transformer's secondary winding to the corresponding C1A and C1B pins has an effect on converter input resistance and maximum output current capability. Generally a minimum value of 1nF is recommended when operating from very low input voltages using a transformer with a ratio of 1:100. Capacitor values of 2.2nF to 10nF will provide higher output current at higher input voltages, however larger capacitor values can compromise performance when operating at low input voltage or with high resistance sources. For higher input voltages and lower turns ratios, the value of the C1 capacitor can be increased for higher output current capability. Refer to the Typical Applications examples for the recommended value for a given turns ratio.

C2 CAPACITOR

The C2 capacitors connect pins C2A and C2B to their respective transformer secondary windings. For most applications a capacitor value of 470pF is recommended. Smaller capacitor values tend to raise the minimum start-up voltage, and larger capacitor values can lower efficiency.

Note that the C1 and C2 capacitors must have a voltage rating greater than the maximum input voltage times the transformer turns ratio.

V_{OUT} AND VSTORE CAPACITOR

For pulsed load applications, the V_{OUT} capacitor should be sized to provide the necessary current when the load is pulsed on. The capacitor value required will be dictated by the load current (I_{LOAD}), the duration of the load pulse (t_{PULSE}), and the amount of V_{OUT} voltage droop the application can tolerate (ΔV_{OUT}). The capacitor must be rated for whatever voltage has been selected for V_{OUT} by VS1 and VS2:

$$C_{OUT}(\mu F) \geq \frac{I_{LOAD(mA)} \bullet t_{PULSE(ms)}}{\Delta V_{OUT}\ (V)}$$

APPLICATIONS INFORMATION

Note that there must be enough energy available from the input voltage source for V_{OUT} to recharge the capacitor during the interval between load pulses (as discussed in Design Example 1). Reducing the duty cycle of the load pulse will allow operation with less input energy.

The VSTORE capacitor may be of very large value (thousands of microfarads or even Farads), to provide energy storage at times when the input voltage is lost. Note that this capacitor can charge all the way to the VAUX clamp voltage of 5.25V typical (regardless of the settings for V_{OUT}), so be sure that the holdup capacitor has a working voltage rating of at least 5.5V at the temperature that it will be used.

The VSTORE input is not designed to provide high pulse load currents to V_{OUT}. The current path from VSTORE to V_{OUT} is limited to about 26mA max.

The VSTORE capacitor can be sized using the following formula:

$$C_{STORE} \geq \frac{(7\mu A + I_Q + I_{LDO} + (I_{PULSE} \bullet t_{PULSE} \bullet f)) \bullet t_{STORE}}{5.25 - V_{OUT}}$$

where 7µA is the quiescent current of the LTC3109, I_Q is the load on V_{OUT} in between pulses, I_{LDO} is the load on the LDO between pulses, I_{PULSE} is the total load during the pulse, t_{PULSE} is the duration of the pulse, f is the frequency of the pulses, t_{STORE} is the total storage time required and V_{OUT} is the output voltage required. Note that for a programmed output voltage of 5V, the VSTORE capacitor cannot provide any beneficial storage time to V_{OUT}.

To minimize losses and capacitor charge time, all capacitors used for V_{OUT} and VSTORE should be low leakage. See Table 6 for recommended storage capacitors.

Table 6. Recommended Storage Capacitors

VENDOR	PART NUMBER/SERIES
AVX www.avx.com	BestCap Series TAJ and TPS Series Tantalum
Cap-XX www.cap-xx.com	GZ Series
Cooper/Bussman www.bussmann.com/3/PowerStor.html	KR Series P Series
Vishay/Sprague www.vishay.com/capacitors	Tantamount 592D 595D Tantalum

Note that storage capacitors requiring voltage balancing resistors are not recommended due to the steady-state current draw of the resistors.

PCB LAYOUT GUIDELINES

Due to the rather low switching frequency of the resonant converter and the low power levels involved, PCB layout is not as critical as with many other DC/DC converters. There are however, a number of things to consider.

Due to the very low input voltages the circuit operates from, the connections to V_{IN}, the primary of the transformers and the SW, V_{IN} and GND pins of the LTC3109 should be designed to minimize voltage drop from stray resistance, and able to carry currents as high as 500mA. Any small voltage drop in the primary winding conduction path will lower efficiency and increase start-up voltage and capacitor charge time.

Also, due to the low charge currents available at the outputs of the LTC3109, any sources of leakage current on the output voltage pins must be minimized. An example board layout is shown in Figure 4.

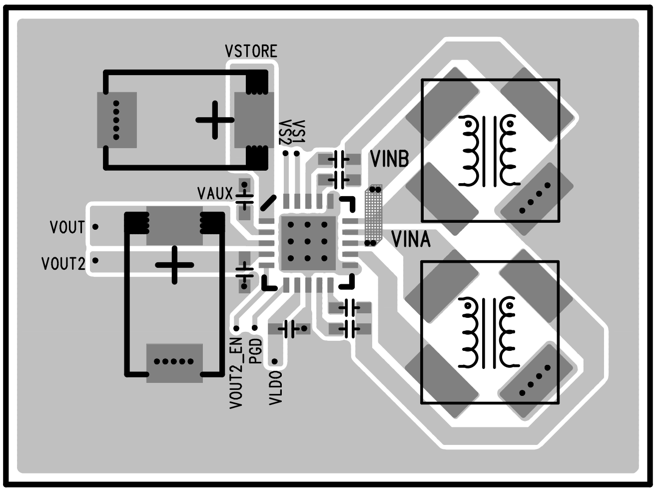

Figure 4. Example Component Placement for 2-Layer PC Board (QFN Package). Note That VSTORE and VOUT Capacitor Sizes are Application Dependent

APPLICATIONS INFORMATION

DESIGN EXAMPLE 1

This design example will explain how to calculate the necessary reservoir capacitor value for V_{OUT} in pulsed-load applications, such as a wireless sensor/transmitter. In these types of applications, the load is very small for a majority of the time (while the circuitry is in a low power sleep state), with pulses of load current occurring periodically during a transmit burst.

The reservoir capacitor on V_{OUT} supports the load during the transmit pulse; the long sleep time between pulses allows the LTC3109 to accumulate energy and recharge the capacitor (either from the input voltage source or the storage capacitor). A method for calculating the maximum rate at which the load pulses can occur for a given output current from the LTC3109 will also be shown.

In this example, V_{OUT} is set to 3.3V, and the maximum allowed voltage droop during a transmit pulse is 10%, or 0.33V. The duration of a transmit pulse is 5ms, with a total average current requirement of 20mA during the pulse. Given these factors, the minimum required capacitance on V_{OUT} is:

$$C_{OUT}\,(\mu F) \geq \frac{20mA \bullet 5ms}{0.33V} = 303\mu F$$

Note that this equation neglects the effect of capacitor ESR on output voltage droop. For ceramic capacitors and low ESR tantalum capacitors, the ESR will have a negligible effect at these load currents. However, beware of the voltage coefficient of ceramic capacitors, especially those in small case sizes. This greatly reduces the effective capacitance when a DC bias is applied.

A standard value of 330µF could be used for C_{OUT} in this case. Note that the load current is the total current draw on V_{OUT}, V_{OUT2} and VLDO, since the current for all of these outputs must come from V_{OUT} during a pulse. Current contribution from the capacitor on VSTORE is not considered, since it may not be able to recharge between pulses. Also, it is assumed that the harvested charge current from the LTC3109 is negligible compared to the magnitude of the load current during the pulse.

To calculate the maximum rate at which load pulses can occur, you must know how much charge current is available from the LTC3109 V_{OUT} pin given the input voltage source being used. This number is best found empirically, since there are many factors affecting the efficiency of the converter. You must also know what the total load current is on V_{OUT} during the sleep state (between pulses). Note that this must include any losses, such as storage capacitor leakage.

Let's assume that the charge current available from the LTC3109 is 150µA and the total current draw on V_{OUT} and VLDO in the sleep state is 17µA, including capacitor leakage. We'll also use the value of 330µF for the V_{OUT} capacitor. The maximum transmit rate (neglecting the duration of the transmit pulse, which is very short compared to the period) is then given by:

$$T = \frac{330\mu F \bullet 0.33V}{150\mu A - 17\mu A} = 0.82\text{sec or } f_{MAX} = 1.2Hz$$

Therefore, in this application example, the circuit can support a 5ms transmit pulse of 20mA every 0.82 seconds.

It can be seen that for systems that only need to transmit every few seconds (or minutes or hours), the average charge current required is extremely small, as long as the sleep or standby current is low. Even if the available charge current in the example above was only 21µA, if the sleep current was only 5µA, it could still transmit a pulse every seven seconds.

The following formula will allow you to calculate the time it will take to charge the LDO output capacitor and the V_{OUT} capacitor the first time, from zero volts. Here again, the charge current available from the LTC3109 must be known. For this calculation, it is assumed that the LDO output capacitor is 2.2µF:

$$t_{LDO} = \frac{2.2V \bullet 2.2\mu F}{I_{CHG} - I_{LDO}}$$

If there was 150µA of charge current available and a 5µA load on the LDO (when the processor is sleeping), the time for the LDO to reach regulation would be only 33ms.

APPLICATIONS INFORMATION

The time for V_{OUT} to charge and reach regulation can be calculated by the formula below, which assumes V_{OUT} is programmed to 3.3V and C_{OUT} is 330µF:

$$t_{VOUT} = \frac{3.3V \bullet 330\mu F}{I_{CHG} - I_{VOUT} - I_{LDO}} + t_{LDO}$$

With 150µA of charge current available and 5µA of load on both V_{OUT} and VLDO, the time for V_{OUT} to reach regulation after the initial application of power would be 7.81 seconds.

DESIGN EXAMPLE 2

In most pulsed-load applications, the duration, magnitude and frequency of the load current pulses are known and fixed. In these cases, the average charge current required from the LTC3109 to support the average load must be calculated, which can be easily done by the following:

$$I_{CHG} \geq I_Q + \frac{I_{PULSE} \bullet t_{PULSE}}{T}$$

where I_Q is the sleep current supplied by V_{OUT} and V_{LDO} to the external circuitry in-between load pulses, including output capacitor leakage, I_{PULSE} is the total load current during the pulse, t_{PULSE} is the duration of the load pulse and T is the pulse period (essentially the time between load pulses).

In this example, I_Q is 5µA, I_{PULSE} is 100mA, t_{PULSE} is 5ms and T is one hour. The average charge current required from the LTC3109 would be:

$$I_{CHG} \geq 5\mu A + \frac{100mA \bullet 0.005sec}{3600sec} = 5.14\mu A$$

Therefore, if the LTC3109 has an input voltage that allows it to supply a charge current greater than just 5.14µA, the application can support 100mA pulses lasting 5ms every hour. It can be seen that the sleep current of 5µA is the dominant factor in this example, because the transmit duty cycle is so small (0.00014%). Note that for a V_{OUT} of 3.3V, the average power required by this application is only 17µW (not including converter losses).

Keep in mind that the charge current available from the LTC3109 has no effect on the sizing of the V_{OUT} capacitor, and the V_{OUT} capacitor has no effect on the maximum allowed pulse rate.

TYPICAL APPLICATIONS

Energy Harvester Operates from Small Temperature Differentials of Either Polarity

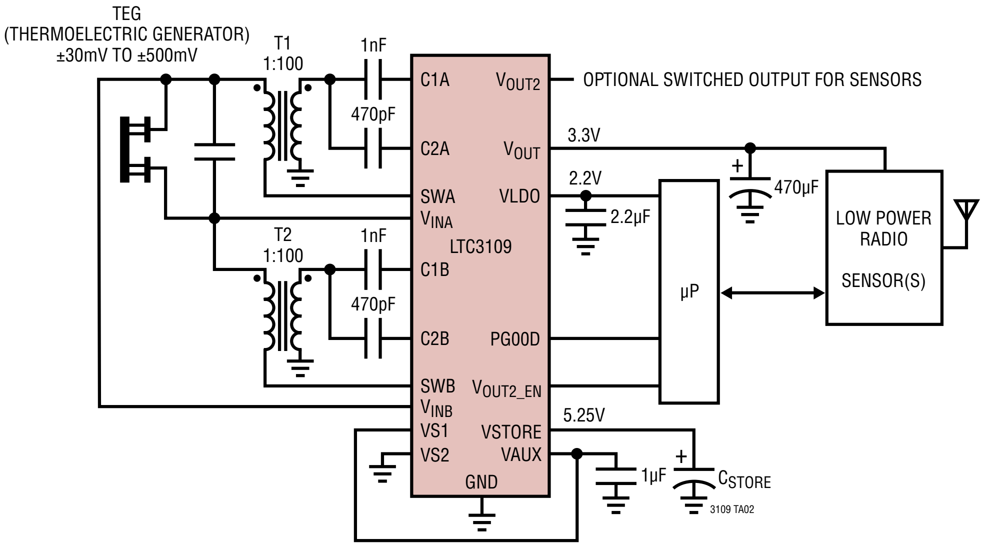

T1, T2: COILCRAFT LPR6235-752SML

Li-Ion Battery Charger and LDO Operates from a Low Level AC Input

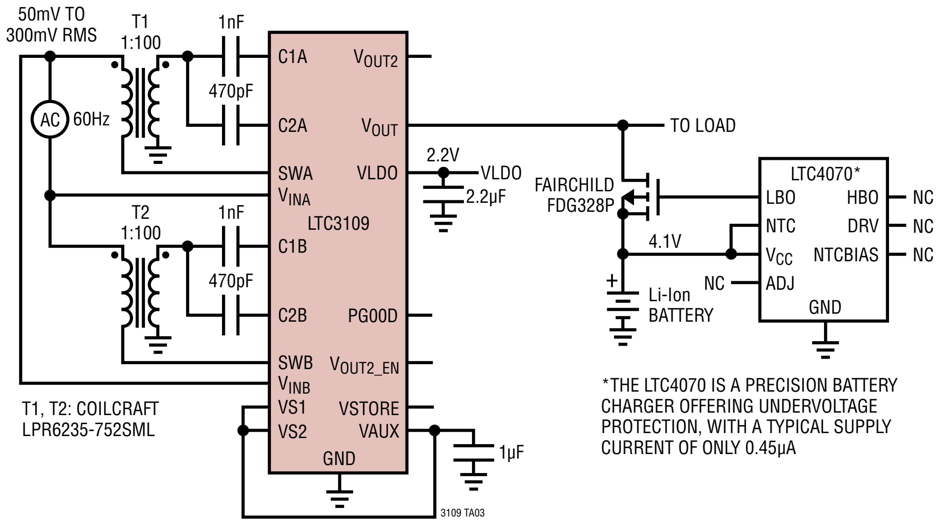

T1, T2: COILCRAFT LPR6235-752SML

*THE LTC4070 IS A PRECISION BATTERY CHARGER OFFERING UNDERVOLTAGE PROTECTION, WITH A TYPICAL SUPPLY CURRENT OF ONLY 0.45µA

TYPICAL APPLICATIONS

Unipolar Energy Harvester Charges Battery Backup

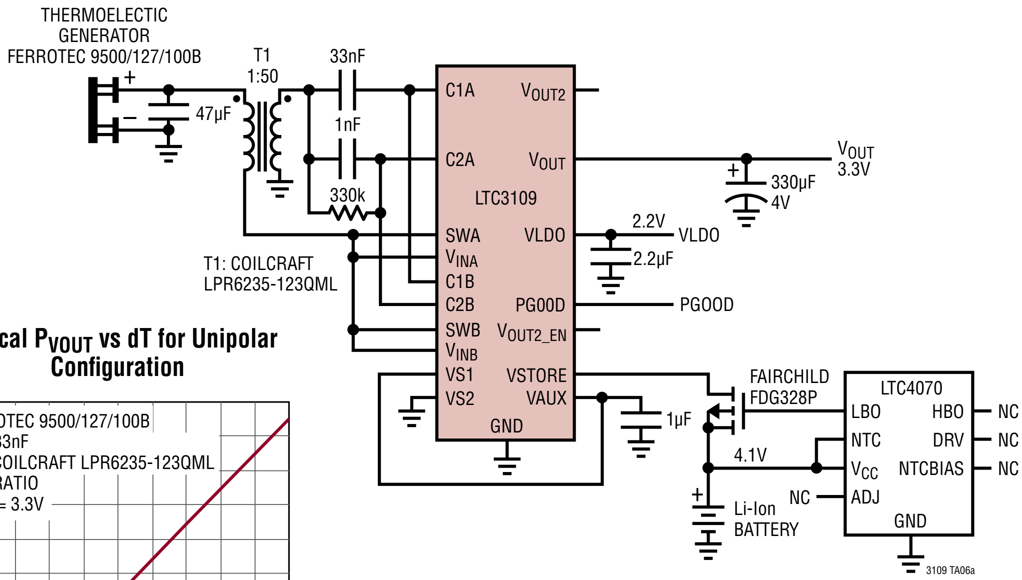

Typical P_{VOUT} vs dT for Unipolar Configuration

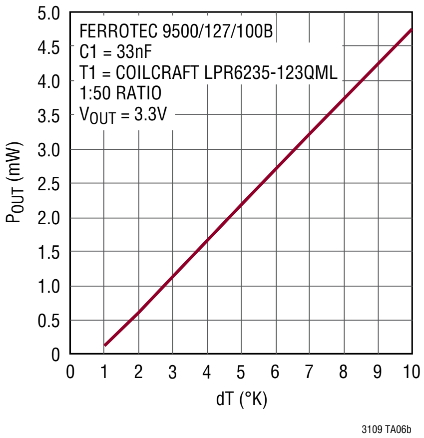

Dual-Input Energy Harvester Generates 5V and 2.2V from Either or Both TEGs, Operating at Different Temperatures of Fixed Polarity

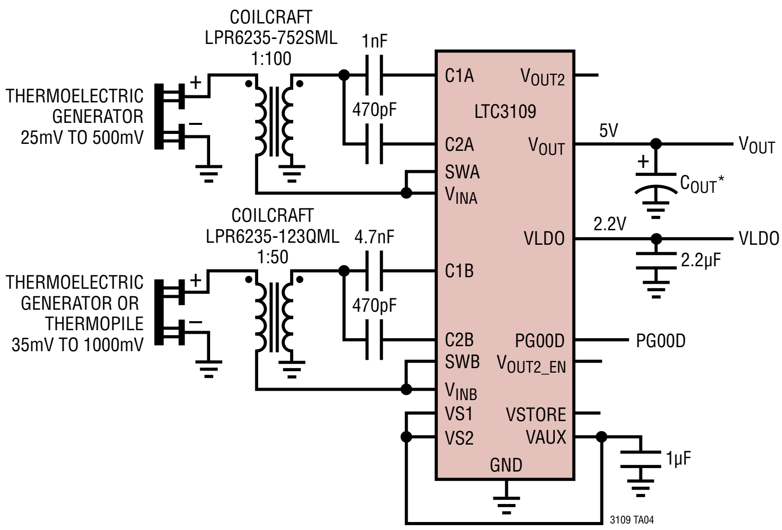

*THE VALUE OF THE C_{OUT} CAPACITOR IS DETEMINED BY THE LOAD CHARACTERISTICS

PACKAGE DESCRIPTION

Please refer to http://www.linear.com/designtools/packaging/ for the most recent package drawings.

UF Package
20-Lead Plastic QFN (4mm × 4mm)
(Reference LTC DWG # 05-08-1710 Rev A)

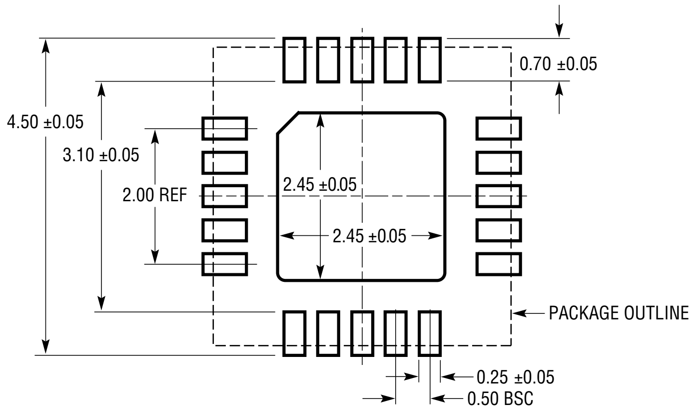

RECOMMENDED SOLDER PAD PITCH AND DIMENSIONS
APPLY SOLDER MASK TO AREAS THAT ARE NOT SOLDERED

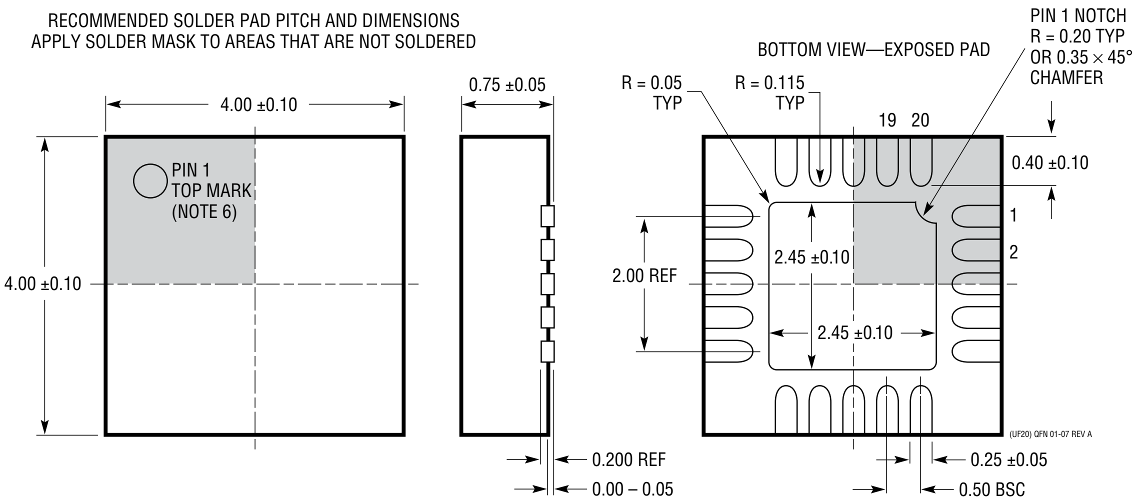

NOTE:
1. DRAWING IS PROPOSED TO BE MADE A JEDEC PACKAGE OUTLINE MO-220 VARIATION (WGGD-1)—TO BE APPROVED
2. DRAWING NOT TO SCALE
3. ALL DIMENSIONS ARE IN MILLIMETERS
4. DIMENSIONS OF EXPOSED PAD ON BOTTOM OF PACKAGE DO NOT INCLUDE MOLD FLASH. MOLD FLASH, IF PRESENT, SHALL NOT EXCEED 0.15mm ON ANY SIDE
5. EXPOSED PAD SHALL BE SOLDER PLATED
6. SHADED AREA IS ONLY A REFERENCE FOR PIN 1 LOCATION ON THE TOP AND BOTTOM OF PACKAGE

PACKAGE DESCRIPTION

Please refer to http://www.linear.com/designtools/packaging/ for the most recent package drawings.

GN Package
20-Lead Plastic SSOP (Narrow .150 Inch)
(Reference LTC DWG # 05-08-1641 Rev B)

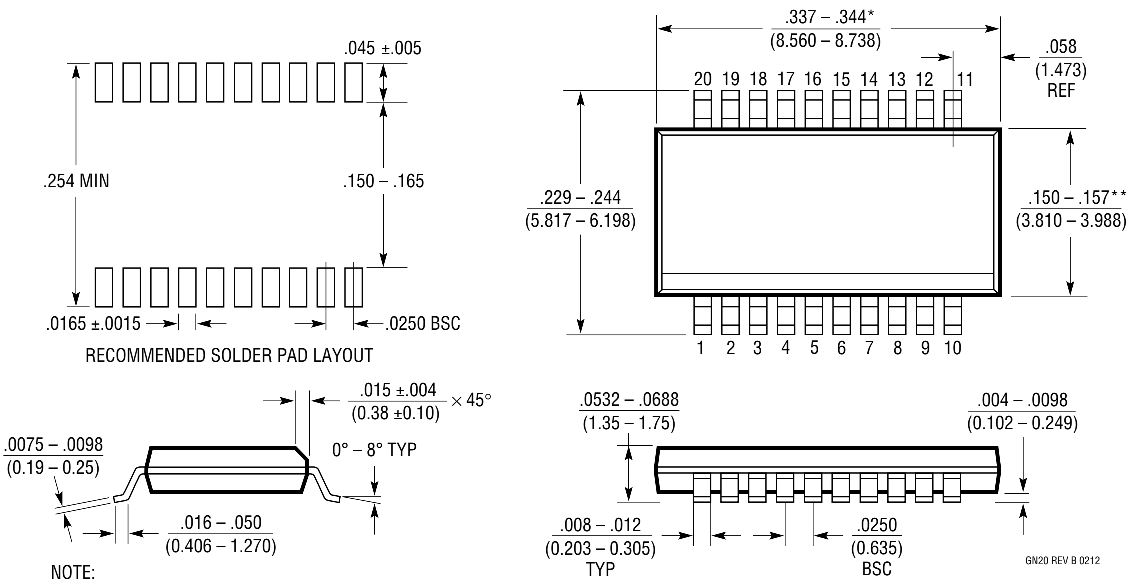

NOTE:
1. CONTROLLING DIMENSION: INCHES
2. DIMENSIONS ARE IN $\frac{\text{INCHES}}{\text{(MILLIMETERS)}}$
3. DRAWING NOT TO SCALE
4. PIN 1 CAN BE BEVEL EDGE OR A DIMPLE

*DIMENSION DOES NOT INCLUDE MOLD FLASH. MOLD FLASH SHALL NOT EXCEED 0.006" (0.152mm) PER SIDE

**DIMENSION DOES NOT INCLUDE INTERLEAD FLASH. INTERLEAD FLASH SHALL NOT EXCEED 0.010" (0.254mm) PER SIDE

REVISION HISTORY

REV	DATE	DESCRIPTION	PAGE NUMBER
A	06/12	Added vendor Information to Table 5	15
B	08/13	Changed Würth transformer part numbers	15

TYPICAL APPLICATION

Unipolar TEG Energy Harvester for Low Resistance/High Current Inputs, Using External Charge Pump Rectifiers

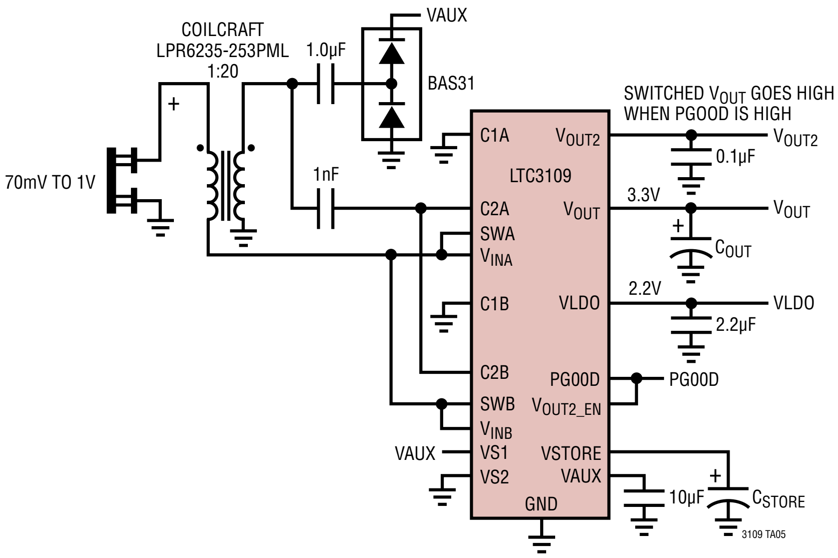

I_{VOUT} vs V_{IN}

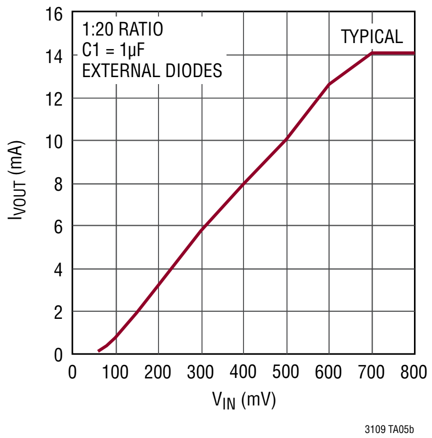

Efficiency vs V_{IN}

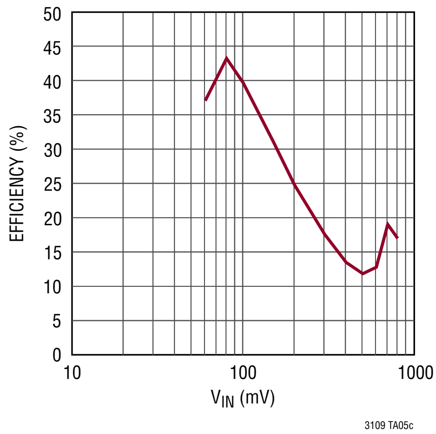

RELATED PARTS

PART NUMBER	DESCRIPTION	COMMENTS
LTC3108/ LTC3108-1	Ultralow Voltage Step-Up Converter and Power Manager	V_{IN}: 0.02V to 1V, V_{OUT} = 2.2V, 2.35V, 3.3V, 4.1V, 5V, I_Q = 6µA, 4mm × 3mm DFN-12, SSOP-16; LTC3108-1 V_{OUT} = 2.2V, 2.5V, 3V, 3.7V, 4.5V
LTC4070	Micropower Shunt Battery Charger	1% Float Voltage Accuracy, 50mA Max Shunt Current, V_{OUT} = 4.0V, 4.1V, 4.2V, I_Q = 450nA, 2mm × 3mm DFN-8, MSOP-8
LTC1041	Bang-Bang Controller	V_{IN}: 2.8V to 16V; $V_{OUT(MIN)}$ = Adj; I_Q = 1.2mA; I_{SD} < 1µA; SO-8 Package
LTC1389	Nanopower Precision Shunt Voltage Reference	$V_{OUT(MIN)}$ = 1.25V; I_Q = 0.8µA; SO-8 Package
LT1672/LT1673/ LT1674	Single-/Dual-/Quad-Precision 2µA Rail-to-Rail Op Amps	SO-8, SO-14 and MSOP-8 Packages
LT3009	3µA I_Q, 20mA Linear Regulator	V_{IN}: 1.6V to 20V; $V_{OUT(MIN)}$: 0.6V to Adj, 1.2V, 1.5V, 1.8V, 2.5V, 3.3V, 5V to Fixed; I_Q = 3µA; I_{SD} < 1µA; 2mm × 2mm DFN-8 and SC70 Packages
LTC3588-1	Piezoelectric Energy Generator with Integrated High Efficiency Buck Converter	V_{IN}: 2.7V to 20V; $V_{OUT(MIN)}$: Fixed to 1.8V, 2.5V, 3.3V, 3.6V; I_Q = 0.95µA; 3mm × 3mm DFN-10 and MSOP-10E Packages
LT8410/LT8410-1	Micropower 25mA/8mA Low Noise Boost Converter with Integrated Schottky Diode and Output Disconnect	V_{IN}: 2.6V to 16V; $V_{OUT(MIN)}$ = 40V_{MAX}; I_Q = 8.5µA; I_{SD} < 1µA; 2mm × 2mm DFN-8 Package

Linear Technology Corporation
1630 McCarthy Blvd., Milpitas, CA 95035-7417
(408) 432-1900 • FAX: (408) 434-0507 • www.linear.com/LTC3109
LT 0813 REV B • PRINTED IN USA

Bibliography

[1] Ltspice getting started guide, 2011. http://cds.linear.com/docs/en/software-and-simulation/LTspiceGettingStartedGuide.pdf.

[2] G. Alonso. Ltspice: Simple steps for simulating transformers, July 2014. http://www.linear.com/solutions/5092l.

[3] S. Beeby and N. White. Energy Harvesting for Autonomous System. Artech House, 2010.

[4] David'K.'Cheng. Fundamentos!de!Electromagnetismo!para!ingenieros. Pearson Addison'Wesley Longman, 1998.

[5] N. Elvin and A. Erturk. Advances in Energy Harvesting Methods. Springer, 2013.

[6] M. Engelhardt. Using transformers in ltspice/switchercad iii. Linear Technology Magazine, pages 23, 24, 2006.

[7] T. J. Kazmirski. Energy Harvesting Systems: Principles, Modeling and Applications. Springer, 2011.

[8] S. Kunijula. Mit sm thesis,. pages 23, 24, 2005.

[9] S. Priya and D. J. Inman. Energy Harvesting Technologies. Springer, 2009.

[10] Y. K. Tan. Energy Harvesting Autonomous Sensor System. Taylor and Francis Group, 2013.